IMPACT LOADING AND TRANSIENT RESPONSE OF PIPES TRANSPORTING GAS OR LIQUID

Roslina Mohammad

A thesis submitted in fulfilment of the requirements
For the degree of Doctor of Philosophy

School of Mechanical Engineering
The University of Adelaide

July 2011

DISCLAIMER

This work contains no material that has been accepted for the award of any other degree or diploma in any university or other tertiary to Roslina Mohammad and, to the best of my knowledge and belief, contains no material previously published or written by another person, except where due reference has been made in the text.

I give consent to this copy of my thesis when deposited in the university library, being made available for loan and photocopying, subject to the provisions of the Copyright Act 1968.

I also give permission for the digital version of my thesis to be made available on the web, via the university's digital research repository, the Library catalogue and also through web search engines, unless permission has been granted by the university to restrict access for a period of time.

Signed …………………………………………….

Date …………………………………………………

ACKNOWLEDGEMENTS

PUBLICATIONS

Journal Papers

1.*Mohammad R, Kotousov A, Codrington J, Blazewicz A. Effect of flowing medium for a simply supported pipe subjected to impulse loading, special ACAM6 issue. Australian Journal of Mechanical Engineering (AJME). 2011; 8(2): 1-10 (see Appendix A).

2.*Mohammad R, Kotousov A, Codrington J. Analytical modelling of a pipe with flowing medium subjected to an impulse load. International Journal of Impact Engineering. 2011; 38(2–3):115–122 (see Appendix B).

3.Kotousov A, *Mohammad R. Analytical modelling of the transient dynamics of pipes with flowing medium. Journal of Physics: Conference Series. 2009; 181 012082, 8pp.

Conference Papers

4.*Mohammad R, Kotousov A, Codrington J. Dynamic behaviour of transporting liquid under impulse loading. 6th Australasian Congress on Applied Mechanics, (ACAM 6); 2010 Dec. 10–12; Perth (Australia).

5.Kotousov A, *Mohammad R. Analytical modelling of the transient dynamics of pipes with flowing medium. 7th International Conference on Modern Practice in Stress and Vibration Analysis (MPSVA); 2009 Sept. 8–10; Cambridge (UK).

Awards and Achievements

Awarded 2nd prize for the *Postgraduate Student Best Paper Award* at the 6th Australasian Congress on Applied Mechanics in 2010 for the paper:

*Mohammad R, Kotousov A, Codrington, J. Dynamic behaviour of transporting liquid under impulse loading. 6th Australasian Congress on Applied Mechanics, (ACAM 6); 2010 Dec. 10–12; Perth (Australia).

ABSTRACT

This thesis focuses on the investigation of the effect of flowing medium on the transient response of a pipe due to dynamically applied loading. The topic is very important in many industrial and military applications including offshore structures, oil and gas, power stations, petrochemical and defence industries where critical pipe components transporting a gas or liquid can be subjected to impact loading due to an accident. In many previous studies, such effects were largely ignored, simplified or considered negligible. The conducted study demonstrated that in many practically important cases, the influence of flowing medium on transient response is not small and has to be taken into consideration.

In the current work, the classical Bernoulli-Euler beam theory is adopted to describe the dynamic behaviour of an elastic pipe and a governing equation of a slender pipe transporting gas or liquid was derived. This governing equation incorporates the effects of inertia, centrifugal and Coriolis forces due to the flowing medium. This equation can be normalised to demonstrate that only two non-dimensional parameters govern the static and dynamic responses of the system incorporating a pipe and flowing medium. Therefore, these non-dimensional parameters can be utilised to investigate various dynamic phenomena using reduced size or scale physical models. Such scale models would be adequate if the values of these parameters were kept the same for the scale model and the real system. This is expected to result in substantial benefits if the experimental approach is adopted for the investigation of the problem under consideration.

The main effort in this thesis is devoted to the development of an analytical procedure utilising the perturbation method and numerical approach adopting a central finite-difference scheme to analyse the dynamic response of the system due to impulsively applied loadings. This is then followed by a validation study against previously published data as well as between both approaches, analytical and numerical. Further, a detailed investigation was carried out on the effects of the flowing medium on the

transient response. It revealed two principally different types of behaviour of a pipe subjected to impulse loading: stable decay and unstable associated with so-called pipe whip.

Special attention is given to the above phenomena, pipe and flow characteristics, which cause growing unlimited displacements of the pipe regardless of how small the value of the applied loading is. Experiments were also conducted to support the theoretical results and were found to follow the theoretically predicted tendencies. The developed theoretical methods provide a framework for analysis of many other dynamic problems of pipes with flowing media subjected to arbitrary boundary and loading conditions. Lastly, the overall conclusion of the conducted research was provided and future work was identified for further investigations, which follows from the obtained results.

CONTENTS

LIST OF FIGURES

LIST OF TABLES

GLOSSARY

Nomenclature

λ_f	density of the flow per unit length (kg/m)
λ_p	pipe density per unit length (kg/m)
V	velocity of the , gas or liquid or their mixture (m/s)
E	Young's modulus (Pa)
I	second moment of inertia of the pipe (m^4)
μ	mass per unit length (kg/m)
τ	characteristic time (s)
L	length of the pipe (m)
$\bar{F}(\bar{x}, \bar{t})$	driving force per unit length (N/m)
$F(x, t)$	dimensionless (normalised) function of the position and time
$W(x)$	dimensionless (normalised) displacement
t	time (s)
γ	specific heat ratio of the gas
$\delta(x - u)$	Dirac delta function
ε and β	two parameters
Y_k	a set of normalised eigenfunctions
A_k	normalisation constants
x^*	position along the pipe
Δx	spatial grid size
Δt	temporal grid size
N_x	The upper bounds of the grid point in the spatial direction
N_t	The upper bounds of the grid point in the temporal direction
A	global evolution matrix
I	identity matrix
R	applied loading

CHAPTER 1

INTRODUCTION

1.1 Background and Significance

The purpose of the research presented in this thesis is to investigate the effect of the flowing medium on the transient response of pipes transporting liquid or gas subjected to impulse loading. This will provide a better understanding of the consequences of a failure so that they can be minimised.

Long flexible pipes such as the one shown in Figure 1.1 are used extensively across many industries to transport liquid or gas or their mixtures. The failure rate of gas or oil pipelines differs significantly, with variances in design factors, construction conditions, maintenance techniques, and the environmental situation.

Figure 1.1: Typical aboveground pipeline in Australian outback

The European Gas Pipeline Incident Data Group presents an overall failure rate of 0.575 per 1000 kilometres/year based on the experiences over $1.47 \ 10^6$ kilometres/years of on-shore gas pipelines [1]. A survey of 185 accidents involving natural gas [2] showed that, of the total, 131 were caused during transportation, by road, railway, ship or pipeline. The analysis of these data clearly shows the relatively high frequency of accidents in pipes: 127 of them occurred in piping systems. The most frequent causes of the accidents were mechanical failure, impact failure, human error and external events. Amongst the accidents arising from impact failure (39 accidents), the most frequent specific cause was excavating machinery (21 accidents), followed by vehicles (5

accidents) and heavy objects (5 accidents). Other specific causes due to external events were ground subsidence (4 accidents) cases and sabotage/vandalism (4 accidents) cases.

Failures from impact loading often caused by third party mechanical interference can be immediate or may occur sometime later due to fatigue. This type of failure is likely to have severe consequences. Historically, some of the most serious pipeline accidents resulting in ruptures have been caused by such incidents. In general, failure of the pipeline can lead to various outcomes; some can pose a significant threat of damage to people and properties in the immediate vicinity of the failure location.

Prior to the recent release of AS 2885.1-2007, Australian pipeline standards mandated burial for all cross-country pipelines carrying gas. The reason was not stated explicitly but would appear to be related to the hazard of pressure in a fluid that could lead to devastating consequences if an aboveground gas line were to rupture. The 2007 revision of AS 2885.1 includes a new section (5.8.3) on 'Pipeline with reduced cover or aboveground', which makes it clear that pipelines may be installed aboveground. The reason for this revision was probably motivated by economical considerations, as aboveground gas pipelines can offer significant benefits while posing relatively low risks. Some gas producers are interested in application of aboveground gas lines so that they could have this option available for production flowlines in remote areas. Hence, the issues surrounding safety and dynamic behaviour of aboveground gas pipelines are very important, specifically for Australia.

On the other end of the structural length scale, various sensor technologies have been develop recently based on in micro-pipes carrying fluid. These technologies involve the use of dynamic measurements. Therefore, there is now a growing interest in studying the transient response of pipes with flowing media caused by dynamic loading.

The behaviour of pipes subjected to dynamic loading has been extensively studied in the past, through analytical, numerical and experimental approaches [15-82]. Many previous studies were focused on the development of theoretical techniques for investigation of linear or non-linear dynamic response within simplified one-dimensional models [17, 33, 35, 59]. However, not many investigations were focused

on the effect of the flowing medium on the dynamic response of pipes. The flowing medium can produce substantial forces on the pipe walls and affect the dynamic response of the whole structure, and at the same time, the pipe response, in turn, can change the flow characteristics in a very complicated manner. Due to the complex coupling of fluid-structure interactions, it is not surprising that in many previous theoretical works that have focused on the impact loading of pipes, the internal flow effects were simply ignored or only partially incorporated into the governing equations, utilising oversimplified assumptions. For example, a number of published theoretical one-dimensional models describe the effects of the transported liquid by means of an attached mass model in which an additional mass is distributed along the pipe with the linear density equal to the one of the liquid [35,44]. The distributed mass is then introduced into the corresponding governing equations. Such simplification could be adequate if the flow velocities and rates of loading are comparatively low; however, at higher flow speeds or rates of loading, such theoretical models can produce large errors in the quantitative assessment of the pipe transient behaviour when it is subjected to dynamically applied loading. For the same reason, which is complexity of the mechanisms governing the transient response, there were no numerical attempts or experimental studies, to focus on the effect of the flowing medium on the transient behaviour of pipes.

The possible large errors in theoretical predictions of pipe response to dynamic loading are not the only reason behind the proposed study. Another major concern, if one disregards the effect of the internal flow in pipes, is that many critical (from a safety point of view) phenomena could be completely neglected, leading to incorrect design decisions. For example, the existence of critical values of the flow was demonstrated, such as flow density and speed, at which any small external disturbance leads to growing unbounded deflections of the pipe. Such behaviour is linked to the dynamic instability of pipes with flowing medium. This behaviour is seen familiarly in the chaos caused by an unrestrained garden hose with running water under relatively high pressure, phenomena called pipe whip. For example, in the case of a full bore failure of an aboveground pipeline, the pipe whip can represent a potential threat to structures and people in the vicinity of the pipeline. Therefore, when designing aboveground pipelines,

the possible instability mechanisms have to be avoided or some special measures have to be undertaken to avoid or minimise the consequences of pipe failures.

The main objective of the thesis is the analytical, numerical and experimental investigation of the effects of the flowing medium on the transient response of a circular pipe carrying gas or liquid, which are subjected to impact loading. These effects can be very important in modern high-pressure pipelines, which now, in accordance with the Australian standards, are permitted to be constructed above ground. Indeed, the potential energy density accumulated in such pipelines is comparable with the energy of some explosive substances. The research will provide a better understanding of the consequences of a failure so that they can be minimised. Further, an attempt is made to provide a theoretical basis for the development of design criteria that avoid possible unstable behaviour of pipes in the case of an accident.

1.2 Aims and Objectives

The overall objective of this research project is to investigate, using analytical, numerical and experimental approaches, the effect of the flowing medium on the transient response of a pipe transporting gas or liquid and subjected to impact loading.
In order to achieve this objective, the following specific aims were formulated for the project:

- Aim 1: Derive simplified governing equations of a pipe model with flowing gas or liquid subjected to external loading.

- Aim 2: Develop an analytical procedure for analysis of the flowing medium effects on the transient response of a pipe, which utilises the perturbation approach. This approach is expected to be accurate at relatively small influence of the internal flow on the overall response.

- Aim 3: Develop a computational tool adopting the central finite-difference scheme for determining the dynamic response of a pipe with flowing medium subjected to arbitrary dynamic load.

5

- Aim 4: Validate the developed theoretical approaches against known analytical and numerical solutions.

- Aim 5: Using analytical and numerical approaches, analyse the dynamic response of a pipe transporting liquid or gas and estimate the internal flow effects.

- Aim 6: Investigate critical parameters of the internal flow leading to the initiation of pipe instability. Estimate the effect of support conditions and develop simple criteria avoiding the initiation of dynamic instability.

- Aim 7: Design an experimental rig for studying the transient response of pipes with flowing medium subjected to impact loading.

- Aim 8: Conduct experimental investigations on the effect of the internal flow on the transient response of pipes transporting liquid.

1.3 Outline of Thesis

The remainder of this thesis is structured as follows. Chapter 2 provides an in-depth critical literature review of the previous research related to the current research topic. This includes a review of major previous studies of the transient response of pipes with and without flowing media and pipes subjected to low speed impact. Due to the great number of articles on the topic, this review is restricted to a summary of the current state of the art in this area including main results and general analytical, numerical and experimental approaches to analysis of such types of problems.

Chapter 3 introduces the governing equation of a long flexible pipe with flowing medium that takes into account the forces generated by the internal flow due to inertia, centrifugal and Coriolis accelerations. Due to the approximate nature of the mathematical modelling, a number of assumptions and simplifications have to be introduced. It is assumed, for example, that the flow velocity and density in the pipe are not affected by the pipe transient response but the pipe itself is subjected to the

additional external forces as a result of the pipe lateral deflections that change the flow direction. Small and, hence, linear deformations are also assumed in the pipe as well as all assumptions utilised in the classical Bernoulli-Euler beam theory. Thus, there is no consideration of plastic deformation, fracture or other phenomena that might accompany the impulse loading of pipes. Further, a scaled transformation of variables is conducted to demonstrate that only two dimensionless parameters affect the transient response. These parameters represent dimensionless combinations of the elastic properties of the pipe, pipe geometry and flow characteristics. In the case of a small influence of the flowing medium on the overall mechanical response of the whole system, the governing equation can be solved using an analytical approach, which is based on the standard perturbation technique. Several examples demonstrating the effectiveness of this approach for particular problems are considered in detail. The asymptotic approach developed in this chapter can be generalised relatively easy for other boundary conditions as well as for arbitrary applied loading.

Chapter 4 presents a numerical method using central finite-differences scheme. In this chapter, the consideration is given to validate the earlier developed analytical approach and the numerical method against published results and classical solutions. Further, as expected, both the approaches, asymptotic and numerical, produce essentially the same results in situations in which the internal flow has a small influence on the mechanical response; for example, this happens at low flow speeds or large moments of inertia of the pipe.

As mentioned above, only two dimensionless parameters fully control the transient response of the system within the adopted assumptions and simplifications. In Chapter 5, a comprehensive investigation of the effect of the flowing medium on the dynamic response of pipes is conducted. Special attention is paid to the conditions that initiate dynamic instability associated with pipe whip phenomena. A simple criterion to avoid such dangerous behaviour is proposed and can be used in the design of aboveground pipelines.

In Chapter 6, a rig is described for experimental investigation of the effect of flow parameters on the dynamic response of circular pipes. The rig essentially represents

encastre pipe with water flowing through it. A laser sensor was used to measure the deflection at the mid-point of the pipe which was impacted by a load cell device. This chapter also presents the results of the experimental investigations followed by a discussion.

Finally, Chapter 7 presents the overall conclusions of the conducted research, along with recommendations for future work.

CHAPTER 2

BACKGROUND AND LITERATURE REVIEW

2.1 Introduction

The aim of this chapter is to provide a general overview of problems, methods and solutions related to the dynamic behaviour of long flexible pipes transporting liquid or gas. A substantial number of sources were reviewed and a brief summary will be provided here. This literature review is comprised of several sections covering various aspects of dynamic behaviour of long flexible pipes having circular cross-sectional area. The present chapter is not intended to provide a comprehensive review of problems and complex phenomena associated with dynamic behaviour of pipes, specifically, vibration and vibration control of pipes conveying gas or liquid, curved pipes and pipes of non-circular cross-section. Instead, it focuses on specific issues that are important for the current study.

Pipes are widely utilised in many industries and across many applications [3] to transport, process, transmit and store fluids and materials that, sometimes, can be hazardous, volatile and flammable. For example, in oil and gas installations (whether on-shore or offshore) circular pipes are commonly used for the conveyance of either crude or products. An accident leading to the loss of the pipe integrity could pose a serious threat to property, environment and people in the close vicinity of the accident location [4]. Therefore, it is not surprising that there were many investigations conducted in the past two decades that are related to the dynamic behaviour, safety and integrity of pipelines and pipe systems [5].

The importance of safety and integrity issues associated with pipelines and pipe systems was highlighted by a number of very serious accidents in the past [6–12]. Figure 2.1 illustrates an example of a pressurised piping system that is in close proximity to mechanical, electrical and electronic equipment and instruments of a power generation aggregate [13]. Mechanical damage to the pipe system could result in a disastrous consequence and severe damage to the power generator and the personnel.
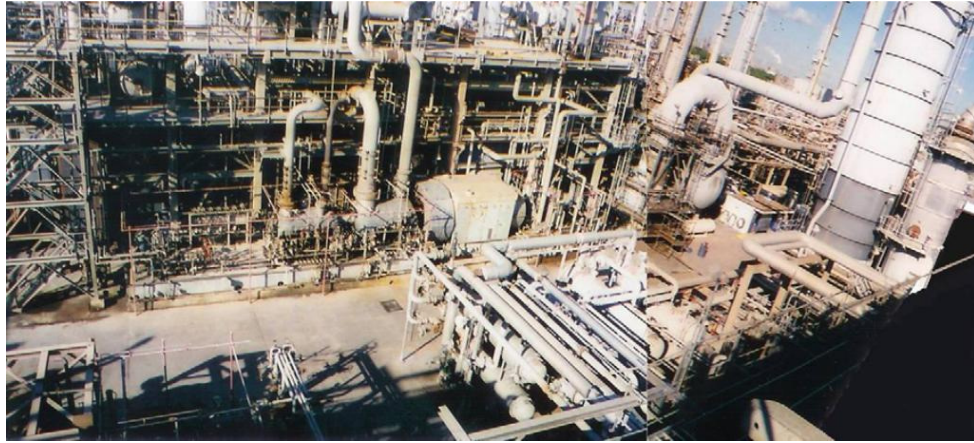
Figure 2.1: The close proximity of piping system to mechanical and electrical equipment in a power generation aggregate [13]

Another typical example is a petrochemical industrial plant, which often incorporates thousands of pipes for various technological purposes, which can potentially fail due to many reasons. The cost of such failures is often much greater than the cost of the initial failed component. Consequences of a pipe failure on the petrochemical plant are shown in Figures 2.2a and 2.2b. These figures display images of the aftermath of an accidental toxic vapour cloud that was discharged following a failure of a pipe component. The initial failure resulted in an explosion that was followed by a series of other explosions that resulted in a US$1.5 billion loss and 23 deaths at the facility [13].

Figure 2.2a: Accidental release of toxic vapour [13]

Figure 2.2b: Aftermath of an accident [13]

As part of the safety precaution measures, effective protection solutions against possible impact loading have to be implemented to any potentially dangerous piping system or pipeline. Subsequently, safety engineers or safety authorities have to demonstrate the proper and adequate design strength not only against quasi-static loading but also in the case of abnormal events such as that caused by impact loadings because this sort of loading is rather frequently found in practice. It can be associated with accidents such as collision with a moving object, struck by a falling object or acts of vandalism.

Numerous surveys carried out on high-pressure pipelines have confirmed that that the impact loading is one of the main reasons of heavy accidents. It is interesting to note that although the accidents due to impact loading are less frequent than, for example, accidents due to mechanical failure, the most serious pipeline accidents [14] resulting in high financial, property or human life losses have been caused by incidents associated with impact. Amongst the accidents arising from impact failure, the most frequent were machinery accidents, followed by vehicles and heavy objects. Other specific causes of such accidents due to external events were ground subsidence and acts of sabotage/vandalism.

The purpose of the current project is to gain a further understanding of dynamic behaviour of pipes under impulse loading (impact-like loading). The study is focused on the investigation of the effects of the internal flow on the dynamic response of pipes,

which was often ignored in many previous studies. Special attention is given to the condition leading to dynamic instability of pipes. Such conditions can occur during an accident resulting in a full bore fracture of a high-pressure pipeline with a relatively small diameter. In this case, the pipe transporting gas or liquid can become unstable and generate substantial damage due to chaotic movements, similar to what almost everyone has experienced when watering a garden with an unrestrained hose. The next section will provide a brief review of simplified one-dimensional theories of pipes based on Bernoulli-Euler assumptions, which will be also utilised and further extended in the current study.

2.2 Bernoulli-Euler Beam Equation

This section will begin with considerations of the classical Bernoulli-Euler beam theory, which is the most popular theory for modelling the transient response of long flexible structures. Many previous studies utilised this theory and many interesting results have been obtained in the past. It was also demonstrated in many previous studies that for sufficiently flexible structures it provides an excellent correlation with experimental results. The Bernoulli-Euler beam theory will be further extended and utilised to model effects of the internal flow on the transient response of pipes.

2.2.1 Review of Bernoulli-Euler Beam Theory and Its Modifications

The Bernoulli-Euler beam theory can be formally derived from the classical linear theory of elasticity using well-developed asymptotic techniques, energy or variational approaches. In general, the theory provides a way to calculate the load-carrying capacity and dynamic deflections of long and flexible beams subjected to various support conditions. Bernoulli-Euler beam theory is also known as simplified beam theory or classical beam theory or engineer's beam theory. This theory can reasonably be applied only for the laterally loaded beams without taking into account the sheer deformation in

the material in contrast to more complicated theories, such as Timoshenko beam theory, which will be briefly discussed later in this chapter. The Bernoulli-Euler beam theory relates to the case of small lateral deflections, which must be much smaller than the characteristic size of the cross-sectional area. The out-of-plane (or transverse) displacement $W(x)$ of a statically loaded beam is described within the Euler-Bernoulli beam theory by the following ordinary differential equation:

$$\frac{d^2}{dx^2}\left[EI\frac{\partial^2 W}{\partial x^2}\right] = p \tag{2.1}$$

where p is the distributed loading (force per unit length) acting in the same lateral or transverse direction as W, E is the Young's modulus of the beam's material (in Pa), and I is the area moment of inertia of the beam's cross-section (in m^4). If E and I (or product of these variables) do not vary with x along the length of the beam, then the beam equation simplifies to the especially simple form:

$$EI\frac{\partial^4 W}{\partial x^4} = p \tag{2.2}$$

which is well known from many engineering textbooks.

This formulation also assumes that the internal damping, externally imposed tension, inertia and pressurisation effects are either absent or can be neglected in comparison with the elastic restoring reaction of the beam under the applied external loading [15,16,17].

The quasi-static theory can be generalised immediately to the case in which the inertia force is not negligible. In this case, the transient deflections, $W(x,t)$ of a long flexible beam will be described by the following partial differential equation (PDE), which incorporates the inertia term (the second term on the left side of the equation below) as

$$EI\frac{\partial^4 W(x,t)}{\partial x^4} + \mu\frac{\partial^2 W(x,t)}{\partial t^2} = F(x,t) \qquad\qquad (2.3)$$

where $W(x,t)$ is already a function of x and t. The first term represents the flexural elastic restoring force and the second term is the lateral inertia force of the beam, where μ is the mass per unit length of the beam (in kg/m). The right-hand side term $F(x,t)$, F is a function of span location and time; it represents the external applied force per unit length (in N/m). In the above equation x is the spatial coordinate along the length of the beam, and t is time. The origin of the coordinate system and time can be selected arbitrary and does not affect the solution of this equation.

Many studies utilised the Bernoulli-Euler beam theory to investigate the dynamic response of beam due to transversely moving point mass [18]. These studies were strongly motivated by the rail industry demands and other industrial applications. In this case, the governing equation can be written in the following form:

$$EI\frac{\partial^4 W(x,t)}{\partial x^4} + \mu\frac{\partial^2 W(x,t)}{\partial t^2} = F\delta(x - u) \qquad\qquad (2.4)$$

where F is the intensity of the applied point force and $\delta(x - u)$ is the ordinary Dirac delta function. The product of the intensity and Dirac function represents the moving point mass at location $x - u$, which also changes with time. For example in [18], the effect of the force travelling velocities, boundary conditions and the ratio of the moving mass to the mass of beam on the dynamic and vibration response of the beam were comprehensively studied.

The Bernoulli-Euler beam framework was subsequently utilised to develop more complicated formulations for analysis of the transient behaviour of long flexible beams [19] incorporating damping. An example of extension of the classical beam theory with linear damping can be written as:

$$EI \frac{\partial^4 W(x,t)}{\partial x^4} + \mu \frac{\partial^2 W(x,t)}{\partial t^2} + c \frac{\partial W(x,t)}{\partial t} \equiv F(x,t) \qquad (2.5)$$

In this equation (2.5), the third term represents damping with c is a positive constant characterising the damping effect; c in this equation in (kg/ms).

The Bernoulli-Euler beam theory was also extended to long flexible pipes having an internal flow of gas or liquid. The linearised equation of motion for a horizontal pipe conveying fluid in the case of negligible damping can be written as:

$$EI \frac{\partial^4 W}{\partial x^4} + MU^2 \frac{\partial^2 W}{\partial x^2} + 2MU \frac{\partial^2 W}{\partial x \partial t} + (M+m) \frac{\partial^2 W}{\partial t^2} = F(x,t) \qquad (2.6)$$

where M is the mass of fluid per unit length, flowing with a steady flow velocity U, m is the mass of the pipe per unit length, W is the lateral deflection of the pipe, x and t are the spatial coordinate and time, respectively; and the right-hand side term is $F(x,t)$ represents the external dynamic loading. The various terms in the above equation can be identified, sequentially, as the flexural restoring force, a centrifugal force, a Coriolis force, and the inertia force. This equation represents the simplest governing equation taking into account the effect of the internal flow on the structural response of the system (pipe–internal flow) [20]. Formally, this equation can also be further extended [21] to incorporate the viscous damping effects, for example, as follows:

$$EI \frac{\partial^4 W}{\partial x^4} + MU^2 \frac{\partial^2 W}{\partial x^2} + 2MU \frac{\partial^2 W}{\partial x \partial t} + (M+m) \frac{\partial^2 W}{\partial t^2} + c \frac{\partial W}{\partial t} = F(x,t) \qquad (2.7)$$

The equation (2.7) was used in [21] to investigate the transient vibrations of a fluid-conveying pipe. The results from experimental and numerical simulations demonstrated that Coriolis force may have a significant damping effect at moderate flow velocities and the damping of the flow in a pipe can be effective and may have potential in engineering applications as a vibration controller. It was also demonstrated that the

damping effect may be exploited to control the vibration of a light and resonant structure, if the pipe carrying the fluid is used as a controller in a cantilever pipe.

Another simplified model was developed to incorporate the axial tensile forces. When such forces are significant, the motion of a pipe can be described by the following fourth order partial differential equation (PDE):

$$EI\frac{\partial^4 W}{\partial x^4} - \left(T_o - M_f U^2\right)\frac{\partial^2 W}{\partial x^2} + 2M_f U\frac{\partial^2 W}{\partial x \partial t} + \left(M_f + M_p\right)\frac{\partial^2 W}{\partial t^2} = 0 \qquad (2.8)$$

where T_o the effective axial force representing the combined effect of an initially imposed force T_o, which will be negative when it is compressive. The effect of the fluid flow produces a centrifugal force due to curvature of the span, and a Coriolis force due to combined flow and rotation of the fluid elements. The centrifugal force is equivalent to a compressive end load, and in vibration problems leads to the reduction of the natural frequencies of the pipe. The Coriolis force causes an asymmetrical distortion of the classical mode shape. The last equation is based on the assumptions that the dynamic deflections are small so that only linear terms are significant. The other assumptions are that mass densities are uniform, transverse shearing and damping are negligible and the fluid velocity and pressure are constant along the pipe.

In [22], the effect of fluid velocity on buckling instability of a pipe with the cantilever-type boundary conditions was investigated. The effect of the axial load P, was analysed utilising the following governing equation:

$$EI\frac{\partial^4 W}{\partial x^4} + (MU^2 + P)\frac{\partial^2 W}{\partial x^2} + 2MU\frac{\partial^2 W}{\partial x \partial t} + (M + m)\frac{\partial^2 W}{\partial t^2} = 0 \qquad (2.9)$$

where, as previously, the first term describes the flexural elastic restoring force, the second term the centrifugal force term together with the effect of axial compression, the third tem takes into account the Coriolis force and the fourth—the inertia term. This

study revealed that flutter or divergence instability may occur, depending on the combination of velocity and axial loading.

There was also an interest to study the stability of a tensioned clamped-pinned pipe conveying fluid. [23]. The study has proven that for small fluid velocities, the pipe is stable. The pipe loses stability by divergence at relatively high fluid velocities. The equation of motion governing the lateral in-plane motion of the pipe without internal and external fluid as a function of the axial distance, x and time, t, [23] it was taken in the following form:

$$EI \frac{\partial^4 W}{\partial x^4} + T \frac{\partial^2 W}{\partial x^2} + m_r \frac{\partial^2 W}{\partial t^2} = F_{int}(x,t) + F_{ext}(x,t), \qquad (2.10)$$

where EI is the bending stiffness of the pipe, m_r is the mass of the pipe per unit length, T is a prescribed axial tension, $F_{int}(x,t)$ and $F_{ext}(x,t)$ are forces acting on the pipe from inside and outside, respectively. The internal fluid flow is approximated as a plug flow, as if it were an infinitely flexible rod travelling through the pipe, all points of the fluid having a velocity U relative to the pipe. This was accepted as a reasonable approximation for a fully developed turbulent flow profile [24].

2.2.2 Influence of Shear Deformations

The effects of shear deformation, which are neglected in the classical beam theory, have been extensively investigated in literature. The Timoshenko's beam theory, for example, can be used to allow for the effect of transverse shear deformation and constitutes an improvement over the standard beam. A numerical example for the supported-clamped pipe was considered by Huang [25]. The influence of rotary inertia, shear deformations, internal dissipation (the dissipation in this work was simulated within Kelvin-Voigt model) on the dynamic response of pipes transporting fluid were studied by Bratt [26]. Stack et al. [27] and Lin and Tsai [28] presented a finite element (FE) approach for non-linear vibration analysis of Timoshenko pipes conveying fluid.

18

The results of the simulations were partially validated using data from experimental studies available in the literature.

A vast majority of the previous studies on the investigation of the effect of shear deformations on the transient response of pipes utilised the Timoshenko theory of beams subjected to transverse loading and were conducted using computer-based techniques. Considering an elastic Timoshenko beam of length L, uniform cross-section area A, and moment of inertia I, subjected to specified boundary conditions at the left and right ends of the beam and applying Hamilton's principle, one can derive the coupled Euler–Lagrange governing equations in the absence of body forces as

$$kG\left(\frac{\partial^2 W(x,t)}{\partial x^2} - \frac{\partial \psi(x,t)}{\partial x}\right) - \rho\frac{\partial^2 W(x,t)}{\partial t^2} = 0 \qquad (2.11a)$$

$$EI\frac{\partial^2 \psi(x,t)}{\partial x^2} + kGA\left(\frac{\partial W(x,t)}{\partial x} - \psi(x,t)\right) - \rho I\frac{\partial^2 \psi(x,t)}{\partial t^2} = 0 \qquad (2.11b)$$

where $W(x,t)$ is the transverse deflection function and $\psi(x,t)$ the slope of the deflection curve due to bending. Parameters E, G and ρ represent the Young's modulus, the shear modulus, and the material mass density, respectively; k represents the Timoshenko shear coefficient that is introduced to account for the geometry-dependent distribution of shear stress. One can rewrite the above system of PDEs as a fourth order single PDE.

Chao et al. [29] developed a set of coupled-non-linear PDEs of motion for pipes with flowing medium using the continuity and momentum equations of unsteady flow as well as Timoshenko beam theory. However, the governing equations are too complicated to allow any analytical solution or simple analysis of various effects. They will not be given here.

Timoshenko beam theory was implemented to study the transient response and stability of relatively pipes transporting fluid by Pramila et al. [30]. The hydro-elastic stability of short simply supported pipes was studied by Tani and Doki [31] also within

Timoshenko beam theory. These researchers investigated the effects of shearing loads and support conditions on the dynamic behaviour. It was demonstrated that an increase in the shearing load reduces the critical velocity leading to pipe instability and raises the number of the corresponding hoop waves. A change of the boundary conditions was found to influence significantly the short pipe dynamics. The dynamics and stability issues of short pipes were re-examined by means of Timoshenko beam theory for pipes and a three-dimensional fluid-mechanical model for the fluid flow [32, 33]. These short pipes were subjected to clamped-clamped or cantilever-type boundary conditions.

2.2.3 Mechanics of Non-linear Problems

The linear models were found incapable of describing dynamics of pipes with flowing medium when the flow velocity approaches a critical value leading to static or dynamic instability [34]. The non-linear dynamics of pipes transporting liquid or gas and subjected to various boundary conditions has been investigated extensively in recent years due to wide applications of the relevant problems in many industrial situations, such as heat exchangers, nuclear reactor piping, power stations and pipelines.

The non-linear equations of pipes with flowing medium are normally derived using the Hamilton's principle or from Newton's second law. An example of a non-linear governing equation derived by Semler et al. [35] in a relatively simple form is given below. It is based on the energy and Newtonian methods and can be written in the following form:

$$\frac{\partial^2 \eta}{\partial \tau^2} + \frac{\partial^4 \eta}{\partial \xi^4} + \alpha \frac{\partial^5 \eta}{\partial \tau \partial \xi^4} + u^2 \frac{\partial^2 \eta}{\partial \xi^2} + 2u\sqrt{\mu} \frac{\partial^2 \eta}{\partial \tau \partial \xi} + \gamma \frac{\partial \eta}{\partial \xi}$$

$$+ \left(\frac{\partial \eta}{\partial \xi}\right)^2 \left(u^2 \frac{\partial^2 \eta}{\partial \xi^2} + 2u\sqrt{\mu} \frac{\partial^2 \eta}{\partial \tau \partial \xi} + \frac{\gamma}{2} \frac{\partial \eta}{\partial \xi}\right)$$

$$+ \left(1 + \alpha \frac{\partial}{\partial \tau}\right) \left(\frac{\partial^4 \eta}{\partial \xi^4} \left(\frac{\partial \eta}{\partial \xi}\right)^2 + 4 \frac{\partial \eta}{\partial \xi} \frac{\partial^2 \eta}{\partial \xi^2} \frac{\partial^3 \eta}{\partial \xi^3} + \left(\frac{\partial \eta}{\partial \xi}\right)^3\right)$$

$$+\left(\sqrt{\mu}\frac{\partial u}{\partial \tau}-\gamma\right)(1-\xi)\left(1+\frac{3}{2}\left(\frac{\partial \eta}{\partial \xi}\right)^2\right)\frac{\partial^2 \eta}{\partial \xi^2}$$

$$-\frac{\partial^2 \eta}{\partial \xi^2}\left(\int_{\xi}^{1}\int_{0}^{\xi}\left(\left(\frac{\partial^2 \eta}{\partial \tau \partial \xi}\right)^2+\frac{\partial \eta}{\partial \xi}\frac{\partial^3 \eta}{\partial \xi \partial \tau^2}\right)d\xi d\xi\right.$$

$$+\int_{\xi}^{1}\left(\frac{1}{2}\sqrt{\mu}\frac{\partial u}{\partial \tau}\left(\frac{\partial \eta}{\partial \xi}\right)^2+2u\sqrt{\mu}\frac{\partial \eta}{\partial \xi}\frac{\partial^2 \eta}{\partial \tau \partial \xi}+u^2\frac{\partial \eta}{\partial \xi}\frac{\partial^2 \eta}{\partial \xi^2}\right)d\xi\left.\right)$$

$$+\int_{0}^{\xi}\left(\left(\frac{\partial^2 \eta}{\partial \tau \partial \xi}\right)^2+\frac{\partial \eta}{\partial \xi}\frac{\partial^3 \eta}{\partial \xi \partial \tau^2}\right)d\xi=0 \tag{2.12}$$

where $\eta = W/L$, W is the lateral deflection of the pipe, L is the pipe length, $\xi = x/L$ is the dimensionless spatial variable, $u = VL/\sqrt{M/EI}$ is the flow parameter, V is the fluid velocity, which can vary with time, EI is the pipe flexural rigidity, $\tau = t\sqrt{EI/(M+m)}/L^2$ is dimensionless time, $\alpha = c\sqrt{EI/(M+m)}/L$, c is the coefficient of Kelvin-Voigt damping of the pipe material, $\mu = M/(M+m)$ is the mass ratio of the linear densities of the pipe and pipe with fluid, and $\gamma = (M+m)gL^3/EI$ is a gravitational parameter.

The first term in the above equation is the linear inertia, the second term is the linear stiffness, and the third term is due to the Kevin-Voigt damping. All terms involving the square the fluid flow speed u^2 are due to the centrifugal force, while those having linear term u are due to the Coriolis acceleration. All terms including γ represent the effect of gravity. The terms in the third line represent the non-linear stiffness due to non-linear curvature; the fifth and the last lines represent non-linear inertial. Terms with time derivative of the flow velocity take into account the unsteady mature of the internal flow. A systematic comparison of the derived equation with previous studies was conducted. However, no quantitative analysis of the governing equation or investigation of the effect of various controlling parameters have been carried out.

The governing equations near the critical fluid velocity above which the lateral deflections become self-excited and unbounded (within the linear theory) were derived by Yoshizawa et al. [36]. The beating phenomena, as predicted by the theory, were observed experimentally at slightly above the critical fluid velocity. Miles et al. [37] demonstrated that as flow through the non-linear stiffened cantilever pipe increases, phase-coupled harmonics of the power-spectral primary frequency grow. For parameters close to those associated with chaotic movements, sub-harmonics become phase coupled to the primary frequency. Cross-bi-spectra indicated that both sum and difference interactions result in non-linear phase coupling and energy exchange between vibration modes.

2.3 Effect of Internal Flow on Dynamic Behaviour of Pipes

The effect of the internal flow on the dynamic behaviour of pipes conveying fluids is essentially based on the interaction of inertia, centrifugal forces and Coriolis forces of the fluid with the pipe structure [38]. The centrifugal and Coriolis forces occur from the fluid flow, while the inertia force is a combination of the fluid and pipes inertias. As mentioned above, the centrifugal force arises from the fluid flowing in a pipe that is curved due to lateral deflection. If the element of the pipe rotates, this rotation generates a gyroscopic or Coriolis force that is proportional to the fluid velocity. From the previous studies, it was highlighted that the Coriolis force has a marked influence on the dynamic pipe behaviour.

Most of the earlier contributions to the dynamics of pipes neglected most of the above mentioned interactions effects. However, later, it was realised that at sufficiently high internal pressure and flow speed in a relatively flexible pipe these effects are significant and can totally change the dynamic or static behaviour of pipes [17,35,39–51]. For example, for a sufficiently high flow velocity, the centrifugal force can overcome the flexural restoring force and the pipe can buckle in its first mode, provided that gravity and external damping are relatively small. This phenomena is also known as divergence

[52,53]. It was also recognised that when the fluid is stationary (the flow speed is negligible or zero) [54], the pipe response as a classical beam to an initial disturbance.

If the centrifugal force in the pipe acts in much the same way as compressive forces in the classical beam theory, the Coriolis force acts to restabilise the pipe after divergence before flutter, or dynamic instability, finally destabilises the whole pipe. Once the pipe becomes unstable, the non-linear effects associated with relatively large pipe displacements become very important and the linear theory is then not applicable beyond this critical flow velocity associated with the initiation of the dynamic instability [55, 56].

The interesting findings are that the pipe systems can be categorised into two types: gyroscopic conservative and non-conservative type system. Gyroscopic conservative systems refer to the pipes not being allowed to move at the downstream end, and it was concluded that such pipes cannot absorb fluid energy. Non-conservative systems take place when the downstream end is allowed to move and fluid energy can be absorbed by the pipe. In the subcritical flow range, the pipe systems of different types response differently. In a gyroscopic conservative system, the Coriolis force does not contribute to damping hence the damping values do not increase because of the increase of flow velocity. In a non-conservative system, the Coriolis force will lead to the generation of dissipation forces for certain modes of pipe oscillation.

Propagation of free harmonic waves in a periodically supported infinite pipe has been studied in [57]. Due to the presence of the Coriolis force from the fluid flowing in a curved path, it was found that the elastic waves travelling in positive and the negative direction propagate at different speeds. As a result of this, no classical deflection modes present in the dynamic response of the pipe.

In simplified beam theories, the centrifugal force acts in the same manner or equivalent to a compressive end load [17]. This can be realised by comparing the governing equation of a pipe taking into account the internal flow,

$$EI\frac{\partial^4 W}{\partial x^4} + MV^2\frac{\partial^2 W}{\partial x^2} + 2MV\frac{\partial^2 W}{\partial x \partial t} + (M+m)\frac{\partial^2 W}{\partial t^2} = 0 \qquad (2.13)$$

with the classical governing equation describing dynamic behaviour of a pipe subjected to a compressive load P at the pipe's ends.

$$EI\frac{\partial^4 W}{\partial x^4} + P\frac{\partial^2 W}{\partial x^2} + m\frac{\partial^2 W}{\partial t^2} = 0 \qquad (2.14)$$

and x, t are the axial coordinate and time, respectively, EI is the flexural rigidity of the pipe, M is the mass of fluid per unit length, flowing from the fixed end to the free one with a steady flow velocity V, m is the mass of the pipe per unit length, and $W(x,t)$ is the lateral deflection of the pipe.

The first term in both equations is the flexural restoring force with $\delta^2 W/\delta x^2 \sim 1/R$, where R is the local radius of curvature. The second term in the former equation is associated with the centrifugal forces as the fluid flows in curved portions of the pipe [24]. The third term is recognised as being associated with the Coriolis acceleration, and the last term represents the inertial effects. In this way, with increasing the flow speed, V, the effective stiffness of the system is diminished, and for sufficiently large V, the destabilising centrifugal force may overcome the restoring flexural force. The resulting divergence is known as buckling or fire-hose instability.

For sufficiently small V, the dynamics of the system is dominated by the Coriolis force $2MV\,\delta^2 W/\delta x \delta t$, and the system is subjected to the flow-induced damping. For sufficiently large V, the centrifugal force $MV^2\,\delta^2 W/\delta x^2$, which may also be viewed as a compressive follower force, overcomes the Coriolis damping effect, and the system can lose stability from single-mode flutter [24].

If the pipe vibrates with periodic motions of period T, it was shown in [58,59,60] that the work done by the fluid on the pipe is equal to:

$$\Delta W = -MV \int_0^T \left[\left(\frac{\delta w}{\delta t} \right)_L^2 + V \left(\frac{\delta w}{\delta t} \right)_L \left(\frac{\delta w}{\delta x} \right)_L \right] dt \neq 0 \qquad (2.15)$$

where $(\delta w / \delta t)_L$ and $(\delta w / \delta t)_L$ are, respectively, the lateral velocity and slope of the free end (for the case of a fixed-free pipe). For small magnitudes of the velocity of the internal flow ($V > 0$), the first term dominates, and the work done is negative; hence, the pipe loses energy to the flowing fluid, and free pipe motions are damped. However, for the high enough velocities, V, the second term will dominate. If the slope and velocity of the free end have opposite signs over a period, or

$$\left(\frac{\delta w}{\delta t} \right)_L \left(\frac{\delta w}{\delta x} \right)_L < 0, \qquad (2.16)$$

then the work done may be positive, and energy flows from the fluid, to the pipe, resulting in amplified oscillations. The fluid is a source of unbounded energy. The opposite-sign characteristic of the free-end slope and velocity corresponds to the dragging and lagging modal form of flutter, observed in experiments and commented in many studies including [61,62,63]. With the situation of $V < 0$, for example an aspirating system, exactly the opposite conclusions may be reached by consideration of the same equation [24].

In [64] it was concluded that in the case of free motions, the pipe absorbs energy from the fluid for all sufficiently small $|V|$ and is therefore subject to flutter. For relatively higher flow speeds $|V|$, the pipe loses energy to the fluid, and hence it is stabilised and its motions are damped. The startling conclusion is that the system is unstable for infinitesimally small $|V|$ or if energy dissipation is taken into account, for very small $|V|$.

2.4 Numerical Techniques

The effect of the flowing medium and stability conditions for circular pipes transporting fluid or liquid has been studied with different numerical approaches, such as the FE method and the spectral element approach. In Langthjem [65], an FE method was developed for a cantilever pipe to investigate the critical conditions when pipe loses stability and experience chaotic movements. The FE method was used by Liang and Tang [66] to examine the dynamic response and stability issues of simply supported pipe. Shizhong and et al. [67], Wang et al. [68], Cui and Tani [69] and Hongwu and Junji [70], used FE to solve the solid-liquid coupling damping matrix and a symmetrical solid-liquid coupling stiffness matrix. The first several natural frequencies of pipes were determined.

Another popular method, a spectral element approach, is often used to predict the flow-induced vibrations accurately. Lee and Oh [71] developed a spectral element model that was formulated from the exact wave solution of the governing equations. It was claimed that the spectral element approach provide much better accuracy in comparison with FE for the uniform pipes regardless its length. Later, Lee and Park [72] derived coupled governing equations for a pipe transporting liquid using Hamilton's principle and the classical governing equations of uncompressible fluid. The obtained non-linear equations were liberalised about the steady-state solution using the frequency-domain approach for the linearised equations.

Stein and Tobriner [73] presented a numerical solution to the governing equations of a pipe conveying fluid and resting on an elastic foundation. An ideal gas and infinite pipe approximations were utilised by Mizoguchi and Komori [74] to investigate the vibration and stability of pipes. This study took into consideration the effect of the fluid boundary layer. The frequencies of pipes were obtained for a wide range of the internal flow velocities ranging from 10 m/s to Mach 3.

Wang and Bloom [75] formulated an analytical model to study the dynamics of submerged and inclined concentric pipes of different length and subjected to different boundary conditions. The discretised dynamic equations were solved numerically.

Lee and Chung [76] suggested a non-linear approach for a clamped-clamped pipe transporting fluid using the classical Euler-Bernoulli beam theory described in the previous section of this chapter and the non-linear Lagrange strain theory. Similar to the previous study, the governing equations were discretised, linearised and solved numerically. Yang and Jin [77] applied the Galerkin method with improved truncation term and Maalawi and Ziada [78] presented a mathematical model for a pipeline composed of uniform modules. As a case study, the developed model was applied to a simply supported pipeline consisting of two and more modules.

The influence of stochastic uncertainties of flexible cantilever pipe material properties, such as Young's modulus, densities was investigated by Ganesan and Ramu [79]. The statistical information was presented in terms of average values, variance and autocorrelation functions. The stochastic equations were solved for the moments of characteristic values and effect of the stochastic uncertainness on the dynamic behaviour was investigated.

2.5 Experiments Investigations of Pipes subjected to Impact Loading

Many experimental studies have been conducted in the past investigating various aspects of pipe integrity and pipe behaviour under dynamic and impulse loading. Many of these studies were driven by industry or military applications. The purpose of this section is to provide a brief overview of key studies focusing on the development of test equipment.

A - FRAME

B - GUIDES

C - DROP WEIGHT

D - SPECIMEN

E - CLAMPING FIXTURE

F - PHOTO CELL

G - ACCELEROMETER

H - L.V.D.T

I - TABLE

VIEW A

SPAN

VIEW A
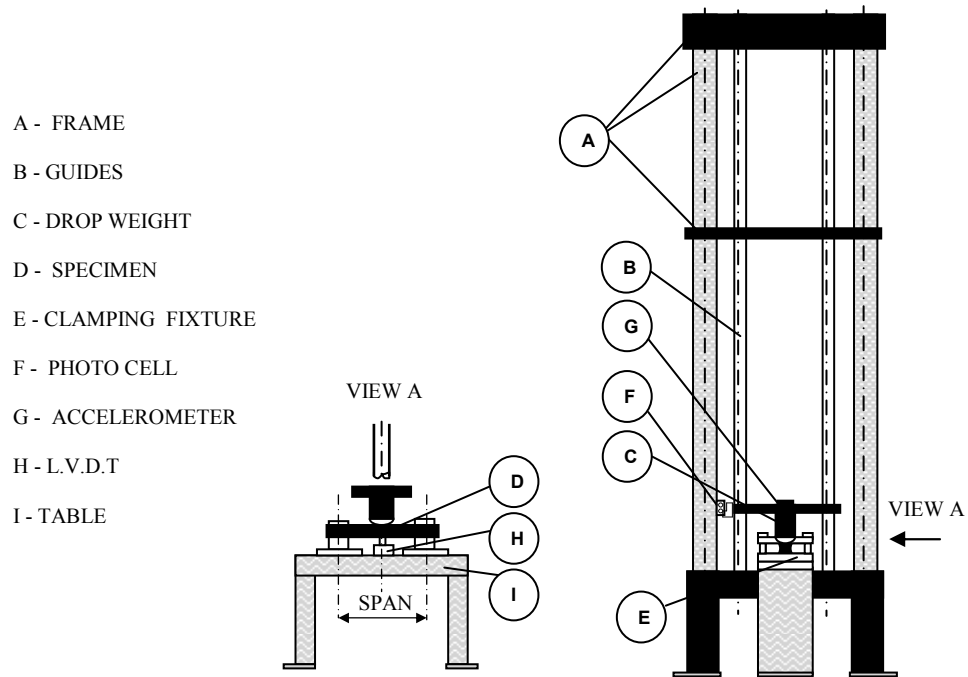
Figure 2.3: Setup of drop-weight impact test [80]

In the laboratory environment, the simulation of impact loading ranges from low velocity drop-weight tests to high velocity ballistic missile tests. For example, the experiment conducted in [80] studied impact response of pipes by setting up a drop-weight test to simulate low velocity impact. The test setup, shown in Figure 2.3, included an instrumented drop weight and data acquisition system. The aims of the experimentations were to relate the mechanical behaviour of the pipe to the loss of kinetic energy of the impactor under low velocity loading conditions. It also aimed to build a standardised test method for low velocity impact studies, since at that time, there were no acceptable standard testing procedures for pipes [80].

A quasi-static behaviour of buried pipelines under localised radial (impact-like) loading was undertaken in [81]. This study was motivated by numerous accidents during pipe excavation. The pipelines were pressurised and radial impulse contact loads were applied on the pipe. This study shows that the response of flat plates can approximate the mechanics of local indentation of pressurised pipes when the indenter is of small in comparison to the diameter of the pipeline. However, the results of this experimental study are limited by the small range of considered geometries and loading condition.

28

In a number of experimental and theoretical papers, it was demonstrated that the structure-fill medium interactions significantly influence the dynamic behaviour. An experimental study carried out indicated that the critical perforation energy and deformation of the wall of the pipes were significantly influenced by the presence of the fluid (water) and fluid pressure [4]. Figure 2.4 depicts the experimental setup.
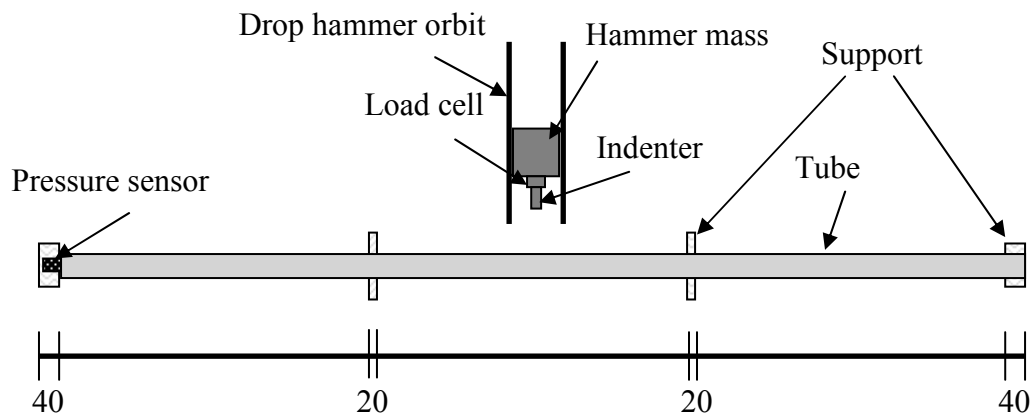
Figure 2.4: Schematic arrangement for the impact test on pressurised pipes [4]

The experiment reported that irrespective of pipe thickness, the limit perforation energy of empty pipes was greater than that filled with water. When the thin wall tube was filled with water and not pressurised, the limit perforation energy dropped by 20–30%, but the energy drop in thick wall tubes are smaller. Figure 2.4 is referred and stated that the ballistic limit of the tubes impacted by a hemispherical-nose indenter is greater than that of the tubes impacted by the blunt and conical ones under the same impact conditions. The thickness of the wall is also an important parameter in perforation of the tube wall with the ballistic energy of the thick wall tube about three times that of the thin-walled pipes. The fill liquid tends to retain the circular shape of the pipe walls and localised the impact point. This change may lead to an increase of the perforation limit.

The experimental studies on pipes with flowing medium were conducted mainly with rubber pipes conveying water or air and with very thin-walled metal pipes conveying oil. The experiments were also extended to a cantilever pipes fitted with various nozzles at the free end [82].
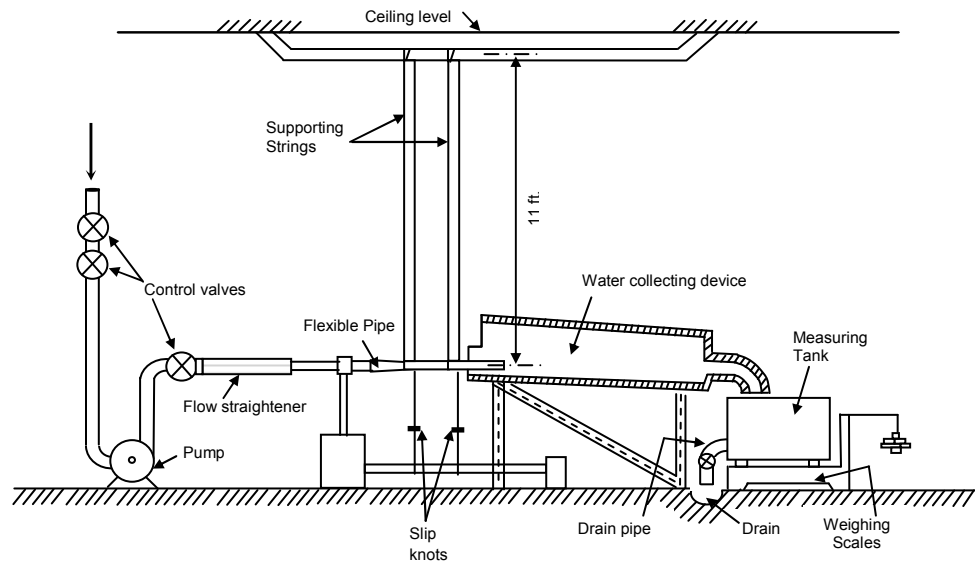
Figure 2.5: Schematic diagram of the apparatus used for experiments with rubber tubes conveying water. [82]

Figure 2.5 shows the apparatus used in experiments with rubber pipes conveying water. The rubber tube was glued to a suitable length of rigid metal pipe that was clamped securely in a horizontal position. The pipe was supported by a number of thin threads hung from the ceiling and of sufficient length to ensure that at least for motions of small amplitude, the tube effectively moved in horizontal plane. The centrifugal pump was used in some cases to boost the available mains pressure. The water, after leaving the flexible pipe, was collected in a tapered duct leading to a tank resting on weighing scales. The apparatus for experiments with air flowing in rubber tubes was essentially the same except that a volumetric flow meter was inserted in the air supply line. The air pressure was always sufficiently low for compressibility effects to be neglected. The experiments appear to prove that neglecting internal friction in the material of the tube and the effect of the surrounding fluid, a universal stability curve is constructed corresponding to conditions of neutral stability and hence separating stable and unstable regimes. It was shown that damping, associated either with energy dissipation in the tube material or with energy transfer to surround fluid, in certain cases may have destabilised the system [82].

30

2.6 Summary

From a wide study of the literature, a few gaps in knowledge were identified:

1. There is a lack of analytical approaches and analytical solutions that can explicitly provide the estimate of the effect of the internal flow on the dynamic response of pipes and serve as a benchmark for numerical solutions. Meanwhile, the speed of the flow represent a suitable parameter for the development perturbation approaches to the investigation of the pipe dynamics.

2. Most of the previous studies were focused on vibration problems in pipes including the calculation of natural frequencies and vibration control. Despite the fact that the vibration and impact loading problems are closely related, it was surprising that not much research has been conducted to investigate the dynamic response of pipes to impulse loading, especially to understand how the internal flow changes the maximum deflections of the pipe.

3. Despite the fact that many previous studies comprehensively investigated problems of stability of pipes conveying fluid or gas, there were no engineering criteria suggested to avoid unstable behaviour. With the recent release of the AS 2885.1-2007 standard, which clearly states that pipelines may now be installed aboveground, such criteria are vital and must be established. In addition, the vast majority of these studies were focused on a particular type of boundary conditions, namely, cantilever-type boundary conditions.

4. A similar gap was found with the previous experimental studies. The focus of these studies was on the investigation of the effect of the internal flow on the integrity or fracture under impulse loading. Many studies were focusing on the investigation of the critical flow speed, which causes the dynamic instability. However, it seems there are no experimental studies on the investigation of the effect of the flowing medium on the impact response of circular pipes conveying fluid or gas.

The current study will partially address these gaps. In the next chapter, an analytical perturbation approach will be developed and validated via a numerical method based on central-difference scheme. It will also present an experimental rig and the

results from the experimental study. This method and validation study will be described in Chapter 4. A detailed study on the effect of the flowing medium on the transient response of pipes subjected to impulse loading will be presented in Chapter 5. A general conclusion will be provided in Chapter 7.

CHAPTER 3

GOVERNING EQUATION AND ASYMPTOTIC APPROACH

3.1 Introduction

In this chapter, a simplified governing equation is formulated that describes the dynamic response of a long flexible pipe carrying gas or liquid and subjected to transverse impulse loading. This equation is developed from the simplified classical Bernoulli-Euler beam theory. Further, a scaling transformation of the governing equations is conducted to demonstrate that the dynamic response within the adopted assumptions and simplifications is controlled by only two parameters. These parameters represent dimensionless combinations of the elastic properties of the pipe, pipe geometry and flow characteristics. In the case of a slight influence of the flowing medium on the overall mechanical response of the whole system, the governing equation can be solved using an original analytical approach that is based on the standard perturbation technique. Several examples demonstrating the effectiveness of the developed in this thesis approach for particular problems are considered in detail. The development of the asymptotic approach presented in this chapter is quite general and can be generalised relatively easily for other boundary conditions as well as for arbitrary applied loading.

3.2 Simplified Classical Bernoulli-Euler Beam Theory

This section describes a simplified mathematical model based on standard assumptions for bending long flexible beams also adopted in [83,84,85] and many other papers. This model will be utilised throughout this thesis (1) to analyse the transient response of a pipe with flowing medium when the pipe is subjected to transverse impulse loading, and (2) for investigation of the effects of parameters of the internal flow (density and velocity) on the overall mechanical response. The classical Bernoulli-Euler beam theory is adopted as a starting point of modelling and this theory is then further extended to incorporate the contribution of flowing medium into the mechanical behaviour of the system. Indeed, the lateral displacement of the pipe leads to the additional forces due to flow inertia, centrifugal acceleration, and Coriolis force because the flow follows along the curved deflected pipe. All these forces will be incorporated into the pipe governing equation. The derived governing equation represents a fourth order non-homogeneous

PDE and will be solved using asymptotic and numerical approaches in Chapter 4. The outcomes of the theoretical investigation are also validated by experiments presented in Chapter 6.

3.3 Mathematical Modelling of Beam with Flowing Medium

Consider a pipe element of length $d\bar{x}$ as shown in Figure 3.1.
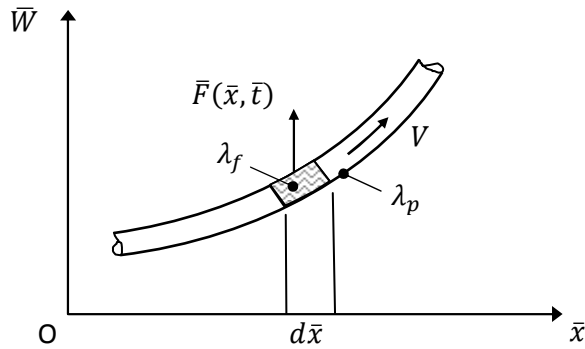
Figure 3.1: Deformation of pipe with flowing medium

Let λ_f and λ_p be the medium and pipe densities per unit length (say 1 meter). In the case of the pipeline's transverse motion, the element is subjected to the inertia force of intensity

$$-\frac{\partial^2 \bar{W}}{\partial \bar{t}^2}\left(\lambda_f + \lambda_p\right) \quad . \tag{3.1}$$

As the flow rotates with angular speed $\partial^2 \bar{W}/(\partial \bar{x} \partial \bar{t})$, the Coriolis force acting on the element $d\bar{x}$ is given by

$$-2\frac{\partial^2 \bar{W}}{\partial \bar{x} \partial \bar{t}}\lambda_f V d\bar{x} \quad , \tag{3.2}$$

where V is the velocity of the medium. With the same sign, we can write the centrifugal force acting on the element due to the flow that follows along the curved deflected pipe:

$$-\frac{\partial^2 \overline{W}}{\partial \bar{x}^2} \lambda_f V^2 d\bar{x} \quad . \tag{3.3}$$

It is assumed for simplicity that the dynamics of the pipe do not affect significantly the flow characteristics such as flow velocity and density. Thus, we can decouple the structural and flow mechanisms of the problem. Taking also into account the elastic response of the pipe element, $d\bar{x}$, the governing dynamic equation can be written in the following form:

$$EI\frac{\partial^4 \overline{W}}{\partial \bar{x}^4} + \frac{\partial^2 \overline{W}}{\partial \bar{t}^2}(\lambda_f + \lambda_p) + 2\frac{\partial^2 \overline{W}}{\partial \bar{x} \partial \bar{t}}\lambda_f V + \frac{\partial^2 \overline{W}}{\partial \bar{x}^2}\lambda_f V^2 = \bar{F}(\bar{x},\bar{t}) \tag{3.4}$$

where E represents Young's modulus and I is the second moment of inertia of the pipe. The right-hand side term $\bar{F}(\bar{x},\bar{t})$ represents a driving force per unit length. We assume that the length of the pipe is finite and $0 \leq \bar{x} \leq L$ and $\bar{t} \geq 0$.

3.4 Scaling Transformation of the Dynamic Governing Equation

It is always advantageous and often necessary to rewrite a governing equation in a dimensionless form. To do so, the following scaling transformations are introduced:

$$x = \frac{\bar{x}}{L}, \qquad t = \frac{\bar{t}}{\tau}, \qquad W(x,t) = \frac{\overline{W}(x,t)}{L} \tag{3.5}$$

where τ is a parameter that will be defined in equation (3.8a). Then, equation (3.4) can be rewritten as

$$\frac{EI}{L^3}\frac{\partial^4 W}{\partial x^4} + \frac{(\lambda_f + \lambda_p)L}{\tau^2}\frac{\partial^2 W}{\partial t^2} + 2\frac{V\lambda_f}{\tau}\frac{\partial^2 W}{\partial x \partial t} + \frac{V^2\lambda_f}{L}\frac{\partial^2 W}{\partial x^2} = \bar{F}(x,t) . \tag{3.6}$$

It is straightforward to show the dimensional consistency of the equation. To proceed with the solution of the governing equation, it is convenient to recast this equation into a more compact form. Dividing both sides by EI/L^3, we obtain

$$\frac{\partial^4 W}{\partial x^4} + \frac{(\lambda_f + \lambda_p)L^4}{EI\tau^2}\frac{\partial^2 W}{\partial t^2} + 2\frac{V\lambda_f L^3}{EI\tau}\frac{\partial^2 W}{\partial x \partial t} + \frac{V^2\lambda_f L^2}{EI}\frac{\partial^2 W}{\partial x^2} = F(x,t) . \tag{3.7}$$

Introduce characteristic time, τ.

$$\tau = L^2\sqrt{\frac{\lambda_p + \lambda_f}{EI}} . \tag{3.8a}$$

Now we define the following dimensionless parameters

$$\varepsilon = \frac{VL\lambda_f}{\sqrt{EI(\lambda_p + \lambda_f)}} \tag{3.8b}$$

and

$$\beta = VL\sqrt{\frac{\lambda_p + \lambda_f}{EI}} \tag{3.8c}$$

and

$$F(x,t) = \frac{L^3}{EI}\bar{F}(x,t) . \tag{3.8d}$$

Then equation (3.6) becomes

37

$$W_{,xxxx} + W_{,tt} + \varepsilon\left(2W_{,xt} + \beta W_{,xx}\right) = F(x,t) \ . \tag{3.9}$$

In the last equation, the following notation for the derivative: $\partial W/\partial x \equiv W_{,x}$ was introduced. The similar rule is applied to the variable t as well as throughout higher order derivatives. Observe also that following the scaling transformation (3.8) and (3.9), the space variable x varies between 0 and 1. Finally, to solve the problem, the initial and boundary conditions must be imposed.

In the derivation of the governing equation (3.9), the effect of axial forces on the transverse movements was also omitted; this can be developed in the pipe as a result of the viscosity of the flow or reactions in the pipe supports. Such forces can also contribute to the dynamic response at large values of pipe deflections or slopes of the deflection curve. However, in the following analysis, it is assumed that the deflections are small and the effect of the axial forces (due to flow viscosity and support reactions) on the transverse movements is negligible in comparison with other forces.

It is important to stress that, within the developed model, only two parameters, ε and β fully control the transient response of the system. Therefore, the derived governing equation (3.9) can be utilised to investigate various dynamic phenomena using reduced size or scaled physical models. Such scaled models would be adequate if the values of the governing parameters ε and β are kept the same for the scaled model and the reference system. This can potentially result in substantial benefits if the experimental approach is adopted for the investigation of the problem under consideration.

3.5 Asymptotic Solution: Cantilever Beam

A boundary-value problem for the governing equation (3.9) can be solved by means of a standard perturbation approach utilising the smallness of parameter ε. To demonstrate the application of the perturbation approach for the analysis of the transient behaviour of pipes, specific boundary conditions at the ends of the pipe $x = 0$ and $x = 1$ must be

prescribed. In this sub-section, consideration is given to the cantilever-type boundary conditions, as shown in Figure 3.2, or

at $x = 0$: $W = W_{,x} = 0$, $\qquad$ (3.10a)

which correspond to zero displacement and zero slope at the fixed end ($x = 0$), and

at $x = 1$: $W_{,xx} = W_{,xxx} = 0$, $\qquad$ (3.10b)

which means zero resultant bending moment and shear force at the free end ($x = 1$).
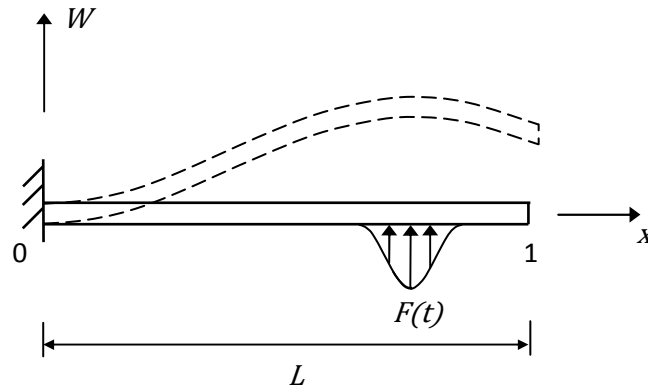
Figure 3.2: Cantilever beam subjected to impulse loading

3.5.1 Solution of Non-homogeneous Classical Beam Equation

The transient analysis of the derived equation (3.9) in the previous section is commenced with a consideration of the classical non-homogeneous beam equation subjected to the boundary conditions given in equations (3.10a) and (3.10b):

$$W_{,xxxx} + W_{,tt} = F(x,t) \ . \qquad (3.11)$$

Assumption is made that the pipe was stationary at $t < 0$, meaning that the applied driving load distribution

$$F(x,t) \equiv 0 \text{ at } t < 0 \tag{3.12}$$

Several solution techniques can be applied to analyse the beam's transient response to an impulse loading, including Laplace-Laplace transforms, the method of undetermined coefficients, variation of parameters, and the Joint transform scheme [86] and [87]. An exact analytical solution of equation (3.11) with boundary conditions (3.10) can be obtained by the standard separation of variables technique and an application of Laplace transform [87]. It can be written as

$$W(x,t) = \sum_{k=1}^{\infty} Y_k(x) \int_0^1 Y_k(u) \int_0^t F(u,\tau) \frac{\sin\big(\omega_k(t-\tau)\big)}{\omega_k} d\tau du \tag{3.13}$$

where $\omega_k = \lambda_k^2$. In the previous equation, Y_k are a set of normalised eigenfunctions corresponding to the solution of the homogeneous equation, i.e. $W_{,xxxx} + W_{,tt} = 0$, subjected to the specified boundary conditions [87]:

$$Y_k(x) = A_k\big[\big(\cosh(\lambda_k x) - \cos(\lambda_k x)\big) - c_k\big(\sinh(\lambda_k x) - sin(\lambda_k x)\big)\big] \tag{3.14}$$

where

$$c_k = \frac{\cosh(\lambda_k) + \cos(\lambda_k)}{\sinh(\lambda_k) + \sin(\lambda_k)} \tag{3.15}$$

with $\lambda_1 = 1.8752$, $\lambda_2 = 4.6942$, $\lambda_3 = 7.8849$, $\lambda_4 = 10.9956$, $\lambda_5 = 14.1373$ and λ_k $(k \geq 6) \approx (2k-1)\pi/2$ [13,14].

The coefficients A_k in Eq. (3.14) are the normalisation constants that ensure the eigenfunctions are not only orthogonal but also orthonormal. For $k \leq 12$, $A_k = 1$,

while for $k > 12$, A_k departs from unity and must be determined (see for example [87]).

Equation (3.13) provides the general analytical expression for the transient spatio-temporal dynamics of a cantilever beam driven by arbitrary load distribution, $F(x, t)$. As an example, consider a spatio-temporal impulse driving force at time $t = 0$ with a magnitude f_a (in scaled variables). We use Dirac's time-and-space delta function to model this impulse. Then, $F(x, t)$ takes the form

$$F(x, t) = f_a \delta(x - x^*)\delta(t) \tag{3.16}$$

where x^* represents the position along the pipe at which the driving impulse is applied. Carrying out the space and time integrations and invoking the basic properties of Dirac's delta function, we obtain

$$W(x, t) = f_a \sum_{k=1}^{\infty} Y_k(x)Y_k(x^*)\, \frac{\sin(\omega_k t)}{\omega_k} \,. \tag{3.17}$$

The above solution is also well known in the literature and describes the mechanical response of a cantilever beam subjected to a spatio-temporal impulse [88–93]. This relationship (3.17) also describes the exact analytical solution of the corresponding problem for a pipe with flowing medium (3.9) when parameters ε as well as β are limited to zero. Such situations, for example, correspond to the case when the velocity of the flowing medium is negligible, or when the pipe has a large bending stiffness (*EI*).

3.5.2 Perturbation Approach

The case of a cantilever pipe with flowing medium can be related to a practically important situation in which, for example, the pipe is ruptured circumferentially due to an accident such as fracture propagation and is subjected to a dynamic loading. In this

case, the simplified governing equation (3.9) was derived in the previous section and, for convenience of the reader, is rewritten below:

$$W_{,xxxx} + W_{,tt} + \varepsilon\left(2W_{,xt} + \beta W_{,xx}\right) = F(x,t).$$

In contrast to the previously considered case (the classical Bernoulli-Euler beam equation neglecting the internal flow considered earlier), an attempt at a standard separation of variables approach to determine the dynamic response fails because it is impossible to satisfy the boundary conditions with a nontrivial solution. However, as was mentioned in Section 3.4.1, at fixed β, (3.18) reduces to the classical Bernoulli-Euler equation when ε is limited to zero. Alternatively, the problem can be solved as a regular perturbation problem developed by the candidate in [83] with, ε as a small parameter; that is, the solution has the form

$$W = W_0 + \varepsilon W_1 + \varepsilon^2 W_2 + \cdots \varepsilon^m W_m + \cdots .\qquad(3.18)$$

If the expansions (3.18) are substituted into (3.9) and like powers of ε are equated, then the following expressions for the transverse deflection of W, correct up to order ε^m, are obtained:

$$
\begin{aligned}
&W_{0,xxxx} + W_{0,tt} = F(x,t) \\[4pt]
&W_{1,xxxx} + W_{1,tt} = F_0(x,t) \qquad F_0(x,t) = -2W_{0,xt} - \beta W_{0,xx} \\[4pt]
&W_{2,xxxx} + W_{2,tt} = F_1(x,t) \qquad F_1(x,t) = -2W_{1,xt} - \beta W_{1,xx} \\[4pt]
&\cdots \\[4pt]
&W_{m,xxxx} + W_{m,tt} = F_{m-1}(x,t) \qquad F_{m-1}(x,t) = -2W_{m-1,xt} - \beta W_{m-1,xx} \ .
\end{aligned}
\qquad(3.19)
$$

These equations are subjected to the specified boundary conditions such as (3.10). This sequence of equations can be considered a recurrent system of differential equations that

can be solved through a step-by-step integration using the general solution for the cantilever beam subjected to arbitrary load distribution (3.13). This solution can also be written using the earlier considered solution for the classical Bernoulli-Euler beam (3.13) as

$$W_m(x,t) = \sum_{k=1}^{\infty} Y_k(x) \int_0^1 Y_k(u) \int_0^t F_{m-1}(u,\tau) \frac{\sin(\omega_k(t-\tau))}{\omega_k} d\tau du \ . \tag{3.20}$$

The above recurrent equations (3.19) and general solution for non-homogeneous beam equation (3.20) provide an analytical tool for the analysis of the effect of the flowing media on the transient response of pipes. Next, the different boundary conditions are considered to demonstrate further the developed approach.

3.6 Asymptotic Solution: Simply Supported Beam

For this sub-section, consideration is given to the simply supported type of boundary conditions, as illustrated in Figure 3.3, or

$$\text{at } x = 0: \ W = W_{,xx} = 0 \text{,} \tag{3.21a}$$

and

$$\text{at } x = 1: \ W = W_{,xx} = 0 \ . \tag{3.21b}$$

These conditions correspond to zero displacement and bending moment enforced at both ends of the pipe.
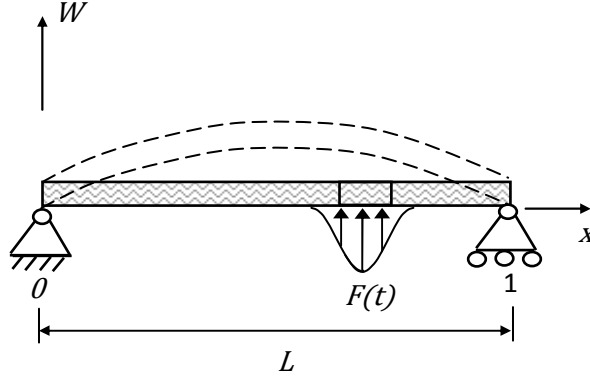
Figure 3.3: Simply supported beam subjected to impulse loading

3.6.1 Solution of Non-homogeneous Classical Beam Equation

Similar to sub-section 3.4, the driving load distribution $\bar{F}(x,t) = 0$ at $t < 0$ is assumed. First, consideration is given to the solution of the non-homogeneous equations for the classical Bernoulli-Euler beam corresponding to the prescribed boundary conditions (simply supported pipe). This solution will be further utilised in the asymptotic approach for a pipe with flowing medium. An analytical solution of equation (3.11) with boundary conditions (3.21) can also be obtained by the separation of variables technique and Laplace transform [86] and can be written as

$$W(x,t) = \sum_{k=1}^{\infty} Y_k(x) \int_0^1 Y_k(u) \int_0^t F(u,\tau) \frac{\sin\big(\omega_k(t-\tau)\big)}{\omega_k} d\tau du \qquad (3.22)$$

where Y_k are the set of normalised eigenfunctions corresponding to the solution of the homogeneous equation $W_{,xxxx} + W_{,tt} = 0$, subjected to the specified boundary conditions:

$$Y_k(x) = \sqrt{2} \sin \lambda_k x, \qquad \lambda_k = k\pi \qquad (3.23)$$

and

$$\omega_k = \lambda^2{}_k = (k\pi)^2 \ . \tag{3.24}$$

The coefficient $\sqrt{2}$ in eigenfunctions, equation (3.23), is a normalisation constant that ensures that the eigenfunctions are not only orthogonal but also orthonormal. Further, the perturbation approach is developed for the simply supported beam.

3.6.2 Perturbation Approach

Similar to the cantilever case considered previously, the problem can be solved as a regular perturbation problem with ε as a small parameter; that is, the solution has the form

$$W = W_0 + \varepsilon W_1 + \varepsilon^2 W_2 + \cdots \varepsilon^m W_m + \cdots \ . \tag{3.25}$$

If this expansion is substituted into (3.9) and like powers of ε are equated, then the similar recurrent expressions for the transverse deflection of W, correct up to order ε^m, can be obtained:

$$\left.\begin{aligned}
&W_{0,xxxx} + W_{0,tt} = F(x,t) \\[4pt]
&W_{1,xxxx} + W_{1,tt} = F_0(x,t) && F_0(x,t) = -2W_{0,xt} - \beta W_{0,xx} \\[4pt]
&W_{2,xxxx} + W_{2,tt} = F_1(x,t) && F_1(x,t) = -2W_{1,xt} - \beta W_{1,xx} \\[4pt]
&\cdots \\[4pt]
&W_{m,xxxx} + W_{m,tt} = F_{m-1}(x,t) && F_{m-1}(x,t) = -2W_{m-1,xt} - \beta W_{m-1,xx} \ .
\end{aligned}\right\} \tag{3.26}$$

Based on the similar approach as adopted in the case of cantilever pipe and omitting computational details, the expansion series terms are

$$W_m(x,t) = 2 \sum_{k=1}^{\infty} \sin(\lambda_k x) \int_0^1 \sin(\lambda_n u) \int_0^t F_{m-1}(u,\tau) \frac{\sin\big(\omega_k(t-\tau)\big)}{\omega_k} d\tau du \ . \tag{3.27}$$

The above recurrent equations (3.26) and general solution for non-homogeneous beam, equation (3.27) with λ_k as given by (3.23), provide an analytical procedure for the analysis of the effect of the flowing media on the transient response of simply supported pipes. Further, several examples are considered to demonstrate the developed approach. For example, first consider a harmonical impulse driving force at time $t = 0$ with a magnitude f_n (in scaled variables); that is

$$F(x,t) = f_n \sin(\lambda_n x)\, \delta(t) \tag{3.28}$$

where n is a positive integer number and λ_n is defined by equation (3.24). Then, in accordance with equations (3.19),

$$W_{n0}(x,t) = f_n \sin(\lambda_n x)\frac{\sin(\omega_n t)}{\omega_n} \tag{3.29}$$

which also describes the transient response of pipe with a stationary filled media. In accordance with equation (3.24),

$$F_{n0}(x,t) = -2f_n\lambda_n \cos(\lambda_n x)\cos(\omega_n t) + \beta \sin(\lambda_n x)\sin(\omega_n x)\ . \tag{3.30}$$

Then, carrying out all integrations and after simplifications, the first-order correction of the deflection function can be written as a sum of two terms:

$$W_{n1}(x,t) = W_{n1}^{Cor}(x,t) + W_{n1}^{Cen}(x,t)\ , \tag{3.31}$$

where

$$W_{n1}^{Cor} = -4\lambda_n f_n \sum_{k=1}^{\infty} \sin(\lambda_k x)\left(\frac{k(1-(-1)^{n+k})}{\pi(k+n)(k-n)}\frac{\cos(\omega_k t) - \cos(\omega_n t)}{(\omega_n + \omega_k)(\omega_n - \omega_k)}\right) \tag{3.32}$$

and

$$W_{n1}^{Cen}(x,t) = \frac{\beta f_n}{2\omega_n^2}\sin(\lambda_n x)\left(\sin(\omega_n t) - \cos(\omega_n t)\omega_n t\right)\ . \tag{3.33}$$

The first term, $W_{n1}^{Cor}(x,t)$, represents the contribution of Coriolis force and the second term, $W_{n1}^{Cen}(x,t)$ is due to the centrifugal acceleration of the flowing media through the curved pipe. It is interesting to note that the first term, $W_{n1}^{Cor}(x,t)$, is limited in time; however, the second term, $W_{n1}^{Cen}(x,t)$, in the first-order correction is growing with time, and is thus demonstrating a synergetic effect of the flowing media in the structural response of the system. Both terms are continuous functions with zero values at $t = 0$. This means that the effect of the flowing medium on the transient response is small within relatively small time intervals from the start of the impulse loading. This effect is characterised by the dimensionless parameter τ (see equation (3.8)). In the case of an arbitrary driving impulse force, the spatial component can be represented in Fourier series as

$$F(x,t) = \delta(t) \sum_{n=1}^{\infty} f_n \sin(\lambda_n x) \ . \tag{3.34}$$

Using the principle of superposition, the general solution can be found by the simple summation of the particular solutions for each harmonic. For example, if the system is subjected to a spatio-temporal impulse driving force, i.e.

$$F(x,t) = f_a \cdot \delta(x^*)\delta(t) \tag{3.35}$$

where f_a is the amplitude of the driving impulse and x^* is the point at where the force is applied, then, the ε^0 - order solution for the pipe deflection is

$$W_0(x,t) = 2f_a \sum_{n=1}^{\infty} \sin(\lambda_n x) \sin(\lambda_n x^*) \frac{\sin(\omega_n t)}{\omega_n} \ . \tag{3.36}$$

The first-order correction of this solution, which incorporates the flowing medium effects, can be found from equation (3.31) as

$$W_1(x,t) = \sum_{n=1}^{\infty} f_n W_{n1}(x,t) \ , \tag{3.37}$$

47

where W_{n1} is given by Eq (3.31) and $f_n = 2f_a \sin(\lambda_n x^*)$.

In the next chapter, a numerical approach is presented for the solution of equation (3.9) in the case of arbitrary (not small) controlling parameters and the obtained analytical solutions are used to validate the numerical approach.

3.7 Summary

In this chapter, the governing equation was derived for a long flexible pipe with flowing medium based on the classical Bernoulli-Euler beam theory. After that, scale transformations were conducted to demonstrate that only two parameters, (ε and β), that govern the transient dynamics of the pipe. This finding can be utilised to investigate various dynamic phenomena using reduced size or scaled physical models. Such scaled models would be adequate if the values of the governing parameters ε and β are kept the same for the scaled model and the reference system. Of course, the physical models have to meet all other conditions corresponding to the adopted assumptions in mathematical modelling. For example, the pipe has to be sufficiently long and flexible, and the loading should not significantly affect the internal flow characteristics.

Further, an asymptotic approach was developed to investigate the transient response of pipes subjected to impulse loading. The approach is based on the standard perturbation technique. The solution represents a recurrent system of equations, each term of which can be obtained by integration. The application of this approach was demonstrated to obtain the first-order correction to the classical solution for the corresponding problem of both a cantilever beam and a simply supported pipe transporting gas or liquid. However, if higher order terms are required, the analytical procedure could become quite cumbersome and time-consuming. Therefore, the derived asymptotic solutions will be used mainly to validate important results obtained by a more comprehensive numerical method to be developed in the next Chapter.

CHAPTER 4

NUMERICAL APPROACH AND VALIDATION STUDY

4.1 Introduction

In Chapter 3, an analytical perturbation approach was developed to obtain solutions for particular problems and analyse the governing equation describing dynamic response of a circular pipe transporting gas or liquid. Due to the asymptotic nature of the developed approach, it has obvious limitations. In particular, the perturbation approach is only applicable to the situations in which the influence of the parameters of the flowing media on the transient response of the pipe is relatively small. Such situations, for example, take place when the velocity and density of the internal flow are low or when the flexural rigidity of the pipe is relatively high. It seems, that other analytical approaches, such as the Fourier transform approach or integral equation method, for analysis of the governing equation, which represents a forth order PDE, are too cumbersome and can lead to significant technical difficulties. Therefore, a more simplified numerical approach is developed, which will be used in the next chapter, Chapter 5 to investigate comprehensively the dynamic response of pipes subjected to impulse loading as well as to study the effects of the flowing medium on the dynamic response.

The numerical approach to be developed in this chapter is based on the central finite-difference scheme. This numerical scheme including convergence and accuracy issues is well investigated and widely described in the literature. It was previously applied to study similar dynamic problems, see for example [87]. In this scheme, the spatial-temporal domain of interest is partitioned with a rectangular uniform grid of mesh size: $\Delta x \times \Delta t$, where Δx represents the spatial grid size and Δt denotes the temporal grid size. The upper bounds of the grid point in the spatial and temporal directions will be denoted by N_x and N_t, respectively. Consequently, the spatial domain is limited by points $n = 0$ and $n = N_x$; and the time domain spreads from $m = 0$ to $m = N_t$. The discredited two-dimensional spatial-temporal domain is shown in Figure 4.1. The inclusion of additional spatial points at $x < 0$ and $x > 1$ is often necessary to implement the specified boundary conditions, which will be discussed later in this chapter.

The following notations are used: the transverse deflection of the beam at a grid point (x_n, t_m) will be denoted as $W(x_n, t_m)$ or, simply as $W_{n,m}$.
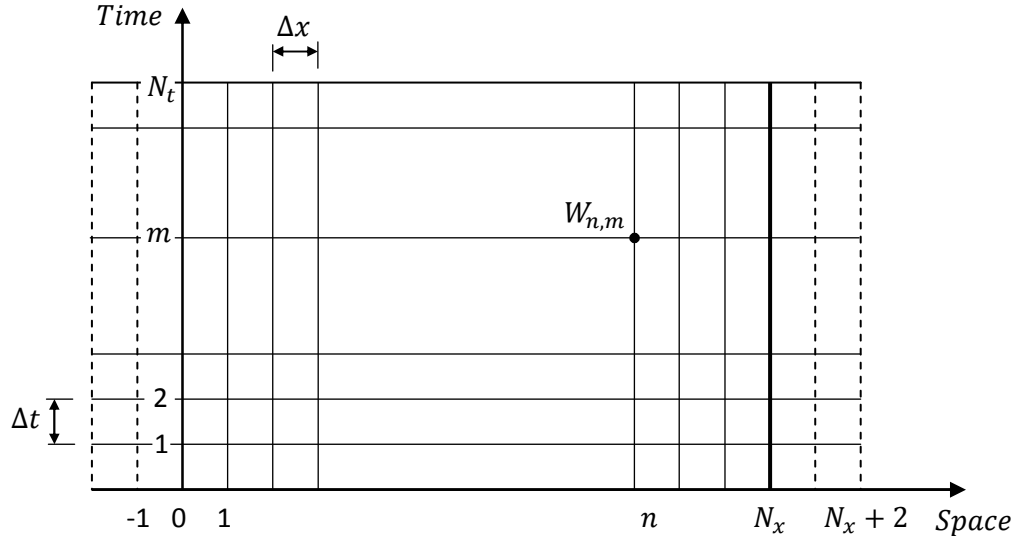
Figure 4.1: Finite-difference grid

The dynamic deformation behaviour of the pipe with flowing medium within the adopted assumptions and simplifications is given by equation (3.9), which can be written in a dimensionless form; and it is repeated below:

$$W_{,xxxx} + W_{,tt} + \varepsilon\left(2W_{,xt} + \beta W_{,xx}\right) = F(x, t) \quad,$$

where the first term in this equation $\left(W_{,xxxx}\right)$ represents the elastic response of the pipe, the second term $\left(W_{,tt}\right)$ is a contribution from the inertia force of pipe material and flowing medium; $\left(2\varepsilon W_{,xt}\right)$ is the contribution from the Coriolis force on the pipe behaviour, $\left(\varepsilon\beta W_{,xx}\right)$ represents the contribution from the centrifugal force of the flow on pipe because the flow follows along the curved deflected pipe, and the right side of this equation, $F(x, t)$, is the applied impulsive force.

In the following the above dimensionless PDE will be discredited and solved using the central finite-difference scheme for various boundary conditions specified at the ends of the pipe, i.e. at points $x = 0$ and $x = 1$.

51

4.2 Central-Difference Numerical Scheme

To implement the central finite-difference scheme, we will first write down the discrete representation of the derivates comprising equations (3.9) or $W_{,xxxx}, W_{,tt}, W_{,xt}$ and $W_{,xx}$. Using Taylor series expansion, we obtain the following representation of the partial derivatives:

$$W_{,t}(n,m) \equiv \frac{\delta W(n,m)}{\delta t}$$

$$\approx \frac{W(n, m + \Delta t) - W(n, m - \Delta t)}{2\Delta t} + 0(\Delta t^2)$$

$$\approx \frac{W(n, m + 1) - W(n, m - 1)}{2\Delta t} \qquad (4.1)$$

and

$$W_{,tt}(n,m) \equiv \frac{\delta^2 W(n,m)}{\delta t^2}$$

$$\approx \frac{W(n, m + \Delta t) - 2W(n,m) + W(n, m - \Delta t)}{\Delta t^2}$$

$$\approx \frac{W(n, m + 1) - 2W(n,m) + W(n, m - 1)}{\Delta t^2} \qquad (4.2)$$

and

$$W_{,xx}(n,m) \equiv \frac{\delta^2 W(n,m)}{\delta x^2}$$

$$\approx \frac{W(n + \Delta t, m) - W(n,m) - W(n,m) + W(n - \Delta t, m)}{\Delta x^2}$$

$$\approx \frac{W(n + 1, m) - 2W(n,m) + W(n - 1, m)}{\Delta x^2} \; . \qquad (4.3)$$

In a similar vein, the spatial derivative term is approximated as

$$W_{,xt}(n,m) \equiv \frac{\delta^2 W(n,m)}{\delta x \delta t}$$

$$\approx \frac{W(n+1,m+1) - W(n+1,m-1)}{4\Delta t \Delta x} -$$

$$\frac{W(n-1,m+1) - W(n-1,m-1)}{4\Delta t \Delta x} \tag{4.4}$$

and

$$W_{,xxxx}(n,m) \equiv \frac{\delta^4 W(n,m)}{\delta x^4}$$

$$\approx \frac{W(n+2,m) - 4W(n+1,m) + 6W(n,m)}{\Delta x^4} -$$

$$\frac{4W(n-1,m) + 4W(n-2,m)}{\Delta x^4} \; . \tag{4.5}$$

Substituting the above equations into the governing equation (3.9) the final discrete representation of the partial deferential equation can be written in the following form

$$W_{n,m+1} = \frac{\varepsilon}{2}\left(\frac{\Delta t}{\Delta x}\right)\left[W_{n-1,m+1} - W_{n+1,m+1}\right]$$

$$-\left(\frac{\Delta t}{\Delta x^2}\right)^2\left[W_{n+2,m} - 4W_{n+1,m} + 6W_{n,m} - 4W_{n-1,m} + W_{n-2,m}\right]$$

$$+\left[2W_{n,m} - W_{n,m-1}\right] + \frac{\varepsilon}{2}\left(\frac{\Delta t}{\Delta x}\right)\left[W_{n+1,m-1} - W_{n-1,m-1}\right]$$

$$+\beta\varepsilon\left(\frac{\Delta t}{\Delta x}\right)^2\left[W_{n+1,m} - 2W_{n,m} + W_{n-1,m}\right]$$

$$+\Delta t^2 F(x,t) \; . \tag{4.6}$$

The central-difference scheme under consideration has a truncation error of $0[\Delta x^4 + \Delta t^2]$. The sufficient condition for stability of this scheme is the condition that

$\Delta t / \Delta x^2 < 0.5$, which indicates that the finite-difference method is stable if the error goes to zero as the truncation error goes to zero. Further, when the both governing parameter, ε and β, equal to zero, we can derive the classical dimensionless form of the beam governing equation (3.11):

$$W_{,xxxx} + W_{,tt} = F(x,t) \ .$$

The finite-difference representation of the last equation is

$$W_{n,m+1} = -\left(\frac{\Delta t}{\Delta x^2}\right)^2 \left[W_{n+2,m} - 4W_{n+1,m} + 6W_{n,m} - 4W_{n-1,m} + W_{n-2,m}\right]$$

$$+\left[2W_{n,m} - W_{n,m-1}\right] + \Delta t^2 F(x,t)$$

$$(4.7)$$

which is a particular case of the derived equation (4.6).

4.3 Initial and Boundary Conditions
4.3.1 Initial Conditions

In the following sub-section, consideration is given to three types of boundary conditions. These are fixed support, free end and simply supported boundary conditions. The initial conditions (deflection and the velocity of the pipe) for all cases are assumed to be zero:

$$W(x,0) = 0 \tag{4.8}$$

and
$$W_t(x,0) = 0 \ . \tag{4.9}$$

In the finite-differences representation, the initial conditions are reduced to the following expressions:

$$W_{n,1} = 0 \tag{4.10}$$

and

$$W_{n,2} = 0 \ . \tag{4.11}$$

Next, consideration is given to the boundary conditions for all cases under consideration.

4.3.2 Boundary Conditions

At the fixed end (which is assumed to be the left end), the deflection and slope have to be zero. It means that for any time t

$$W(0, t) = 0 \tag{4.12}$$

and

$$W_x(0, t) = 0 \ . \tag{4.13}$$

In terms of finite-differences representation, these can be expressed as follows:

$$W_{0,m} = 0 \tag{4.14}$$

and

$$W_{-1,m} = W_{1,m} \tag{4.15}$$

which is valid for any time step m.

The boundary conditions at the free end (without losing the generality, we will assume that these conditions apply to the left end of the pipe or at $x = 0$) are

$$W_{xx}(0, t) = W_{xxx}(0, t) = 0 \tag{4.16}$$

which means that the bending moment and shear force have to be zero. These conditions can be expressed in terms of the finite differences as

$$W_{1,m} - 2W_{0,m} + W_{-1,m} = 0 \tag{4.17}$$

and

$$\frac{1}{2}W_{2,m} - W_{1,m} + W_{-1,m} - \frac{1}{2}W_{-2,m} = 0 \ . \tag{4.18}$$

Finally, for simply supported boundary conditions, the deflection and bending moment have to be zero, or

$$W(0,t) = 0 \tag{4.19}$$

and

$$W_{xx}(0,t) = 0 \tag{4.20}$$

The corresponding finite-differences representations of these conditions are

$$W_{0,m} = 0 \tag{4.21}$$

and
$$W_{1,m} - 2W_{0,m} + W_{-1,m} = 0 \tag{4.22}$$

One can see that many boundary conditions include virtual special points $n = -1$ and $n = -2$ for the left end of the pipe. The similar points have to be introduced for the right part of the part, or at $n = N_x + 1$ and $n = N_x + 2$ to model the appropriate boundary condition. They are shown as dashed line in Figure 4.1.

4.4 Computational Flow

In this section, the matrix approach is introduced to obtain a computational numerical solution. Once the central finite-difference scheme has been established, the evolution equation (4.6) is set in a matrix form. The number of unknowns must match the number of equations and for this reason, the initial and boundary conditions are merged with the main numerical scheme of equation. The matrix forms of the equations are developed for the three earlier considered boundary conditions: fixed end, free end and simply supported end. The evolution equation together with the boundary conditions is combined into the global evolution matrix $\mathbf{A}$ and it is then programmed in MATLAB and solved numerically as follows:

$$\mathbf{A}\,\mathbf{W} = \mathbf{R} \tag{4.23}$$

$$(\mathbf{A}^{-1}\mathbf{A})\,\mathbf{W} = \mathbf{A}^{-1}\,\mathbf{R} \tag{4.24}$$

and

$$\mathbf{I}\mathbf{W} = \mathbf{A}^{-1}\mathbf{R} \tag{4.25}$$

where $\mathbf{I}$ is the identity matrix and $\mathbf{R}$ represents the applied loading $F(x, t)$, which is a function of the position and time. The complete MATLAB code is listed in Appendix C.

As mentioned above, for solution using the finite-difference scheme, the natural grid (the natural domain boundaries are within the bold lines in Figure 4.1) must include virtual grid points (on vertical dashed lines) to accommodate the appropriate boundary conditions. By examining the boundary condition, one needs to extend the natural grid of size $N_x \times N_t$ by introducing the virtual nodes. These grid nodes correspond to indices $n = -1$ and $n = -2$ on the left-hand side of the spatial grid representation, and to $n = N_x + 1, N_t + 2$ on the right-hand side.

To generate the first $W_{n,3}$ grid point, the central-difference scheme must be combined with known initial and boundary conditions. The computational flow proceeds as follows. First, the initial conditions require that these equations be evaluated, where the

57

range of the space index, n, extends from -1 or -2 to $N_x + 1$ or $N_x + 2$ (depending on the boundary conditions). Then, the time increment evolution begins. For each successive time step m, starting $m = 3$, the general formulation in equation (4.9) is applied to compute $W_{n,m+1}$. For this expression, the spatial component index varies between 1 and N_x. Thereafter, the boundary equations specified by the boundary conditions, equations (4.12) to (4.22), are applied. In order to complete the list of data needed to compute numerical results from either analytical formula or the finite-differences scheme, we need to specify the grid parameters. In this study, the scaled values selected $\Delta x = 0.025$ and $\Delta t = 0.00005$. These results in stability factor of 0.08, much lower than the minimum required $\Delta t / \Delta x^2 < 0.5$. The time step $\Delta t = 0.00005$ was selected to insure convergence of the numerical results with 5% error in the time interval $0 < t < 1$.

A shifted spatio-temporal delta impulse is modelled as a point load applied to a specific grid node within a short period, normally $\Delta t = 0.025$. A comparison of the finite-size spatio-temporal load impulse with analytical results obtained for delta impulse, which will be presented later in this chapter, demonstrated that the results are similar. The total number of simulation time steps is arbitrary. However, as time progresses, numerical error accumulate, resulting in a slight time lag due to the well-known limitations in accuracy of the finite-differencing numerical schemes. The computational flow is shown in Figure 4.2.
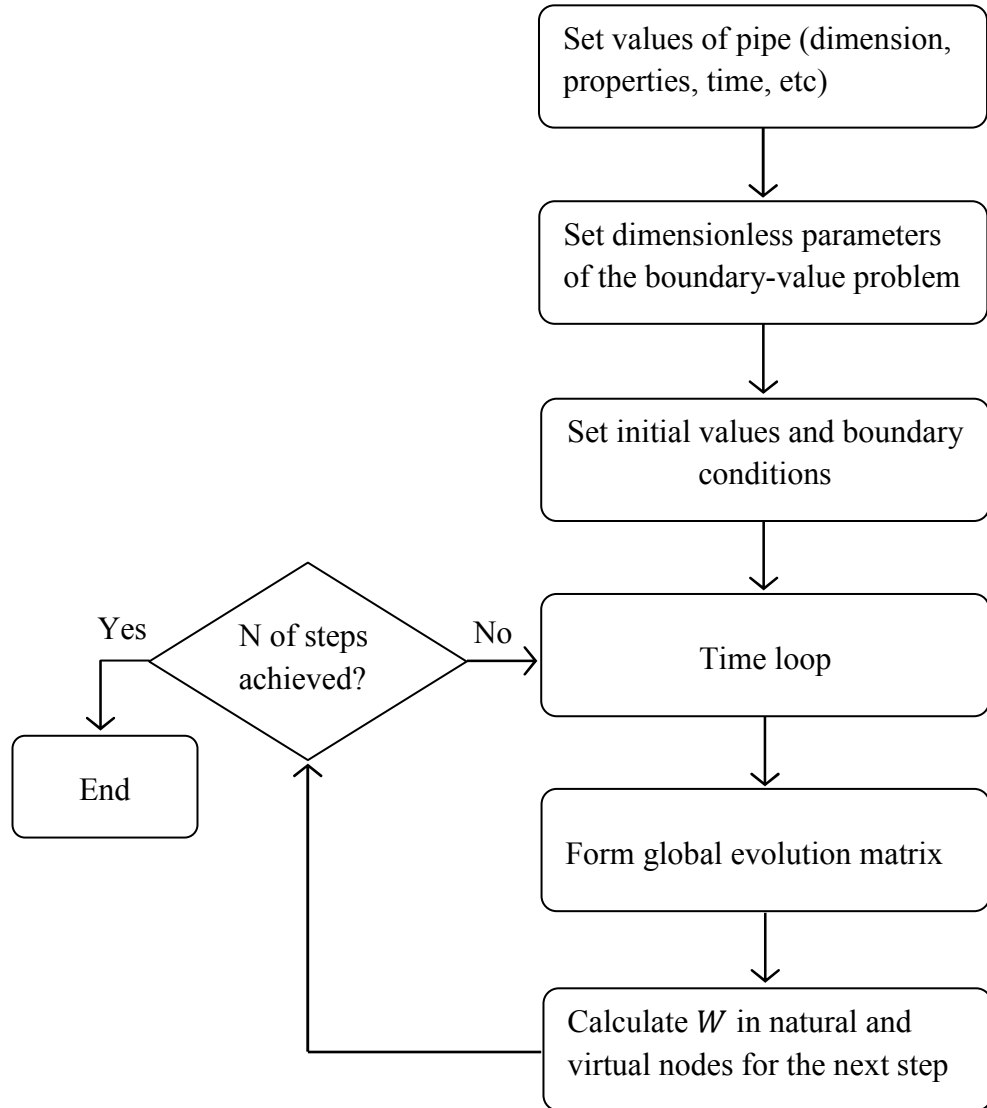
Figure 4.2: Computational flow

4.5 Validation Study

Before conducting the study on the effect of flowing media parameters on the dynamic response of a pipe in Chapter 5, it is first necessary to validate the developed numerical and analytical approaches. This will be achieved through the comparison of the numerical results with the known analytical solutions described in Chapter 3, as well as by comparison of the numerical method results with the perturbation method, which is

possible at small values of ε and β, where the perturbation approach can be applied to model the dynamic response of the pipe. Below, the consideration is given to the three particular cases that demonstrate the accuracy of the developed approaches.

4.5.1 Numerical Approach *versus* Exact Analytical Solution

In this sub-section, the results of the calculations are compared using the developed numerical approach with the exact analytical solution presented in Section 3.6. Recall that the dynamic behaviour of the pipe is controlled by two dimensionless parameters ε and β. In the case of a finite value of parameter β and when $\varepsilon = 0$, the governing equation (3.9) can be reduced to the classical beam equation; and the dynamic deflection of pipe (beam) can be obtained analytically. It can be written in the form of a series as described in Chapter 3, equation (3.13) and given below:

$$W(x,t) = \sum_{k=1}^{\infty} Y_k(x) \int_0^1 Y_k(u) \int_0^t F(u,\tau) \frac{\sin(\omega_k(t-\tau))}{\omega_k} d\tau du$$

where $\omega_k = \lambda_k^2$, k number of modes in the series solution. In the previous equation, Y_k are a set of normalised eigenfunctions corresponding to the solution of the homogeneous equation, i.e. $W_{,xxxx} + W_{,tt} = 0$. For a cantilever

$$Y_k(x) = A_k\left[\left(\cosh(\lambda_k x) - \cos(\lambda_k x)\right) - c_k\left(\sinh(\lambda_k x) - sin(\lambda_k x)\right)\right] \quad ,$$

$$c_k = \frac{\cosh(\lambda_k) + \cos(\lambda_k)}{\sinh(\lambda_k) + \sin(\lambda_k)} \quad ,$$

with $\lambda_1 = 1.8752$, $\lambda_2 = 4.6942$, $\lambda_3 = 7.8849$, $\lambda_4 = 10.9956$, $\lambda_5 = 14.1373$ and λ_k $(k \geq 6) \approx (2k-1)\pi/2$.

The numerical calculations are conducted for a pipe with fixed left end ($x = 0$) and while the right end ($x = 1$) is free. The corresponding boundary conditions are given by equations (4.12) to (4.22). The results of the numerical and analytical calculations are

shown in Figure 4.3 for the displacement of the pipe's free end ($x = 1$) for the total of 2 and 10 first terms in the analytical series solutions (3.16). In this figure, the pipe displacement W was normalised by the magnitude of the applied load. The impulse loading of magnitude, f_a, is applied at the half-way point along the pipe length ($x^* = 0.5$) for duration of $\Delta t = 0.025$. The analytical solution based on first 10 term series expansion agrees very well with the results obtained from the numerical approach with the spatial and time steps: $\Delta x = 0.02$ (or $N_x = 40$) and $\Delta t = 0.00005$, respectively. In this case, the both graphs are virtually not distinguishable, which indicates a very good accuracy of the numerical approach as well as applicability of the finite-size spatio-temporal distribution adopted in the numerical approach to model impulse loading.

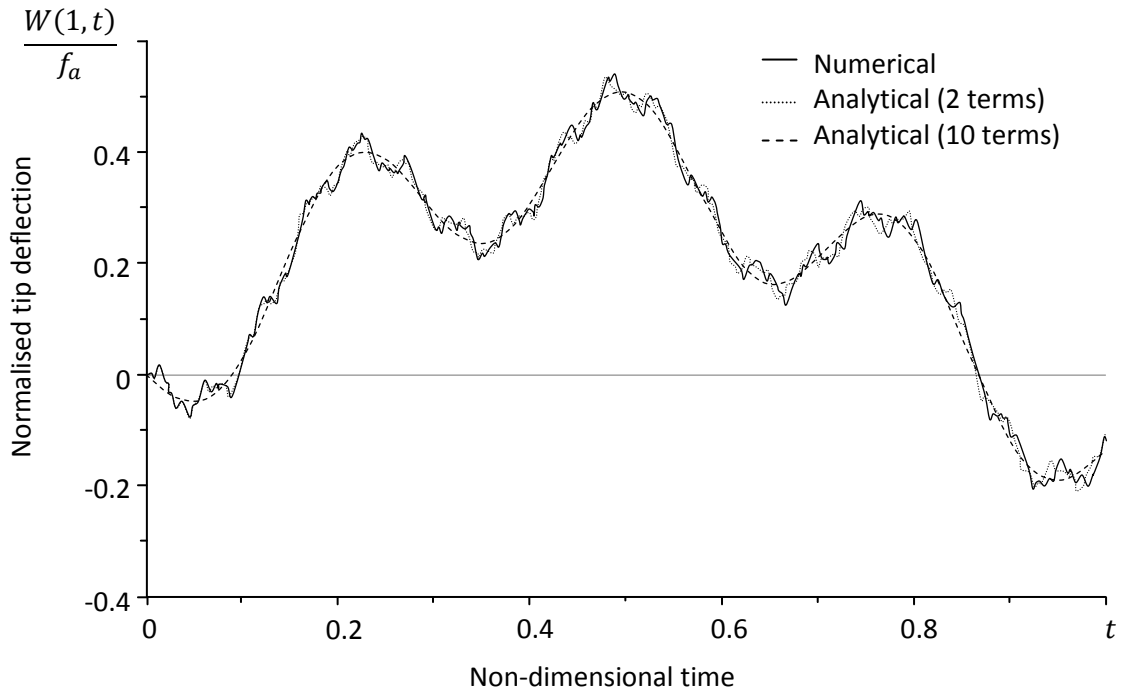**Figure 4.3: Comparison of the exact analytical (3.16) and numerical solutions for**

$$\varepsilon = \beta = 0$$

As time increases, the error in the numerical solution starts to build up due to the numerical approximations and the finite spatial and temporal grid sizes. Reducing the grid sizes will further improve the numerical results; however, this will be at the cost of increased computational requirements.

4.5.2 Numerical Solution *versus* Asymptotic Analytical Approach

For small values of the controlling parameters, the developed perturbation approach via equations (3.18) to (3.20) is implemented. Figure 4.4 displays the first-order perturbation correction (only one term was retained from the analytical asymptotic solution) for the case of $\varepsilon = 0.2$ and $\beta = 0.1$, along with the numerical results. Calculations were performed for a cantilever pipe the left end of which was fixed and the right end is free. The results shown in Figure 4.4 are for the pipe free-end displacements in the case of an impulse load applied as described previously at the pipe mid-point. The numerical and analytical results again match well with any differences being due to only using the first-order perturbation correction and, as before, the finite approximations of the numerical approach.
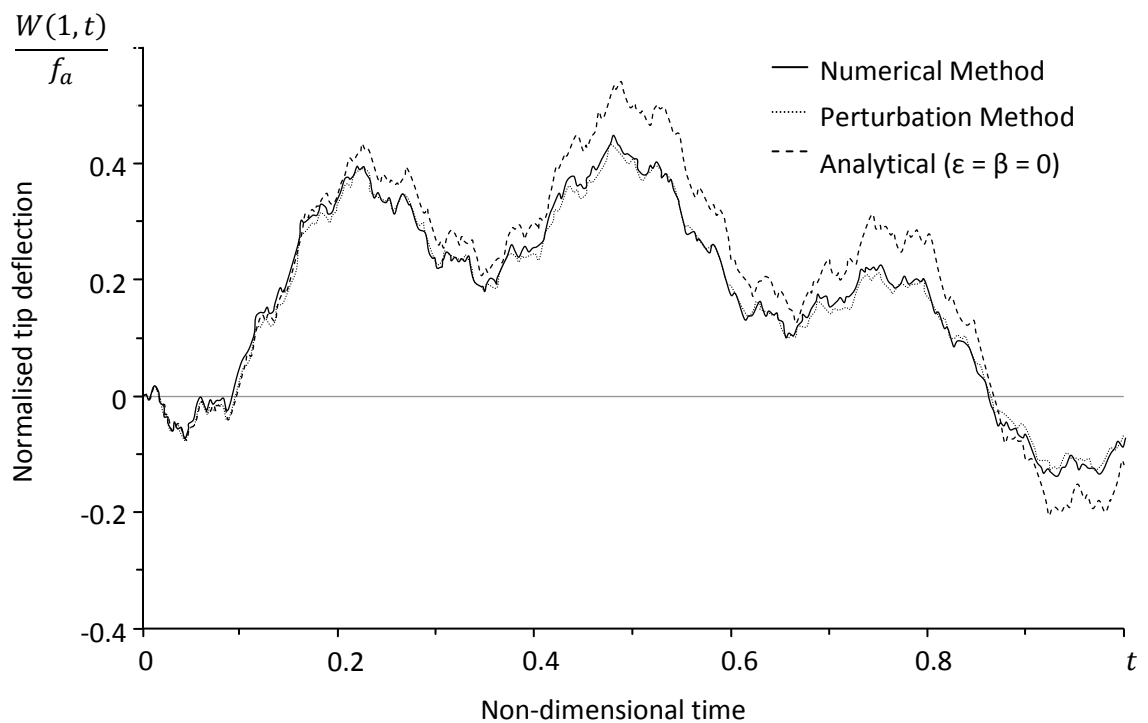
Figure 4.4: Comparison of the analytical and numerical solutions for $\varepsilon = 0.2$ and $\beta = 0.1$, analytical solution for $\varepsilon = \beta = 0$ is given for comparison only

The following results describe the transient response of a simply supported pipe. The impulse load of magnitude, f_a, is applied, in this case, again at the half-way point along the beam length ($x^* = 0.5$). Figure 4.5 displays the first-order perturbation correction calculations for the case of $\varepsilon = 0.2$ and $\beta = 0.1$, along with the numerical results, for the displacements in the centre of the pipe. In this figure, the pipe displacement W has been normalised by the magnitude of the applied load, f_a, and the following computational parameters: $\Delta x = 0.02$ (or 40 subdivisions) and $\Delta t = 0.00005$ is used.

As can be seen from Figure 4.5, the numerical and analytical results match very well. Although both graphs are almost not distinguishable, as time increases, the error in the numerical and analytical solutions starts to build up due to the numerical approximations, and the asymptotic nature of the perturbation approach.
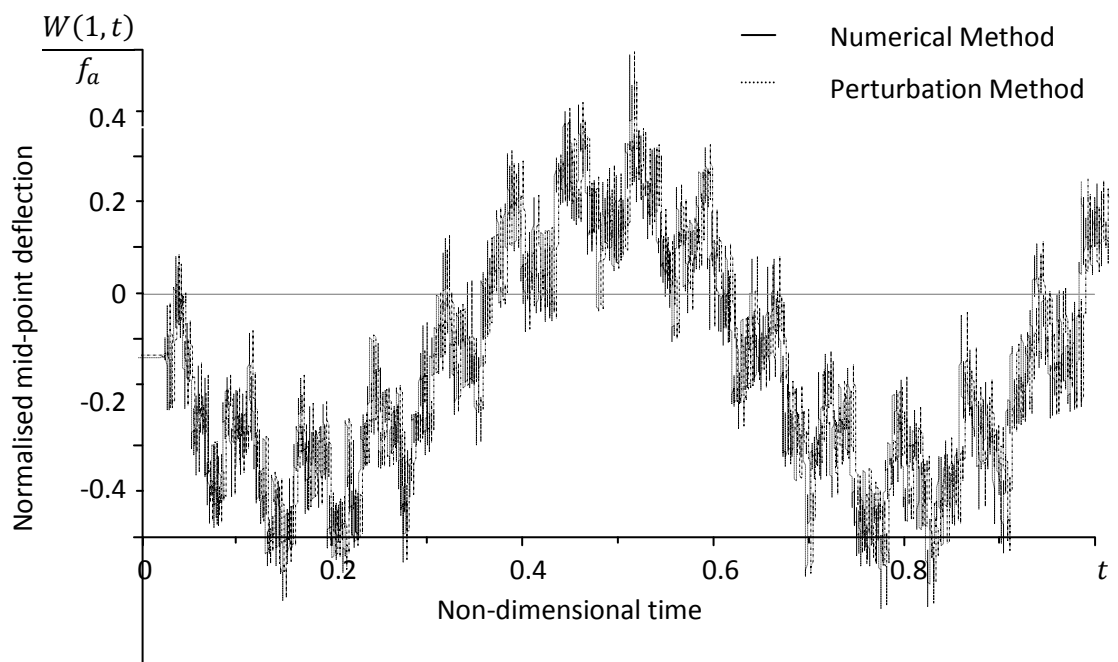

Figure 4.5: Comparison of the analytical and numerical solutions for ε =0.2 and β = 0.1 (the numerical and perturbation graphs are not distinguishable in this case)

4.6 Summary

In this chapter, the central finite-difference scheme was developed for the analysis of the governing equation describing the dynamic behaviour of pipes with flowing medium. The variables in this approach, such as the time step and number of spatial grid points, were selected from computational results testing the convergence and stability of the numerical scheme. Further, a validation study was completed that demonstrated a high accuracy and good convergence of the numerical approach. The numerical approach was also used to validate the previously developed perturbation approach (see Chapter 3). This demonstrated that both approaches are in agreement and can be confidently applied. Due to technical difficulties with the development of analytical solutions using perturbation approach as well as its limitations (the assumption that the flow has a relatively small influence on the pipe response), the numerical approach developed in this chapter will be a major tool for the investigation of the effect of parameters of the flowing medium on the transient response of the pipe to be presented in Chapter 5.

CHAPTER 5

EFFECT OF THE INTERNAL FLOW

ON DYNAMIC RESPONSE

5.1 Introduction

This chapter presents a systematic study of the effect of the flowing medium on dynamic response of circular pipes subjected to impulse loading. The numerical approach developed in the previous chapter is used to investigate the influence of the boundary conditions, flow speed and its density on the dynamic behaviour of pipes. It was demonstrated in Chapter 3 that within the adopted assumptions and simplifications, the dynamic response of a pipe transporting gas or liquid is governed by two dimensionless parameters

$$\varepsilon = \frac{VL\lambda_f}{\sqrt{EI(\lambda_p + \lambda_f)}} \qquad\qquad (3.8b)$$

and

$$\beta = VL\sqrt{\frac{\lambda_p + \lambda_f}{EI}} \qquad\qquad (3.8c)$$

where λ_f and λ_p are the   fluid and pipe densities per unit length; E represents Young's modulus of the pipe's material, I is the second moment of inertia of the cross-sectional area of the pipe, L is the characteristic length of the pipe and V is the speed of the flowing gas or liquid or their mixture.

Therefore, the effect of the flowing medium on the dynamic response of pipes will be expressed through these two parameters. An increase of the flow speed or its density will lead to the increase of ε and β. While parameters ε and β are proportional to the flow speed, the change of the flow density (linear density) is proportional to the product of ε and β.

First, general features of the dynamic response of pipes will be investigated and characterised. After that, a sensitivity study will be carried out to quantify the effect of the above dimensionless parameters on the dynamic response of the pipe subjected to impulse loading. Then, an important dynamic effect, a possible unstable behaviour of

the pipe, so-called pipe whip, will be investigated numerically and analytically. The effect of the boundary (support) conditions will be studied leading to a simple engineering criterion that can be used to avoid the unstable behaviour of a pipe during accidents such as, for example, full bore rupture of a high-pressure pipeline. Further examples will demonstrate that the developed criterion is relevant to the typical high-pressure aboveground pipelines, which are now allowed to be built in remote areas.

5.2 General Features of Dynamic Response

The numerical simulations with various controlling parameters ε and β reveal two principally different types of behaviour of a pipe subjected to impulse loading: stable decay behaviour (a typical response is shown in Figure 5.1) and unstable behaviour (a typical response is shown in Figure 5.2). As in the previous chapter, the impulse load of magnitude f_a was applied at the mid-point of the pipe. The figures plotted below represent the normalised deflection of the tip mid-point of pipes as a function of the non-dimensional time.
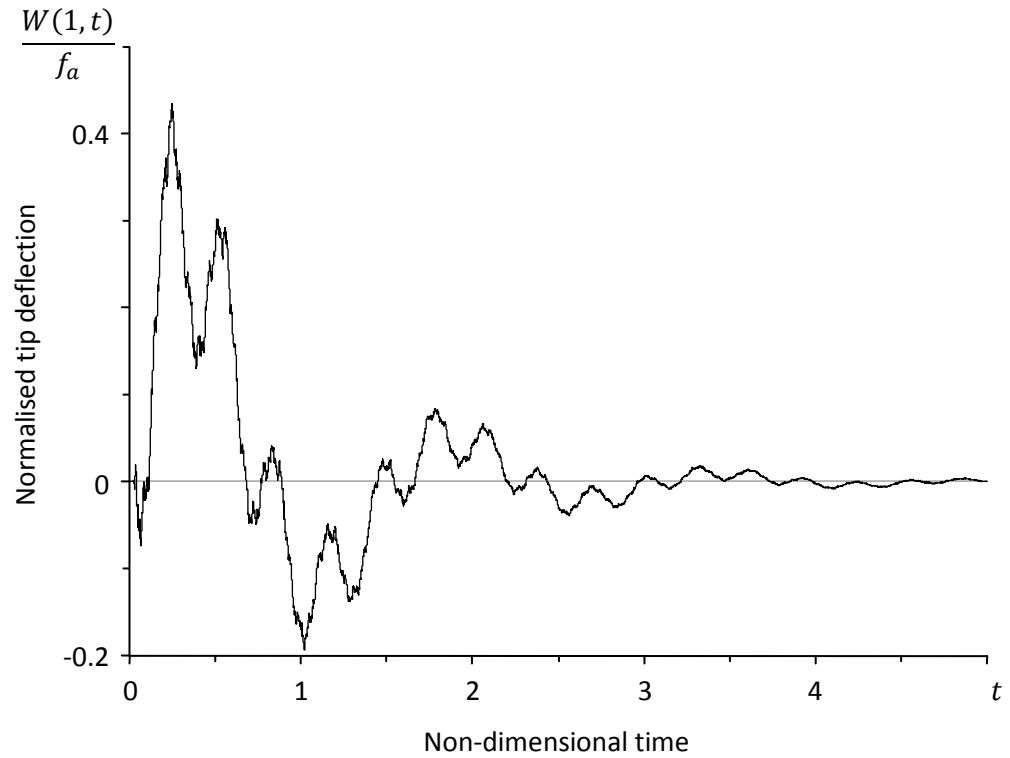
Figure 5.1: Example of stable response of a cantilever pipe with flowing medium (at ε=0.5 and β=10)

The numerical results were obtained with a spatial grid size of $\Delta x = 0.02$ and time step, $\Delta t = 0.00005$, this provides the stability factor of 0.125, which is well below the critical factor, 0.5. From the validation study in the previous sections, it was demonstrated that these parameters ensure stability of the numerical finite-difference scheme as well as good accuracy.

The stable type behaviour (see Figure 5.1) is associated with a transient response of the pipe having a magnitude that decays with time. The effect of the flowing medium in this case is that it provides a damping on the transient pipe response.
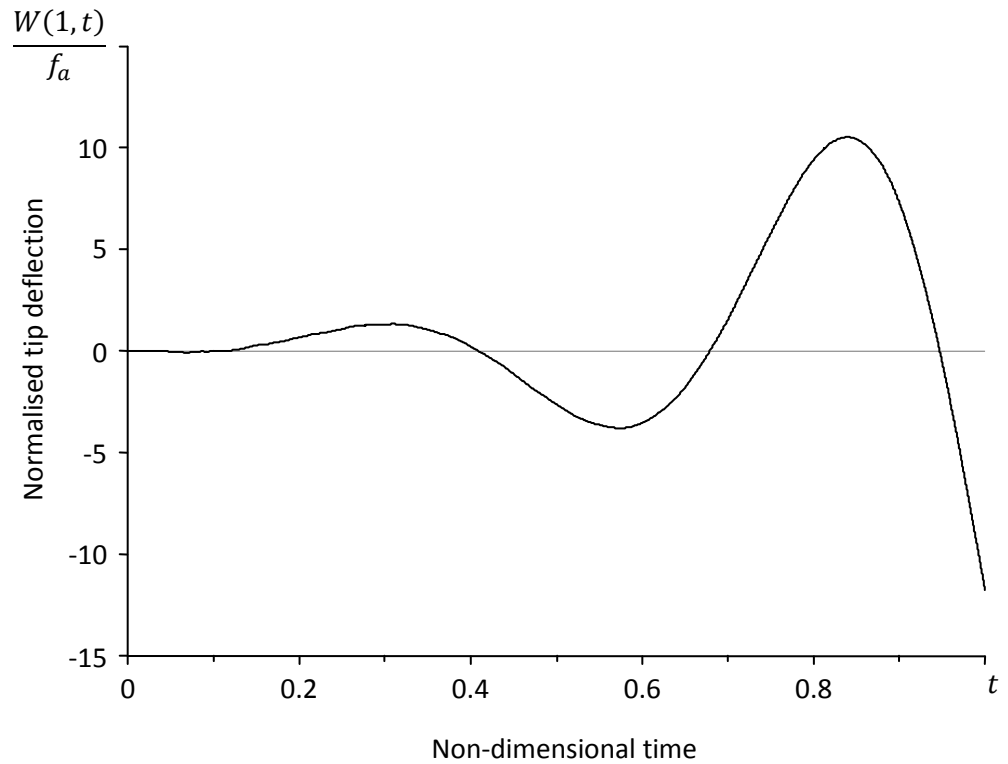
68

$$\frac{W(1,t)}{f_a}$$

Figure 5.2: Example of unstable response of a cantilever pipe with flowing medium (at $\varepsilon = 0.5$ and $\beta = 60$)

The opposite takes place for the unstable type of dynamic behaviour. In this case, the presence of the internal flow serves as a source of an additional energy, powering the development of growing unbounded deflections, i.e. dynamic instability (see Figure 5.2). It was found numerically that the unstable behaviour is a property of the system (pipe-flowing medium) and is independent of the location and amplitude of the applied impulse loading regardless of the location of the applied force. It means that regardless of the magnitude and location of the applied dynamic loading, the pipe will experience growing and unlimited deflections. Of course, in practical situations, the amplitude of the pipe deflections will be limited due to non-conservative energy consumption mechanisms, such as friction or thermal dissipation.

Later in this chapter, the critical conditions of the dynamic instability will be investigated in detail using numerical and analytical approaches. Further, the effect of variation of the dimensionless controlling parameters on the dynamic response will be systematically studied.

69

5.3 Effect of Dimensionless Parameters and Boundary Conditions on Dynamic Response

Figures 5.3 and 5.4 show the transient beam deflection of the tip of the cantilever pipe (fixed-free support condition) subjected to impulse loading for various combinations of dimensionless parameters ε and β.
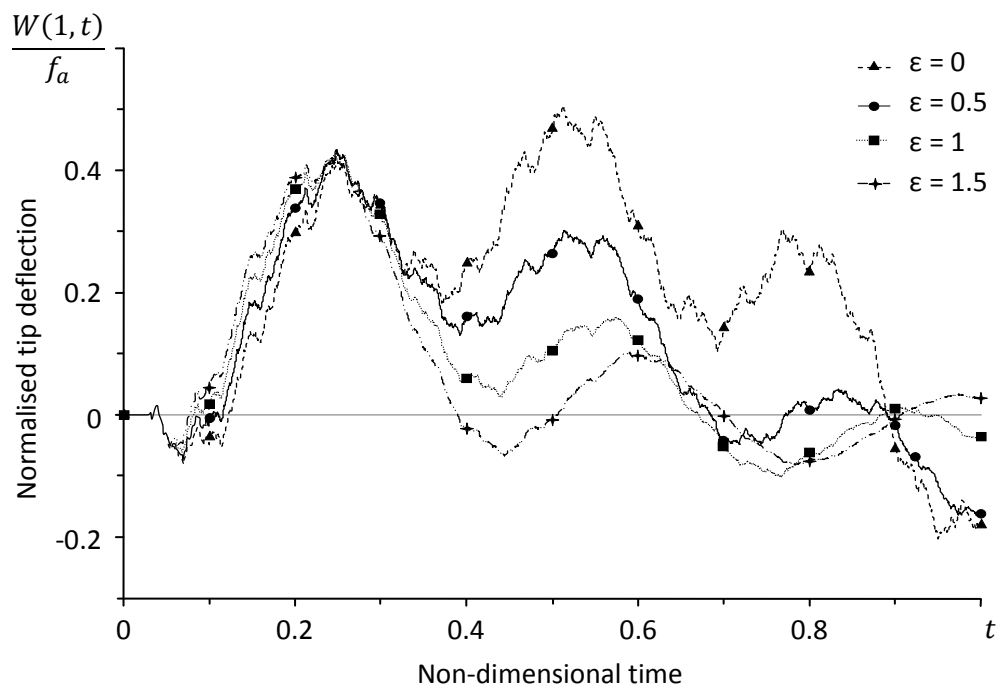

Figure 5.3: Transient response of a cantilever pipe for various values of ε while parameter β is kept constant ($\beta = 10$)

Figure 5.3 depicts a transient response of a cantilever pipe for various values of ε while parameter β is kept constant. From this figure, one can see that the magnitudes of the normalised deflections are decreased with increase of ε. Thus, this parameter can be associated with damping properties of the system and the increase of this parameter leads to a faster dissipation of the energy supplied by the impact loading.

Figure 5.4 shows a transient response of a cantilever pipe for various values of β while dimensionless parameter ε (both parameters are defined in the beginning of this chapter as well as in Chapter 3) is kept constant.
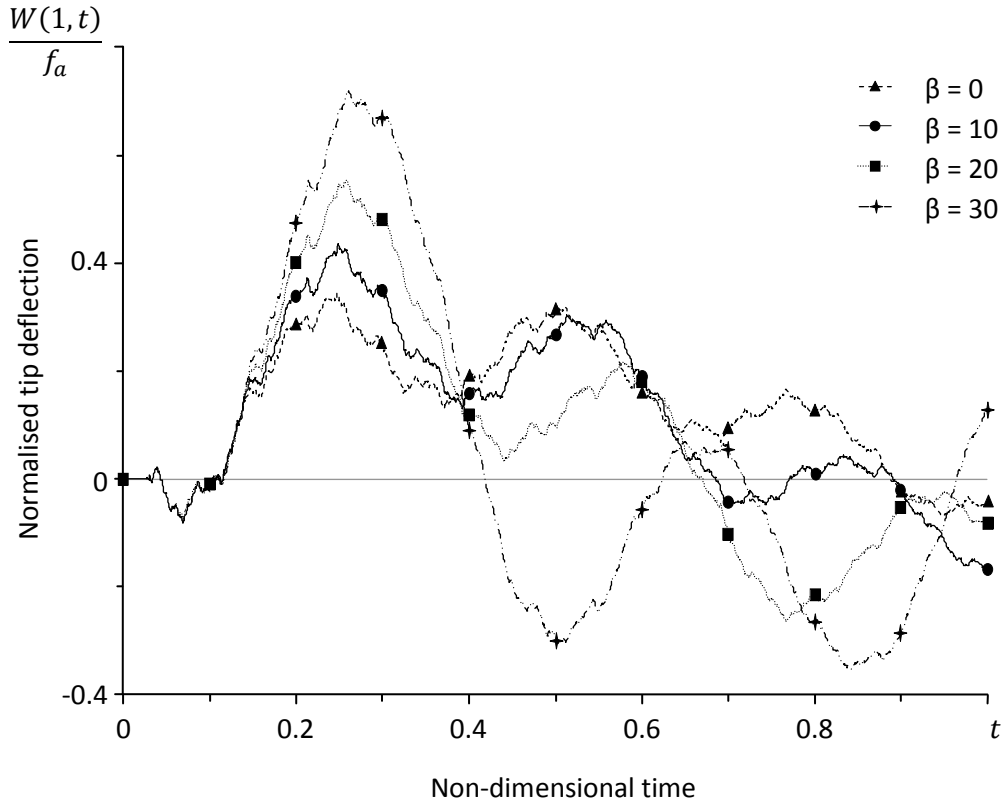

Figure 5.4: Transient response of a cantilever pipe for various values of β while dimensionless parameter ε is kept constant ($\varepsilon = 0.5$)

In the above figure, the parameter β was set at 0, 10, 20 and 30 with $\varepsilon = 0.5$. In contrast to the previous numerical test, the magnitudes of the normalised deflections are increased with time with the increase of the magnitude of β. Thus, higher values of parameter β lead to decreasing the damping properties and, likely to lead to the initiation of the dynamic instability of the system.

To confirm these general tendencies, a number of simulations will be presented for different boundary conditions, which encastre pipe, propped cantilever pipe and simply supported pipe.

71

5.3.1 Encastre Pipe

Figure 5.5 shows a transient response of an encastre pipe (fixed-fixed support condition), for various values of ε while parameter β is kept constant.
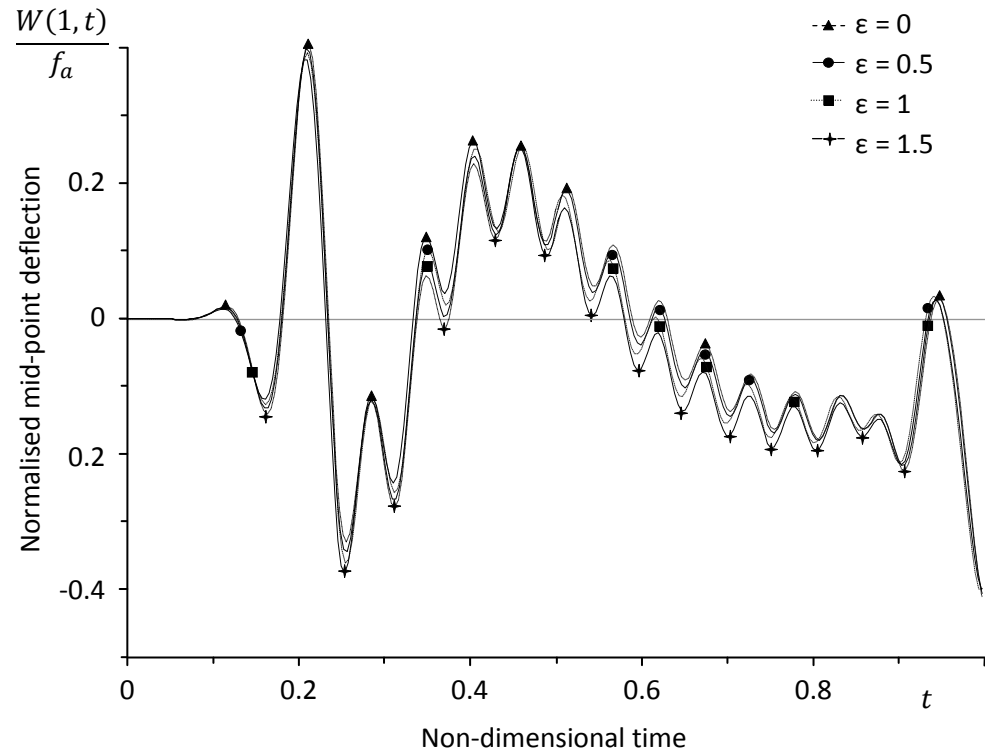

Figure 5.5: Transient response of an encastre pipe for various values of ε while parameter β is kept constant ($\beta = 10$)
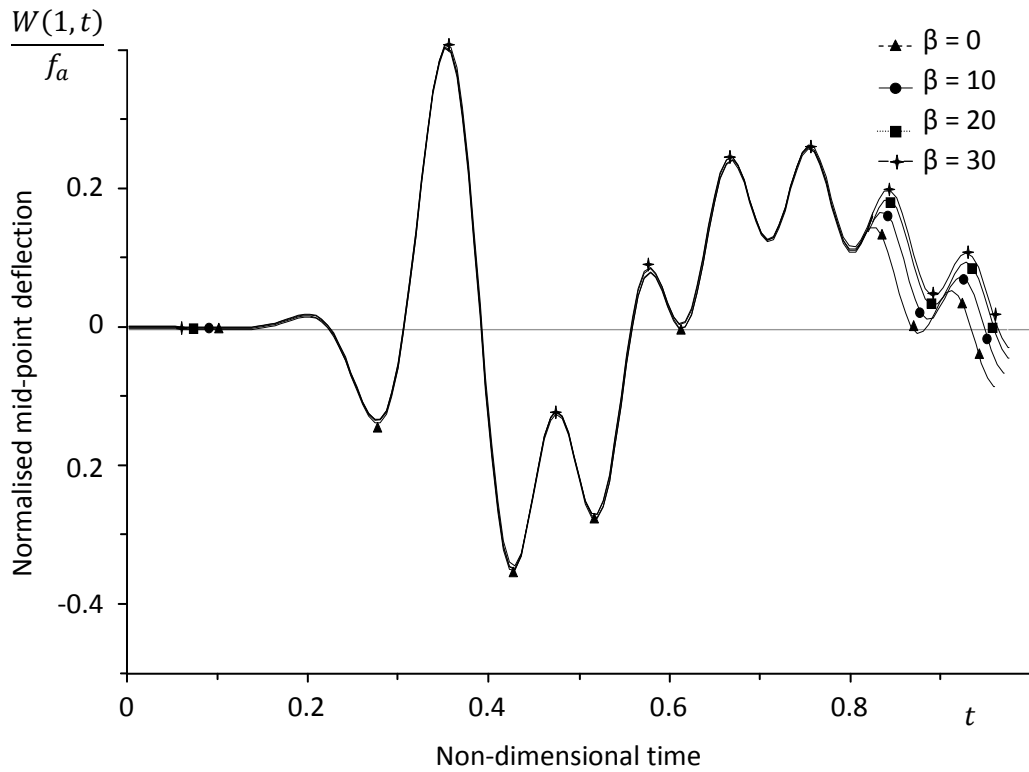
Figure 5.6: Transient response of an encastre pipe for various values of β while dimensionless parameter ε is kept constant ($\varepsilon = 0.5$)

From Figures 5.5 and 5.6, one can see that the effect of flow damping when changing dimensionless controlling parameters is significantly weaker in comparison with the previous case (cantilever pipe). This is obviously connected with the boundary conditions, which in the current case provide more resistance against any unstable behaviour, similar to the classical theory of instability of long flexural beams. However, the general tendencies essentially stay the same: an increase of parameter ε leads to a faster dissipation of the energy supplied by the impact loading and an increase of parameter β leads to a reduction of the dissipation due to the internal flow.

5.3.2 Propped Cantilever Pipe

Figure 5.7 shows a transient response of a propped cantilever pipe (fixed at the left end and simply supported at the right condition) for various values of ε while parameter β is kept constant. All simulations are limited by dimensionless time $t = 1$, after this time, the dynamic behaviour is essentially the same; however, the magnitude of the deflections steadily decays. One can see two major modes of the dynamic response: one is associated with global mode of vibration of the pipe and the second mode is related to the transient response of the pipe to impact loading.

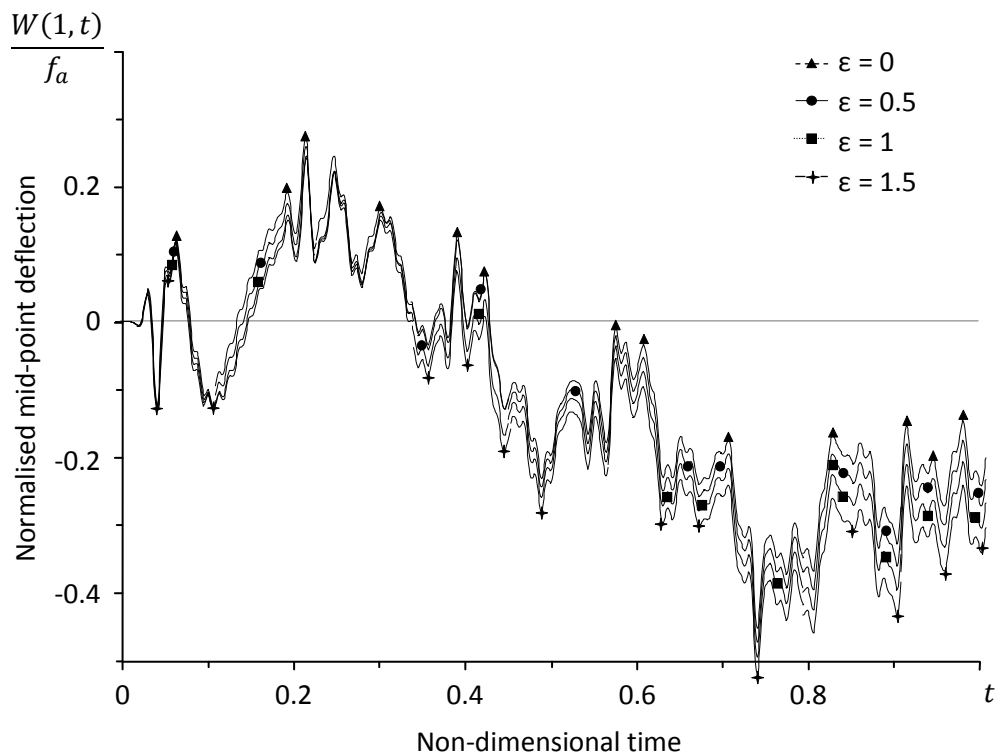

Figure 5.7: Transient response of a propped cantilever pipe for various values of ε while parameter β is kept constant ($\beta = 10$)

Figure 5.8 shows a transient response of a propped cantilever pipe for various values of β while dimensionless parameter ε (both parameters are defined in the beginning of this chapter and in Chapter 3) is kept constant.
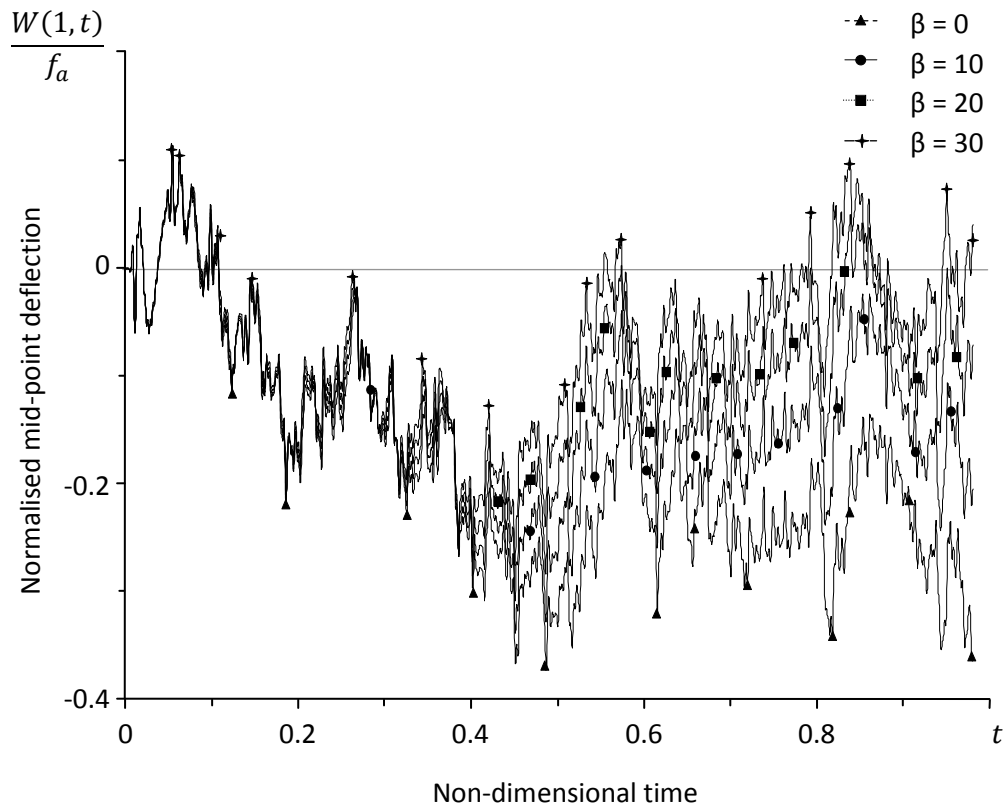
Figure 5.8: Transient response of a propped cantilever pipe for various values of β while dimensionless parameter ε is kept constant ($\varepsilon = 0.5$)

5.3.3 Simply Supported Pipe

Figure 5.9 shows a transient response of a simply supported pipe for various values of ε while parameter β is kept constant and Figure 5.10 shows a transient response of the same type of boundary conditions for various values of β while dimensionless parameter ε is kept constant.

Figure 5.9 also shows the transition from stable behaviour at $\varepsilon = 0$ and 0.5 to unstable behaviour, which takes place at $\varepsilon = 1$. This is characterised by an unlimited deflection of the pipe.

Figure 5.9: Transient response of a simply supported pipe for various values of ε while parameter β is kept constant ($\beta = 10$)
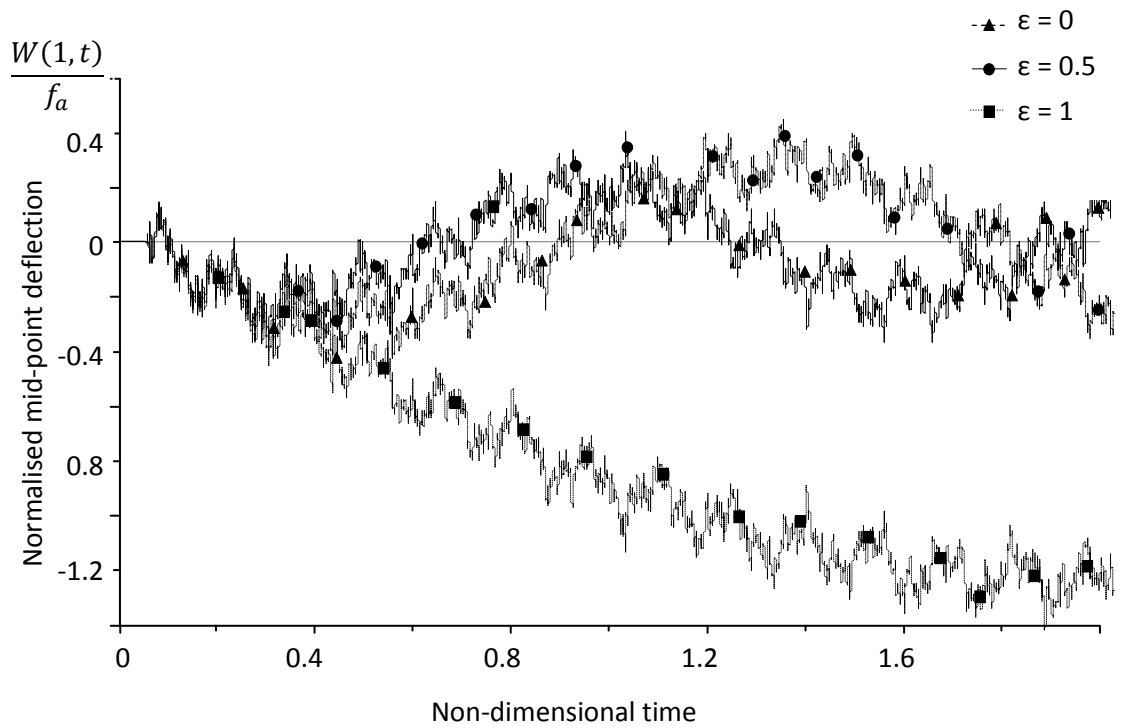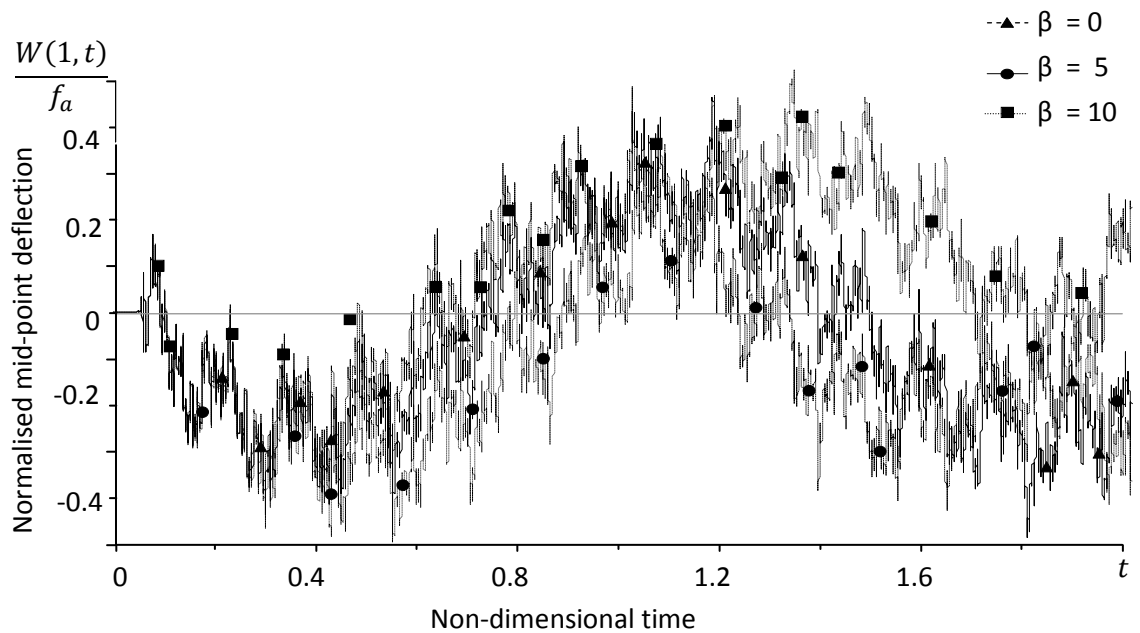
Figure 5.10: Transient response of a simply supported pipe for various values of β while dimensionless parameter ε is kept constant ($\varepsilon = 0.5$)

5.4 Initiation of Instability (Pipe Whip)

The stability of pipes conveying a fluid was first recognised by Marcel Brillion in 1885, [85,90], but it did not attract much attention from the research community until the 1950s, when RH Long, Jr began his pioneering investigations [91]. However, his approach pertained to the pipes with relatively small velocities of the internal flow, considerably below the threshold of instability. In fact, it seems he was unaware of an instability threshold. Instead, he perceived and confirmed by experimentation that, in contrast to simply supported pipes, forced motions of cantilevers are damped by internal flow at relatively low flow velocities.

In 1963, Gregory and Paidoussis [91–93] became the first researchers to confirm both theoretically and experimentally that at sufficiently high flow velocities, cantilevered pipes are subject to oscillatory instability (flutter) behaviour. They also pointed out that

at zero flow velocity, the cantilever pipe system under consideration was lightly damped with the pipe oscillated in its first dynamic mode. At a somewhat higher flow velocity, the system became critically damped. At higher flow velocities, the system became less heavily damped and the pipe oscillated in its second mode. With a further increase in flow velocity, the pipe eventually became unstable spontaneously. Gregory and Paidoussis [91–93] reported further that decreasing the flow velocity to the point where instability first occurred did not avoid the oscillation in progress. These facts, along with the reported results that show the onset of instability depended upon the amplitude of the applied excitation displacement, vividly demonstrate the non-linear behaviour of the cantilever system.

The conditions discussed above of the initiation of the dynamic instability for a cantilever are also very important in the aerospace industry, when designing nozzles of rocket engines. The nozzle of a rocket engine can be viewed as a cantilever with variable flexibility along the length, and the high speed of the gas, which is a product of burning reaction in the chamber of the rocket engine, passing through the nozzle can cause the similar dynamic instability of the rocket engine [15,84].

A new impulse for more thorough investigations of possible unstable behaviour of pipes was caused by the recent release of AS 2885.1-2007. Before this release, the Australian pipeline standards mandated burial for all cross-country pipelines carrying gas. It was realised that in the case of a full bore failure of an aboveground pipeline, the unstable behaviour of the pipe can represent a potential threat to structures and people in the vicinity of the pipeline. Therefore, when designing aboveground pipelines, the possible instability mechanisms must be avoided at the design stage or, alternatively, special measures have to be undertaken to avoid or minimise the consequences of pipe failures. Such an engineering criterion will be formulated later in this chapter.

First, it will be demonstrated that the unstable behaviour of pipes transporting gas or liquid is possible for other boundary conditions then those considered earlier in previous studies (i.e. for cantilever pipe).

Figures 5.11 and 5.12 demonstrate the development of dynamic instability for a propped cantilever pipe and simply supported pipe, respectively. Therefore, the unstable behaviour is also possible in the case of other boundary conditions.
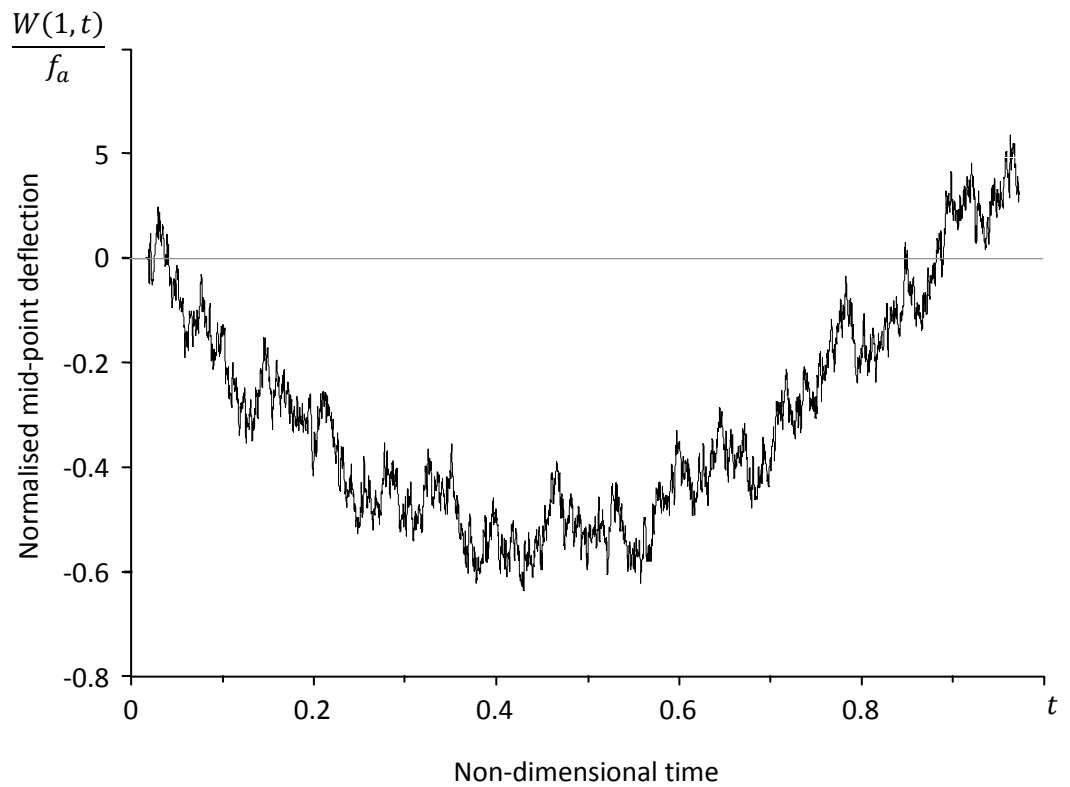

Figure 5.11: Unstable behaviour (initiation of dynamic instability) of a propped cantilever pipe at $\varepsilon = 1$ and $\beta = 5$
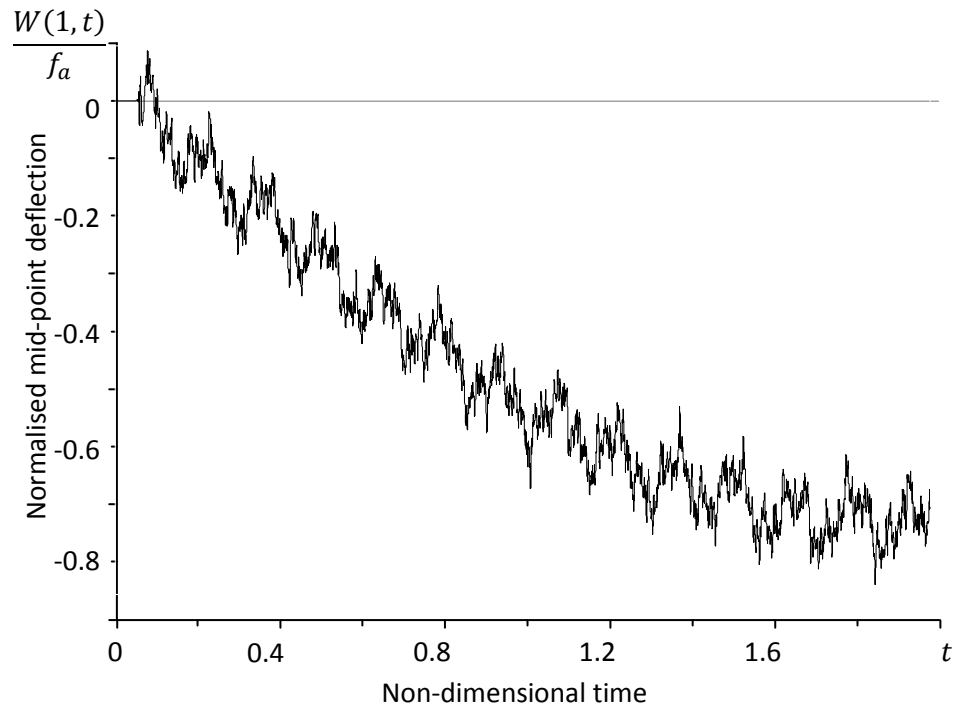
Figure 5.12: Unstable behaviour of a simply supported pipe characterised by dimensionless parameters $\varepsilon = 1$ and $\beta = 10$

In the next section, an analytical approach to the instability of pipes transporting gas or liquid will be presented and validated through numerical simulations. This analytical approach will result in the formulation of an engineering criterion to avoid the possible unstable behaviour of high-pressure pipelines.

5.5 Analytical Modelling Approach to Instability in Pipes

In this section, consideration is given to conditions corresponding to the initiation of the dynamic instability of the pipe. For the convenience of the reader, the homogeneous governing equation of a pipe with the flowing medium is presented again below:

$$W_{,xxxx} + W_{,tt} + \varepsilon\left(2W_{,xt} + \beta W_{,xx}\right) = 0. \tag{3.9}$$

Further, assuming the solution in the form

$$W(x,t) = w(x)e^{(\eta+i\omega)t}, \tag{5.1}$$

then the governing equation (5.1) can be rewritten as

$$w_{,xxxx} + (\eta + i\omega)^2 w + \varepsilon\left(2(\eta + i\omega)w_{,x} + \beta w_{,xx}\right) = 0. \tag{5.2}$$

Mathematically, the dynamic instability takes place when the real part of exponent index $\eta + i\omega$ of the assumed solution (5.1) takes positive values. In this case, theoretically, the amplitude of oscillations can grow unbound with time. However, in practice, the amplitude of oscillations is limited and controlled by the damping properties of the pipeline structure, which always exist in real conditions. Neglecting the damping, the problem is reduced to determination of the domain of parameters ε and β variation, at which $\eta > 0$. Thus, at fixed ε and $\beta = 0$, we need to determine minimum β that satisfies equation (5.2) with an additional condition $\partial \eta / \beta > 0$ that corresponds to the transition from stable conditions to dynamic instability characterised by the growing amplitude of oscillations with time.

Following [83, 94, 95] we represent the solution in the interval $0 \le x \le 1$ in the following form

$$w(x) = \sum_{n=0}^{\infty} C_n x^n . \tag{5.3}$$

From the boundary conditions at the left end (fixed end) follows that $C_0 = C_1 = 0$. The remaining boundary conditions (free end) take the form

$$\sum_{n=0}^{\infty} C_n n(n-1) = 0 \tag{5.4a}$$

and

$$\sum_{n=0}^{\infty} C_n n(n-1)(n-2) = 0 \quad .$$ (5.4b)

Now, we transform the complex form of equation (5.2) to the real-valued one. Representing solution w as

$$w = w_1 + i w_2$$ (5.5)

and complex coefficients

$$C_n = A_n + i B_n \,,$$ (5.6)

such that

$$w_1 = \sum_{n=0}^{\infty} A_n x^n$$ (5.7a)

and

$$w_2 = \sum_{n=0}^{\infty} B_n x^n \,,$$ (5.7b)

where A_n and B_n are real constants, which can be obtained by substituting equations (5.5) to (5.7b) into equation (5.2) producing the following recurrent equations for the coefficients A_n and B_n:

$$A_n = \frac{1}{n(n-1)(n-2)(n-3)}\{-\varepsilon\beta A_{n-2}(n-2)(n-3)$$

$$-2\varepsilon\eta A_{n-3}(n-3) + (\omega^2 - \eta^2)A_{n-4}$$

$$+2\varepsilon\omega B_{n-3}(n-3) + 2\eta\omega B_{n-4}\}$$ (5.8a)

and

$$B_n = \frac{1}{n(n-1)(n-2)(n-3)}\{-\varepsilon\beta B_{n-2}(n-2)(n-3)$$

$$-2\varepsilon\eta B_{n-3}(n-3) + (\omega^2 - \eta^2)B_{n-4}$$

$$-2\varepsilon\omega A_{n-3}(n-3) - 2\eta\omega A_{n-4}\} \quad .$$ (5.8b)

With these equations, the boundary conditions (5.4a) and (5.4b) can be rewritten as

$$aC_2 + bC_3 = 0 \qquad\qquad (5.9a)$$

and

$$cC_2 + dC_3 = 0 \qquad\qquad (5.9b)$$

where a, b, c, d are complex constants.

Specifying, for example, $C_1 = 1$ ($A_1 = 1$ and $B_2 = 0$), and $C_3 = 0$ ($A_3 = B_3 = 0$), from equations (5.4a) and (5.4b) we have

$$a = \sum_{n=0}^{\infty} A_n n(n-1) + iB_n n(n-1) \qquad\qquad (5.10a)$$

and

$$c = \sum_{n=0}^{\infty} A_n n(n-1)(n-2) + iB_n n(n-1)(n-2)\,. \qquad\qquad (5.10b)$$

Similar to the previous case, if we specify $C_2 = 0$ and $C_3 = 1$, i.e. we set $A_2 = B_2 = B_3 = 0$, $A_3 = 1$, then we obtain

$$b = \sum_{n=0}^{\infty} A_n n(n-1) + iB_n n(n-1) \qquad\qquad (5.11a)$$

and

$$d = \sum_{n=0}^{\infty} A_n n(n-1)(n-2) + iB_n n(n-1)(n-2)\,. \qquad\qquad (5.11b)$$

where A_n and B_n are given by recurrent equations (5.8a) and (5.8b).

The condition of existence of a nontrivial solution for the homogeneous system of linear algebraic equations (34) is that the determinant formed from the coefficients must be equal to zero or

$$\det \begin{bmatrix} a & b \\ c & d \end{bmatrix} = 0 \tag{5.12}$$

from which the critical parameters of the initiation of the dynamic instability can be obtained by means of a simple numerical procedure for determining the roots of a non-linear algebraic equation.

The analytical approach assumes the cantilever-type boundary conditions. However, it can be easily generalised for other boundary conditions. Below, a particular problem relevant to pipeline industry will be considered. Namely, what would be conditions to avoid the dynamic instability in the case of full bore rupture of an aboveground high-pressure pipeline? As it is always difficult to model boundary conditions accurately for real problems, two limiting cases will be considered: pinned and clamped supports at the left end of the pipe, as shown in Figure 5.13.
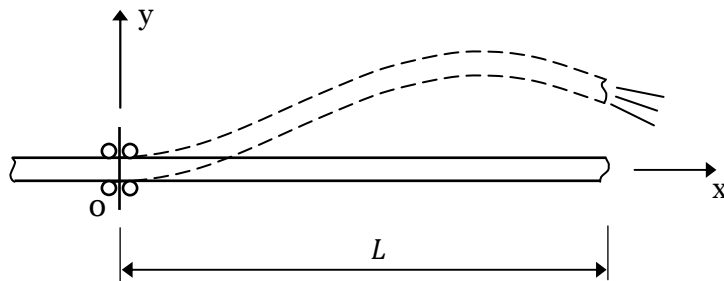
Figure 5.13: Dynamic instability

As explained previously, the strategy is to determine minimum β (at fixed ε and $\beta = 0$), which satisfies equation (5.2). An additional condition is $\partial \eta / \beta > 0$, which corresponds to the transition from stable conditions to dynamic instability characterised by the growing amplitude of oscillations with time. Results of the analytical calculations for two different support conditions are shown in Figures 5.14 and 5.15, where the region of the unstable behaviour is located above the solid line.

Figure 5.14: Critical parameters corresponding to the initiation of the dynamic instability when one end of the pipe is pinned and another one is free

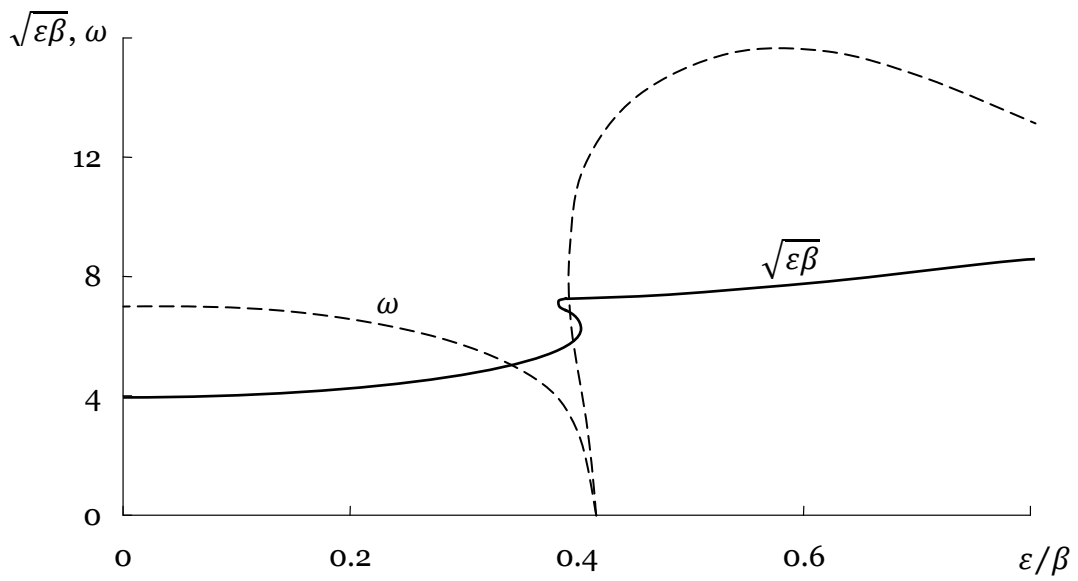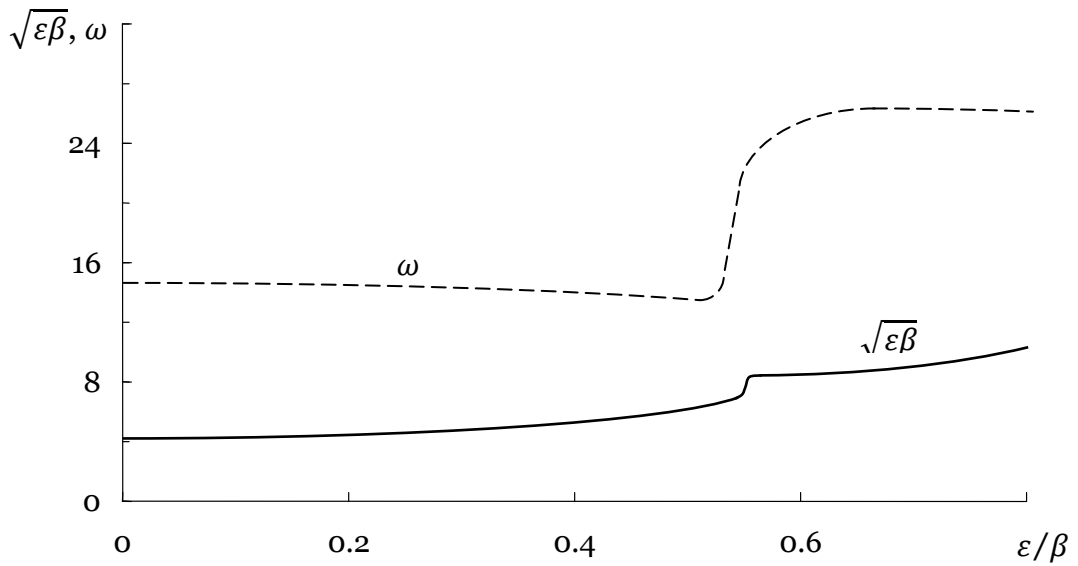**Figure 5.15: Critical parameters corresponding to the initiation of the dynamic instability when one end of the pipe is clamped, and another one is free**

85

These results show that for gas pipelines (when parameter $\varepsilon/\beta = \lambda_f/(\lambda_f + \lambda_p)$ is small) the criterion to avoid the initiation of the pipe whip, regardless of the support conditions, can be written as

$$\sqrt{\varepsilon\beta} = VL\sqrt{\frac{\lambda_f}{EI}} < 4 \tag{5.13}$$

The results of analytical calculations are also supported by numerical calculations using the approach developed in the previous chapter (see Figure 5.16). From this figure, one can see some differences between the analytical and numerical solutions, which are likely caused by the error in the numerical calculation and a criterion of instability implemented the numerical solution. The area below the curves corresponds to the case when flowing medium generates the damping effect and in the area above the theoretical curves, it powers the development of unstable and unbound deflections.
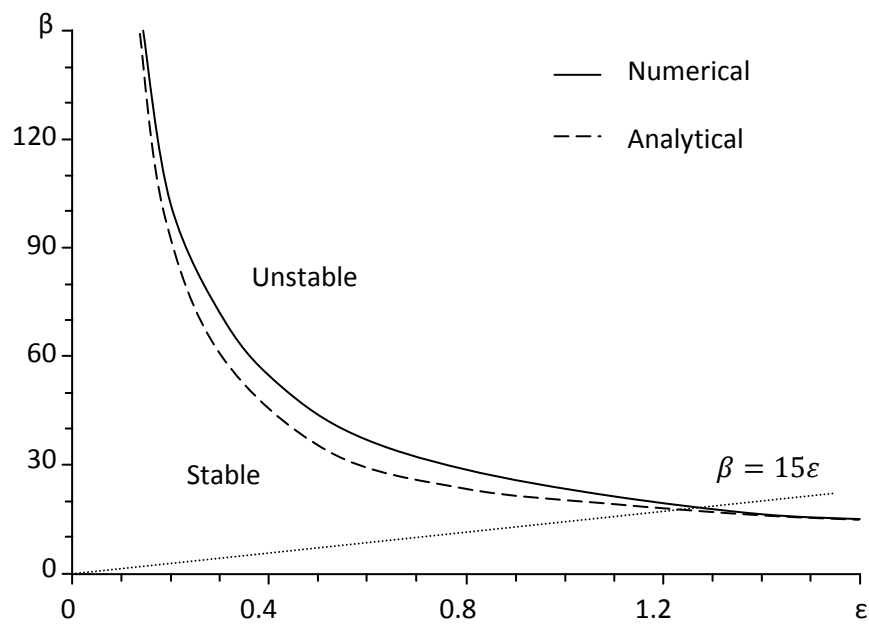

Figure 5.16: Critical conditions for initiation of dynamic instability for cantilever

5.6 Discussion and Conclusion

A numerical method to analyse the effect of flowing medium on the elastic transient response of a pipe transporting gas or liquid and subjected to dynamic loading was systematically employed in this chapter. It was previously demonstrated above that the dynamic response is governed by two non-dimensional parameters, namely ε and β, incorporating mechanical properties of the pipe and characteristics of the flowing medium. It was found that the first parameter (ε) increases the damping properties of the system and the increase of its value leads to the faster dissipation of the energy supplied by the external loading (impact). The other non-dimensional parameter (β) acts in the opposite way. An increase of its value reduces the damping properties of the system and can lead, eventually, to the initiation of dynamic instability.

As an example of the usefulness of the obtained results, the initiation of dynamic instability investigated in this work has to be considered a major risk factor for high-pressure aboveground pipelines as a full bore failure can provoke the development of such behaviour. In this case, significant damage can be expected due to chaotic movements of the pipe. The derived conditions of the initiation of instability can be considered a conservative estimate, as the present mathematical model does not take into account other important factors, for example, friction or gravity, which can contribute significantly into the damping properties and energy absorption mechanisms.

To assess the relevance of the derived conditions of the initiation of instability to practical problems, consider, for example, a full bore failure in a hypothetical aboveground gas flowline of a diameter $D_i = 160\ mm$ and wall thickness $t = 4\ mm$, subjected to operating pressure $P_0 = 10\ MPa$. Let the gas density at operating conditions be $\rho_0 = 100\ kg/m^3$ and the specific heat ratio of the gas, $\gamma = 1.3$, which represent typical values for raw natural gas. The velocity of the gas flow through the orifice can be roughly estimated using the simplified gas dynamics model presented [89] and this is found to be around 350 m/s. The gas flow density behind the decompression wave is approximately 60 kg/m^3. Further, we can find the ratio $\beta/\varepsilon = \frac{\lambda_p + \lambda_f}{\lambda_f} \approx 15$. The line $\beta = 15\varepsilon$ intersect the critical curve (see Figure 5.16) at

$\varepsilon = 1.25$. From equation (5.13), the critical length of the pipe is found to be around 15 meters.

This example explicitly demonstrates that the pipe whip phenomena or dynamic instability is relevant to the typical operating conditions normally occurring in high-pressure aboveground pipelines of relatively small diameter; and to avoid this potentially dangerous dynamic effect, the pipe has to be restrained against lateral movements, in the case considered above, every 15 meters. The anchor spacing can be increased by selecting pipes with large moment of inertia (lager diameter and wall thickness) and by reduction of the operating pressure or gas density.

The equations derived here may also be useful in reducing potential damage from other equipment working under high-pressure conditions. The criterion (equation 5.13) can be applied, for example, when designing pipe attachments, exhausts or dispensers of relatively small diameter or flexible connections.

It is important to mention that the derived model represents a simplest extension of the Bernoulli-Euler beam theory, and, of course, cannot capture all mechanisms and effects associated with pipe-flow interactions and more sophisticated models might be required for more accurate assessments. The latter will be a subject of further investigations.

CHAPTER 6

EXPERIMENTAL STUDY

6.1 Introduction

An experimental study was conducted to gain a further understanding of how the characteristic of the internal flow affects the transient response of circular pipes. The scope of the experimental study was limited to the case of a long flexible pipe with fixed-fixed support conditions or encastre pipe, as schematically shown in Figure 6.1. This configuration was selected because of the simplicity of the rig design and an ability to modify relatively easy the speed of the flow. The speed of the flow leads to the change of the dimensionless controlling parameters ε and β introduced in Chapter 3. All other parameters of the test rig including the pipe cross-section and span were kept constant. The dynamic response of the pipe to impulse loading was measured using a displacement sensor for a range of flow speeds. This will be discussed in detail in the following sections. This chapter first outlines the setup and experimental approach and then discusses the results derived from the experimental measurements.
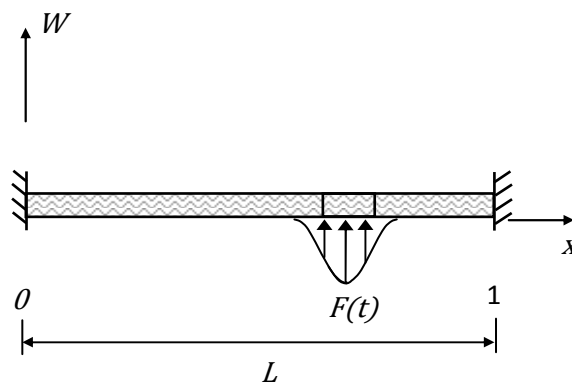

Figure 6.1: The schematic diagram of impact experiments

6.2 Experimental Setup

6.2.1 Flow Tank

Two flow tanks with the closed loop system have been designed and fabricated. The experimental rig consists of a supply tank that delivers fluid, which is tap water, to an open receiver tank through a 2 m long pipe section. The pipe section forms the working area to be used in the experimental study. This pipe section was fixed from both ends.

The supply tank is made from 10 mm thick PVC plates and the receiver tank is made from 10 mm clear acrylic plates to allow visualisation of the flow. Figure 6.2 shows a photo of the experimental setup and Figure 6.3 is the schematic diagram of the flow facility.
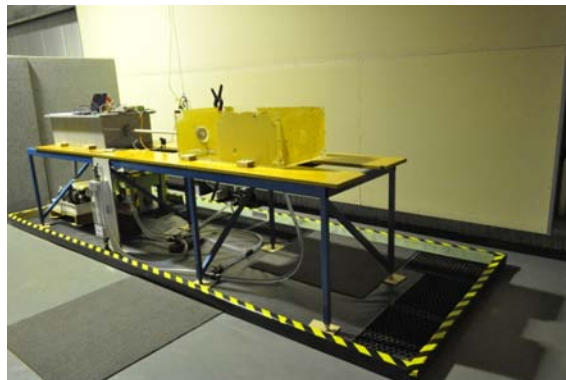
Figure 6.2: The experimental setup
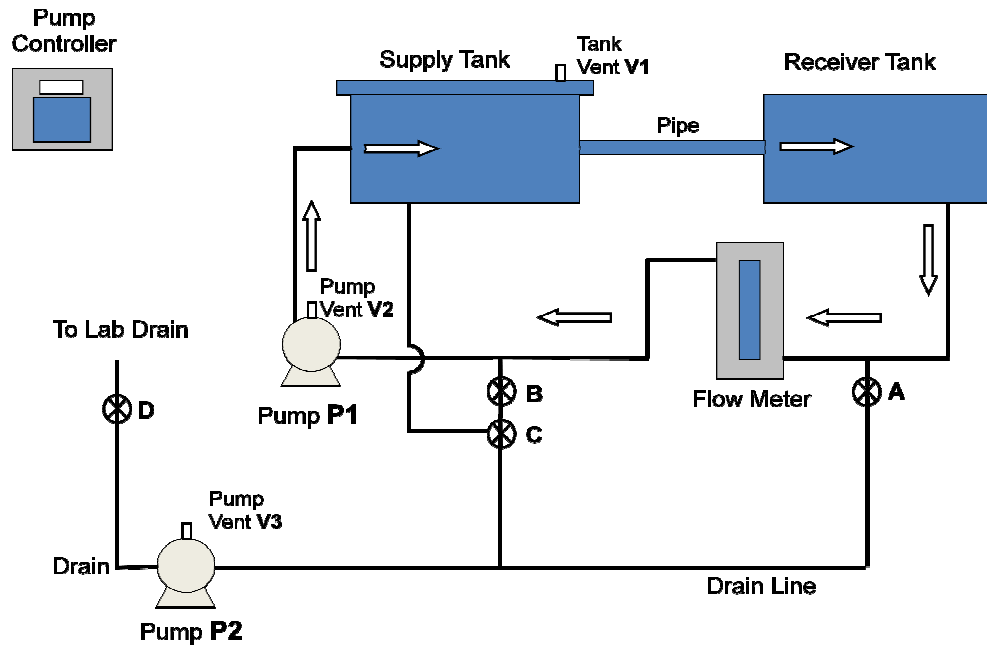
Figure 6.3: The schematic diagram of the flow facility

Flow circulation is achieved via a 2 hp 240 V Onga pump as shown in Figure 6.4. The pump delivers fluid through the supply tank to the pipe working section. The fluid (water) then flows into the receiver tank, out through a flow meter and back into the supply tank (see Figure 6.3). The pump is operated by a variable frequency controller that provides pump speeds from 0 to 25 Hertz.

Figure 6.4: A 2 hp 240 V Onga pump

The supply tank was designed to provide a low turbulence flow with uniform velocity distribution across the cross-sectional area of the pipe. This was achieved using a

carefully designed flow distributor at the inlet, followed by perforated plates and flow screens, discharging into a large settling chamber.

Figure 6.5: The supply tank with the top removed, showing the flow conditioning features
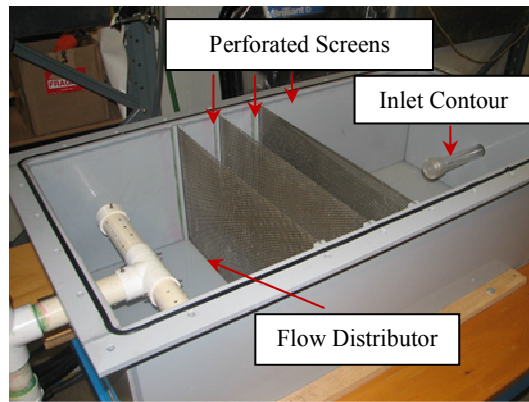
The flow entered the pipe through a contoured inlet, designed according to guidelines provided [96–101]. A 10 mm thick PVC plate is affixed to the top of the supply tank by 30 bolts. A rubber seal is used to prevent pressure leakage. Figure 6.5 is a photo of the supply tank with the top removed, showing the flow conditioning features.

A 20 mm inside-diameter polyvinyl chloride (PVC) pipe was used (with relatively low Young modulus $E = 3.4$ GPa, and the density, $\rho = 1.38\text{x}106\text{g/m3}$). The pipe length, L, was 2 m with the ends clamped to simulate the fixed-fixed support conditions. Although it should be noted that rubber-O-rings at the pipe connection to the tanks did allow some movement. In general, it is very difficult to achieve the idealised boundary conditions in practice. This represents a major source of discrepancies between analytical or numerical studies and experiment. The test pipe is connected between the receiver tank and supply tank. Figures 6.6 (a), (b) and (c) show the connection of the PVC pipe. The material of the pipe (PVC) was selected to ensure sufficient flexibility of the pipe, as it was demonstrated in Chapters 3 and 4 that the effect of the internal flow is negligible if the pipe has high bending stiffness.
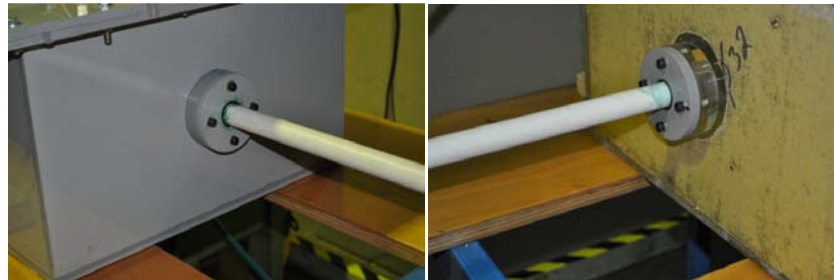
Figures 6.6 (a), (b) and (c): Fixed-fixed PVC pipe section

The flow velocity of the fluid was measured using a Solarton-Morbrey Crawley $1\frac{1}{2}''$ series no KS012342-2 variable-area flow meter (as shown in Figures 6.7 (a) and (b)). This provided a value for the volumetric flow rate, which was converted to flow velocity. The flow meter is driven by a variable frequency controller starting from 0 to 25 Hertz.
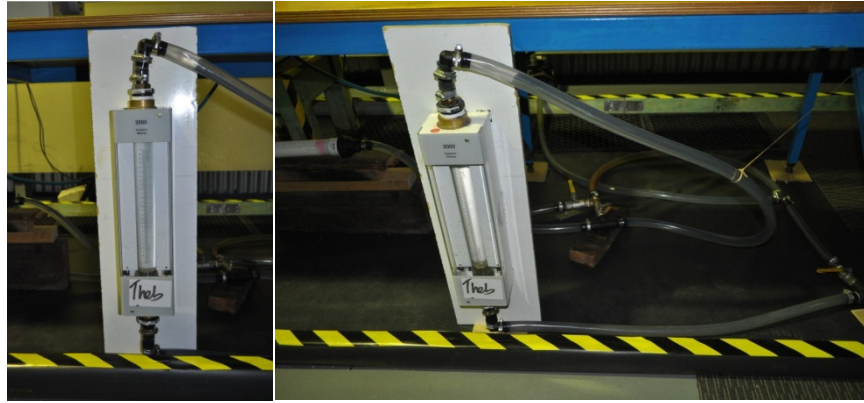
Figures 6.7 (a) and (b): A Solarton-Morbrey Crawley $1\frac{1}{2}''$ series no KS012342-2 variable-area flow meter to measure the flow rate.

6.2.2 Data Acquisition

To enable the investigation of the flowing medium the pipe response, it was necessary to measure the displacement of the pipe after it had been loaded by an impact force. This section discusses the transducers and data logging equipment used for the experiments.

A laser sensor, Wenglor YP05MGV80, was used to measure the deflection at the mid-point of the pipe. The reflex sensor has a working range of 43–53 mm (10 mm measuring range) and a resolution of less than $20\mu m$. The output of the sensor was a 0-10 V signal, which is proportional to the measured lateral deflection of the pipe. The sensor was placed on the pipe. This was chosen to be the mid-point where the maximum deflections are expected. The use of this sensor is justified by a very easy procedure for the alignment and measurements. The deflection-measuring laser setup is shown in Figures 6.8 (a), (b) and (c).
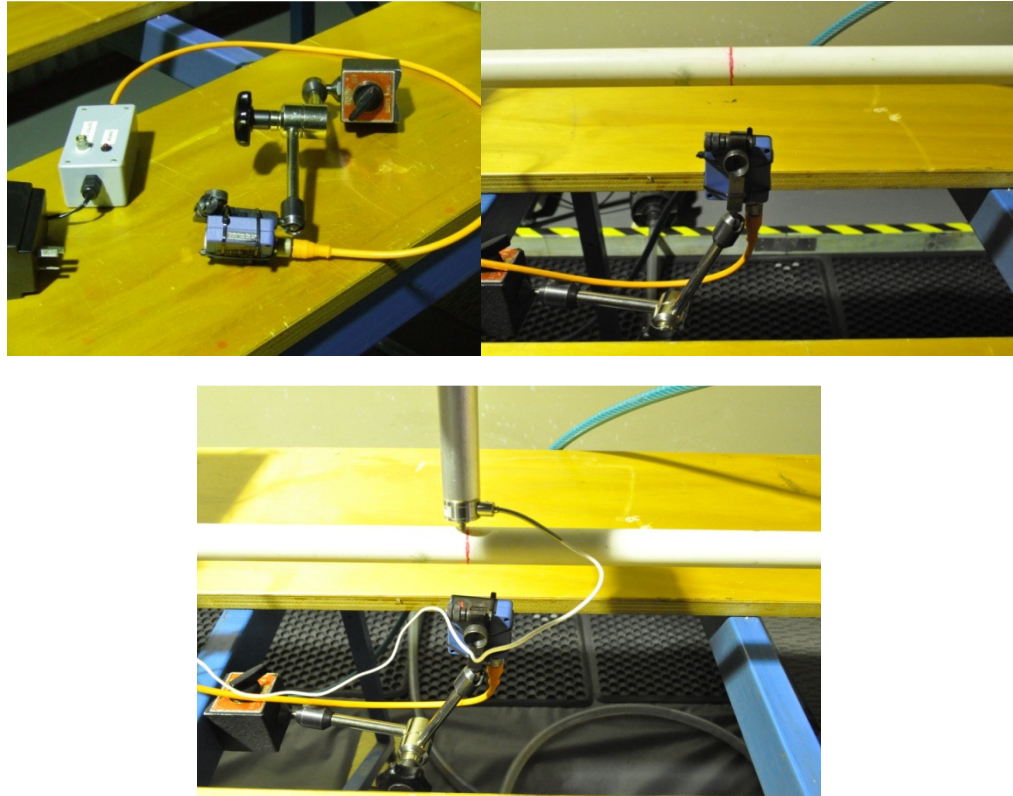
Figures 6.8 (a), (b) and (c): Sensor laser to measure deflection

The pipe was loaded by hitting it with a specially designed impact device. The device consists of a load cell attached to an aluminium handle. The load cell used was a WMC Miniature Sealed Stainless Steel load cell with a measuring capacity of ±50lbf. The load cell utilised strain gauges in a full bridge, which provides for temperature compensation and maximum sensitivity. Figures 6.9 (a) and (b) shows how the load cell is screwed onto the aluminium handle. When the handle is to be used to impact the pipe, the cover is taken off.

Figures 6.9 (a) and (b): Load cell is screwed onto the aluminium handle

Figure 6.10 shows the load cell that is fitted to the handle used to impact the pipe. The pipe was impacted at the mid-point along its length.
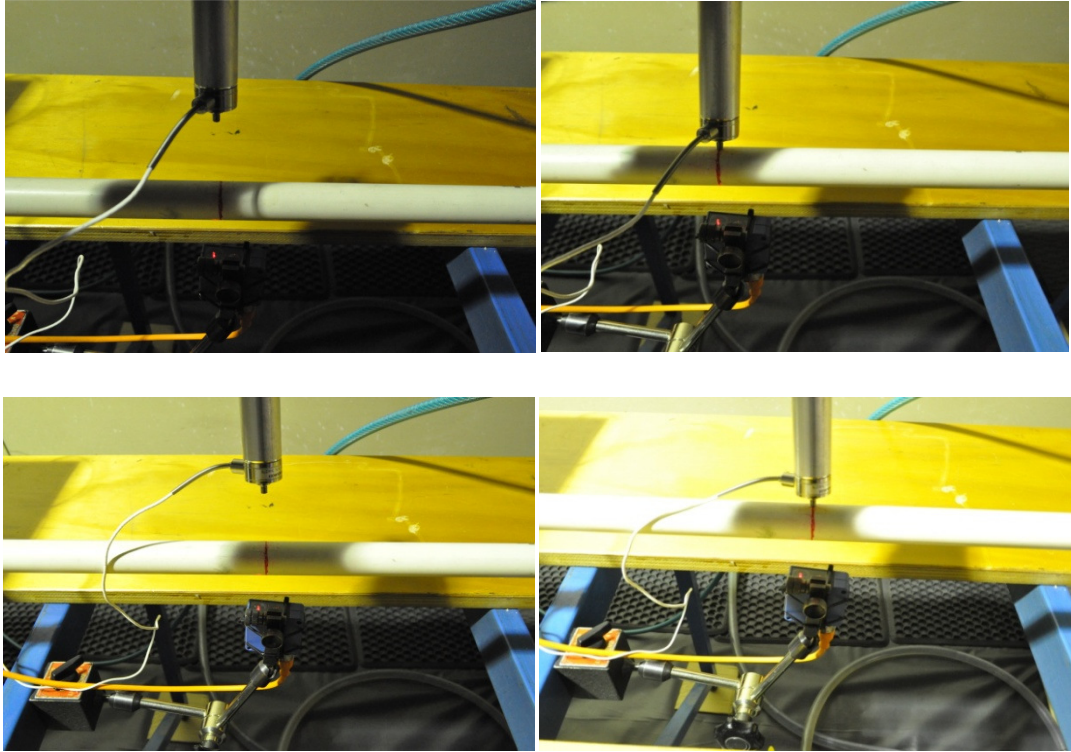
Figure 6.10: Load cell that is fitted to the handle and used to impact the pipe

The load and deflection data was recorded using a Measurement Computing USB-1208FS acquisition board. The data acquisition system, USB-1208FS, shown in Figure 6.11 was a low cost, USB-based module with four channels of 12-bit differential input. The load cell was connected to a bridge amplifier before passing to the data acquisition card. The laser sensor connected directly to the data acquisition card. All data was recorded at a sampling frequency of 500 Hz for later processing.
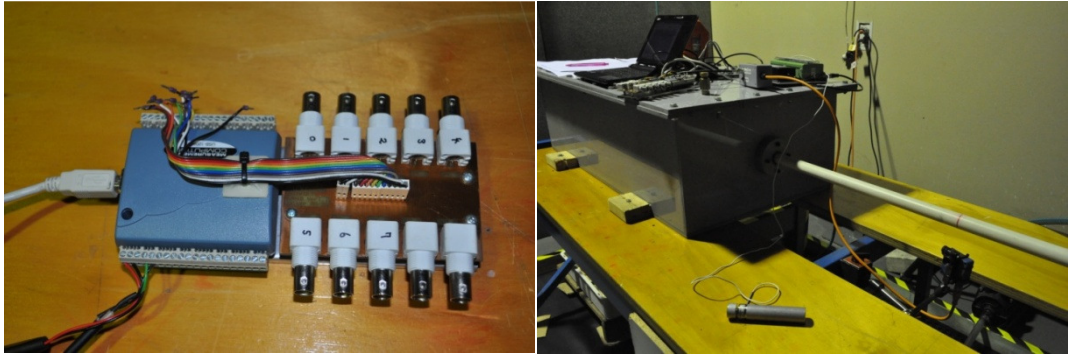
Figure 6.11: Data acquisition system—USB-1208FS

6.3 Experimental Procedure

6.3.1 Filling/Emptying the Tank System

Before conducting the program of experiments, the tanks have to be filled in according to a special procedure, which was developed to meet the necessary electrical safety precautions. To fill the tank, the drain line valves A, B and C are first closed as shown in Figure 6.12. The supply tank vent V1 is opened to bleed out air from the receiver tank. The main water supply tap then is opened so that the supply and receiver tanks are filled with water. When both tanks are sufficiently full, the main water supply tap is turned off.
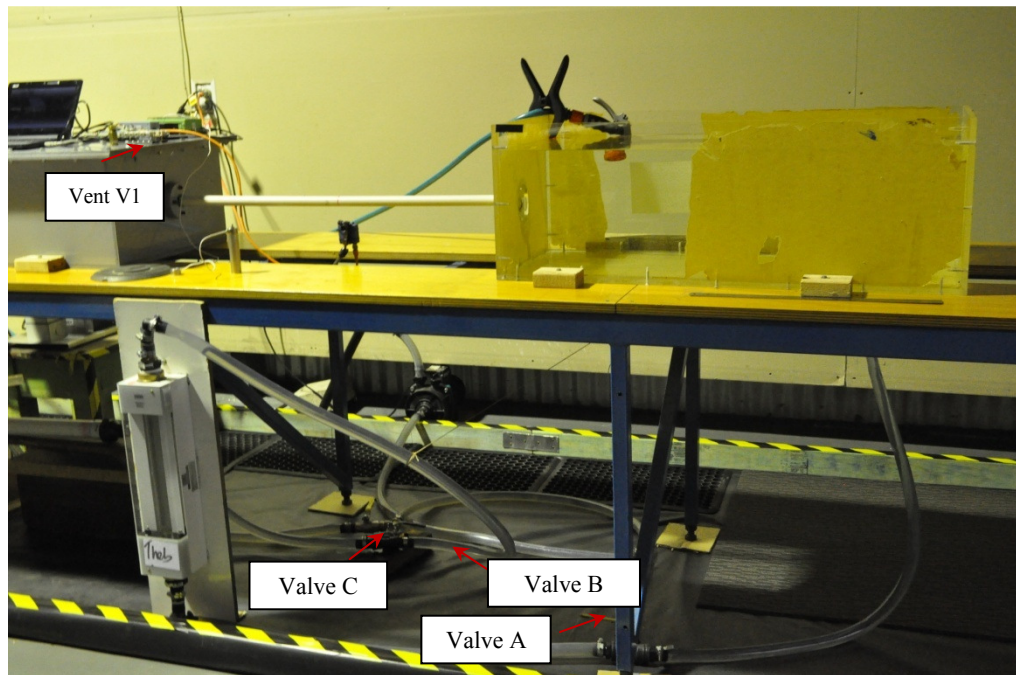
Figure 6.12: Filling two-tank facility

When water in the supply tank has displaced the air, vent V1 is closed. Vent V2 is then opened to bleed out air from the pump. The filling time of the tanks takes approximately 20–30 minutes. The facility should be monitored during filling to ensure no water leaks and overflows. The filling procedure is shown in Figure 6.13.
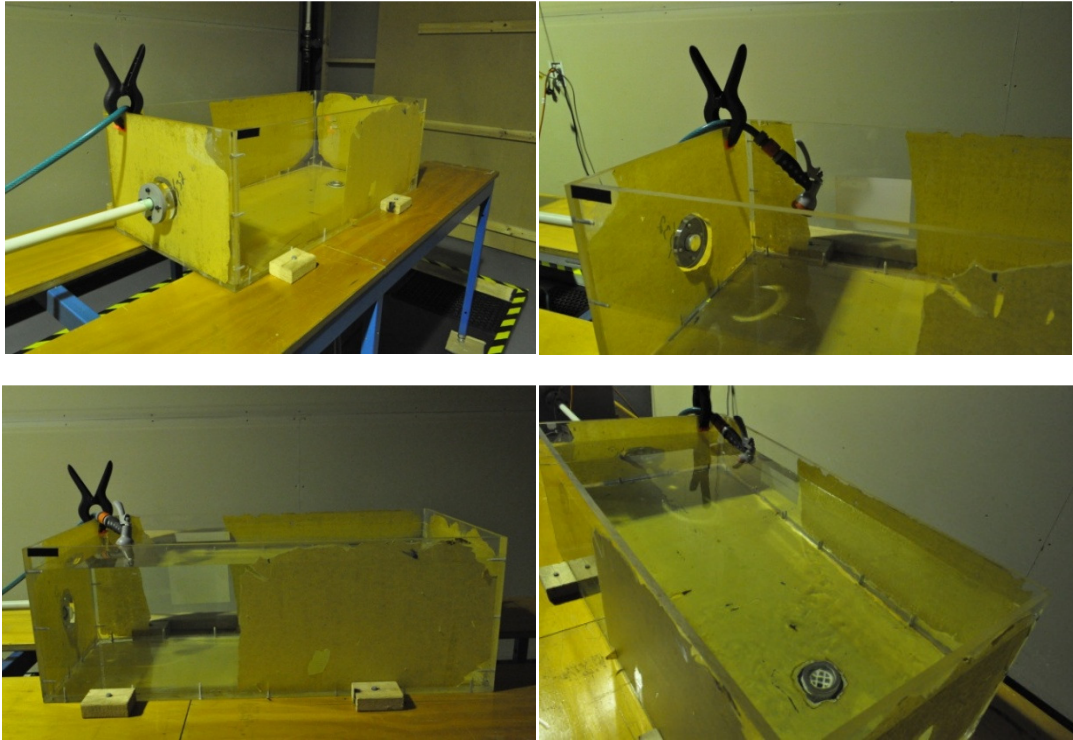
Figure 6.13: Process of filling two-tank facility

To empty the system, the main water supply is closed. The drain line valves A, B and C are opened. Vent V1 is opened and air is bled from drain pump P2 via bleed valve V3. Then valve D is opened (see Figure 6.14) and the drain pump P2 is turned on (see Figure 6.15). When the supply and receiver tanks are empty, pump P2 is switched off and valve D is closed. It takes about 10 minutes for the tanks to be emptied of water. The process of emptying two-tank facilities is shown in Figure 6.16.
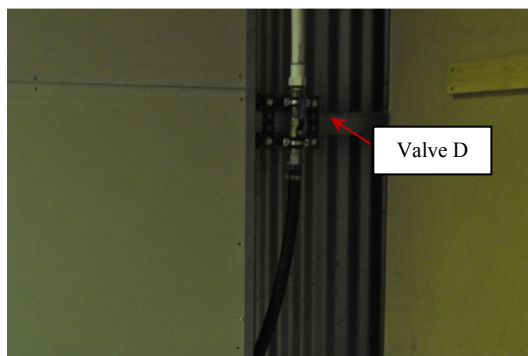
Figure 6.14: Valve D
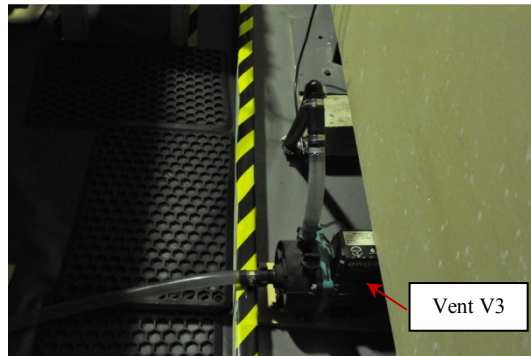
Figure 6.15: Pump P2 via Vent V3
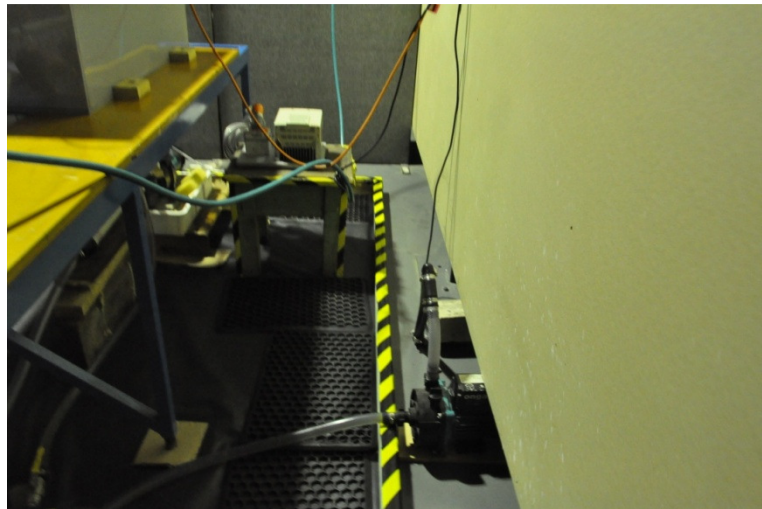
Figure 6.16: Process of emptying two-tank facility

6.3.2 Operating the System Pump (P1)

The pump controller can be seen in Figure 6.17. Before operating the pump, air is bled from the pump casing via vent V2 as shown in Figure 6.18. In operation, a pump is not allowed to be void of water. It is important to ensure the system pump P1 is turned off in the event of water overflowing the tanks. Pump P1 is turned off and valves A, B and C are opened. Water supply to the facility should be turned off.
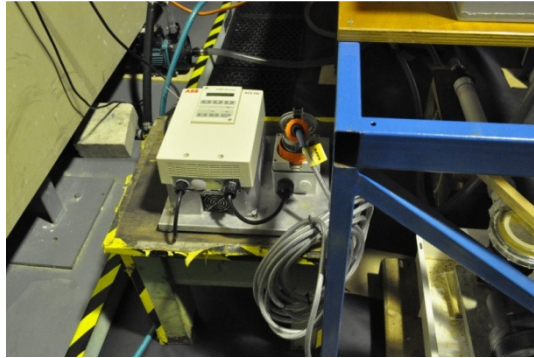
Figure 6.17: Pump controller
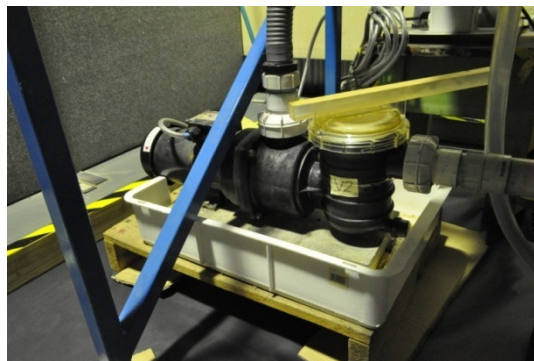
Figure 6.18: Position of Vent V2

6.3.3 Experiments

The impact test was conducted when water has filled the supplier tank and water was flowing in the pipe. The pump was operated at various frequencies so that various flow rates are obtained. A photo of the test setup during experiments is shown in Figure 6.19.

Figure 6.19: The test setup during use

The dynamic response of the pipe was then measured using a displacement sensor for a range of flow conditions as shown in Table 6.1.

Table 6.1: Different range of flow conditions

No.	Velocity (m/s)	ε	β
1	0.19	0.0653	0.0718
2	1.21	0.4137	0.4548
3	2.22	0.7620	0.8377
4	3.01	1.023	1.1250

As one can see, the selected design of the test rig provides a wide range of the controlling parameters, which can be changed to investigate the internal flow effects. However, both controlling parameters change simultaneously with the change of the speed of the water flow and with the current experimental set up it was unachievable to vary these parameters independently.

6.4 Results and Discussions

An impulse load was applied to the centre point of the pipe. Figure 6.20 shows a typical diagram of load intensity normalised by its maximum value (f/f_{max}) as a function of dimensionless time, t, introduced in Chapter 3:

$$t = \frac{\bar{t}}{\tau}$$

where $\bar{t}$ is the actual time in sec and

$$\tau = L^2 \sqrt{\frac{\lambda_p + \lambda_f}{EI}}$$

λ_f and λ_p be the medium and pipe densities per unit length, L is the pipe length, E is Young modulus and I is the second moment of inertia of the pipe's cross-section. τ is the characteristic time and can vary in a wide range, say from 1 for the laboratory tests and up to 10^3 for high-pressure pipelines.
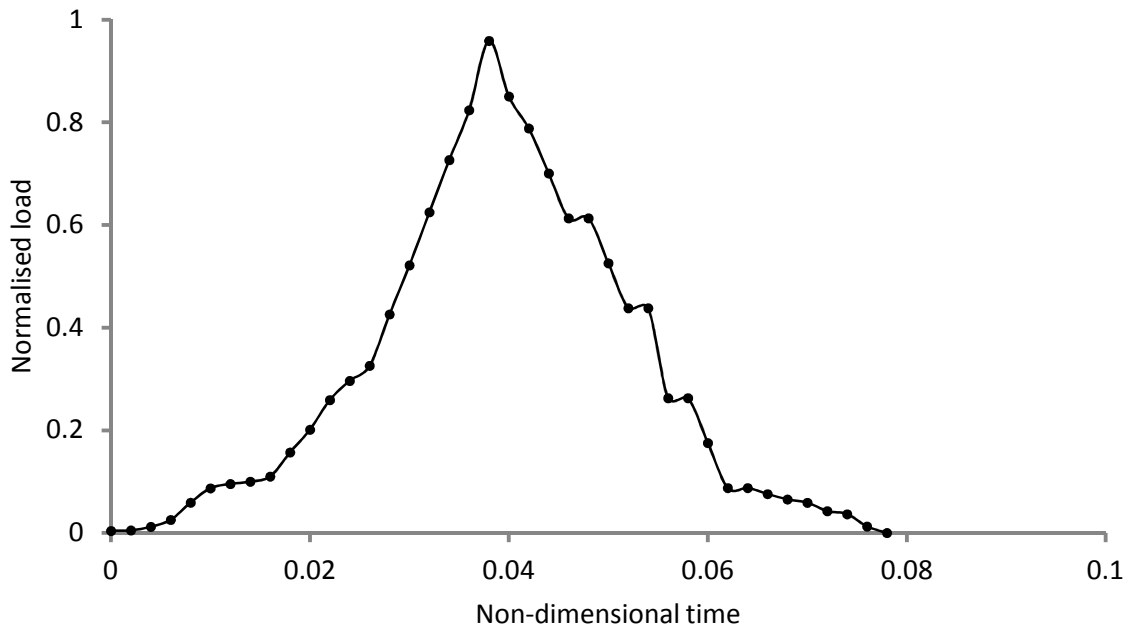
Figure 6.20: Load intensity as a function of time

The next four figures show the transient response of the pipe, normalised deflections at the mid-span, to the quasi-impulse loading.
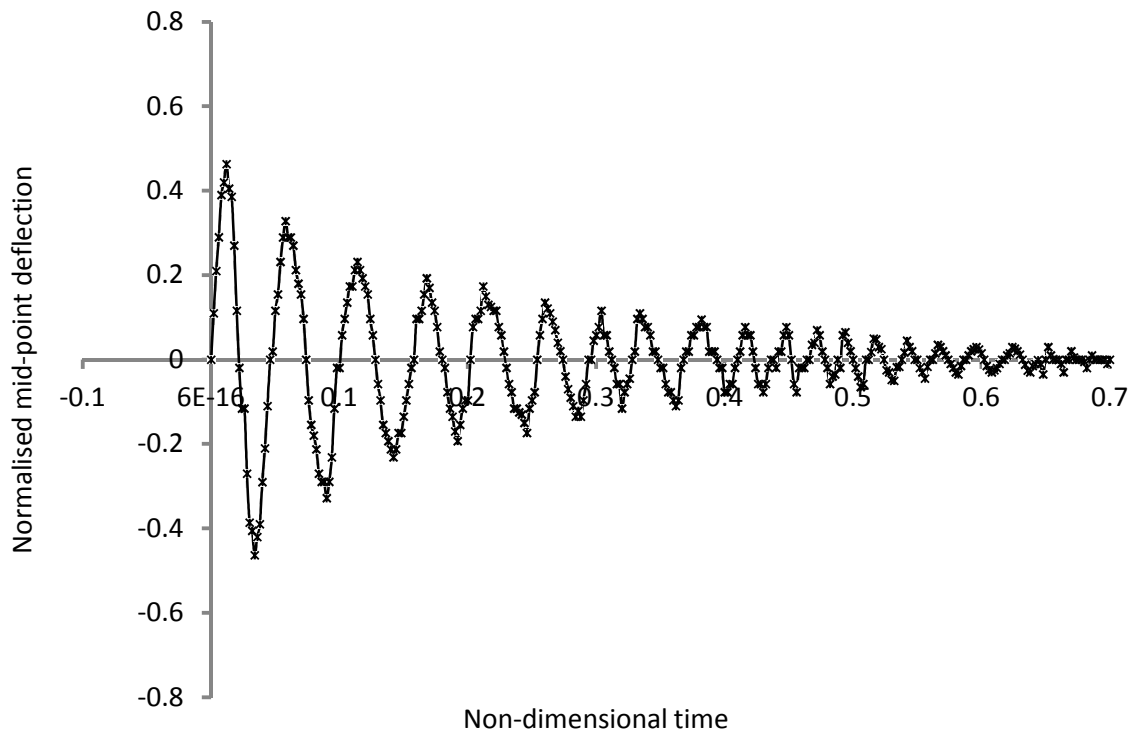
Figure 6.21a: Transient response of pipe mid-section at V = 0 m/s
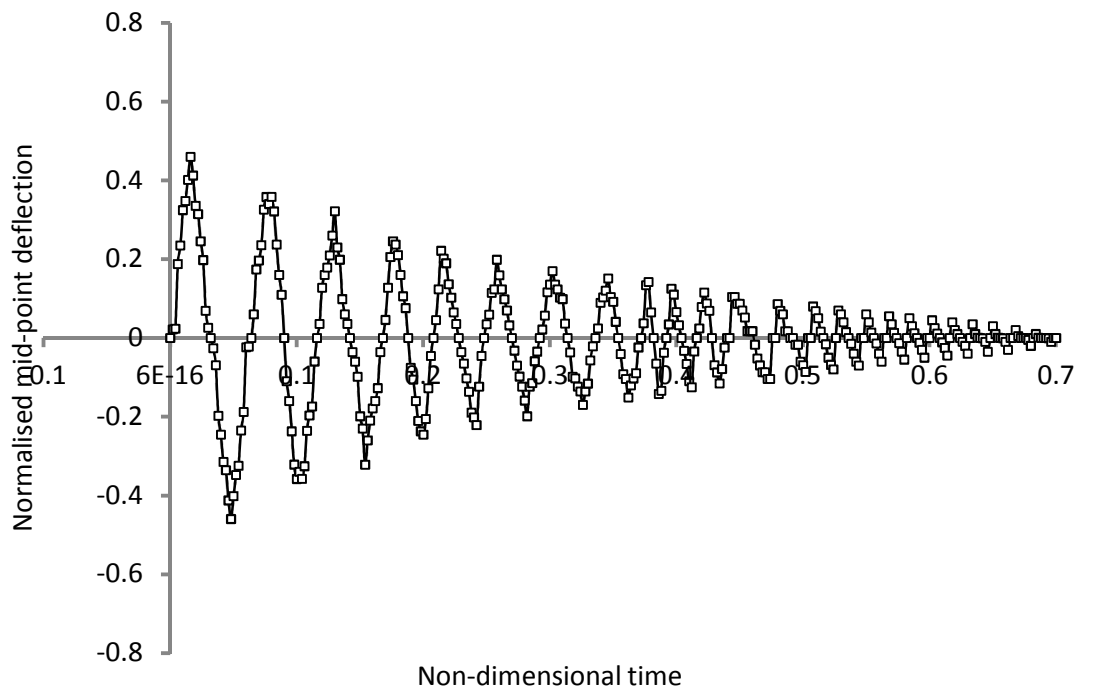
Figure 6.21b: Transient response of pipe mid-section at V=1.21 m/s
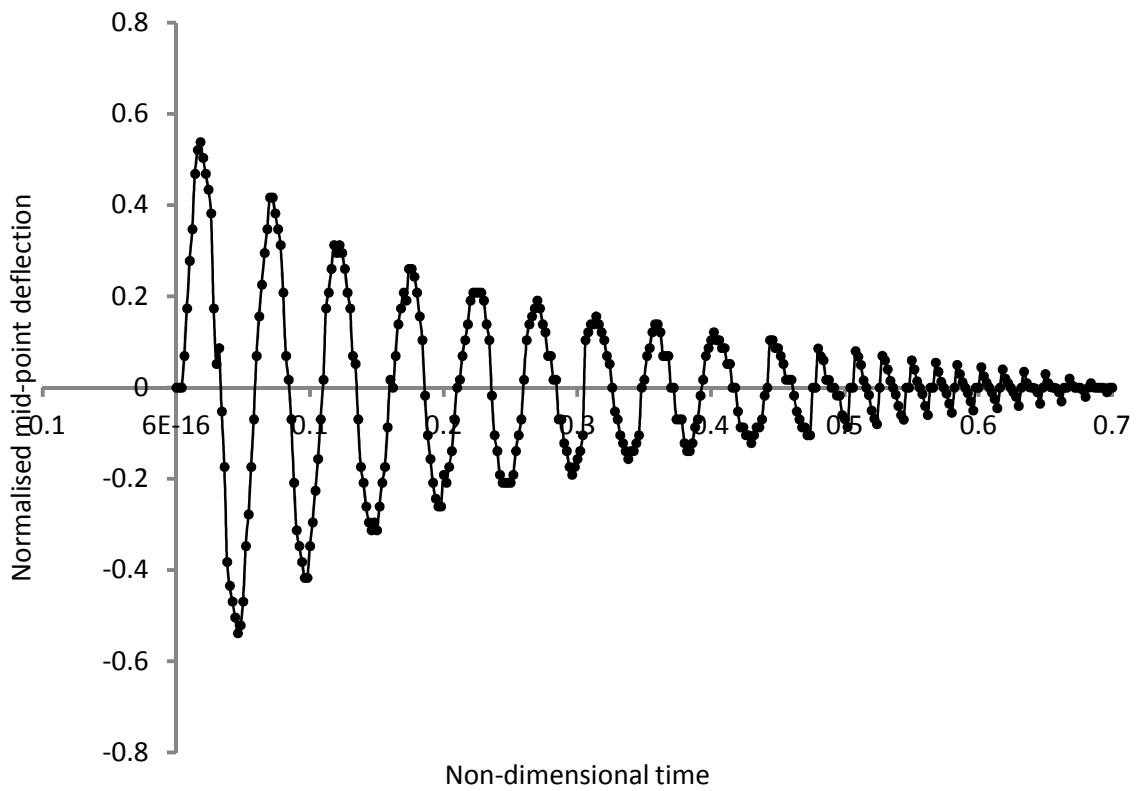
Figure 6.21c: Transient response of pipe at mid-section at V=2.22 m/s
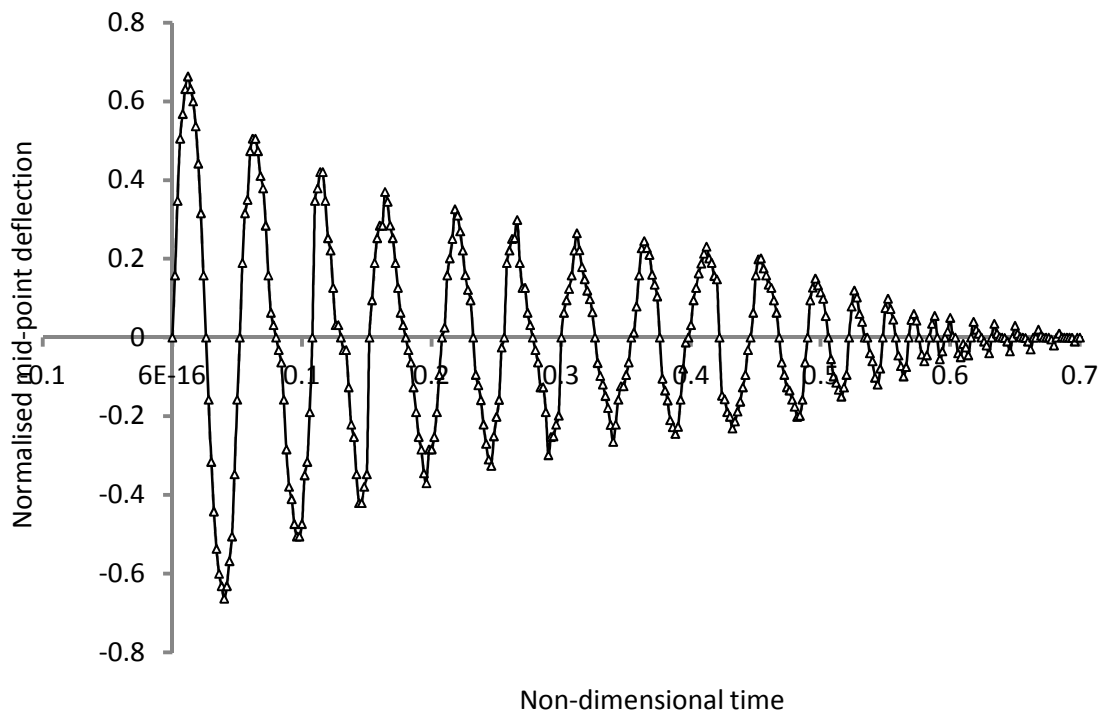
Figure 6.21d: Transient response of pipe at mid-section at V=3.0 m/s

106

All four sets of experiments were combined in a single diagram shown in Figure 6.22. The first resonant frequency dominates in the dynamic response of the system. This is caused by the internal damping, which always exists in real systems. The resonant frequency of the pipe is almost not affected by the flow speed, at least at the first few oscillations.

From the comparison, one can see a significant influence (up to 30% in terms of the normalised deflections) of the parameters of the internal flow on the transient response of the pipe. It can be clearly seen from this figure that the increase of the flow speed leads to the increase of negative damping effect. This effect tends to increase or, at least, to support the intensity of pipe deflections at higher speeds of the internal flow. As discussed in the previous sections, the Coriolis force is responsible for the 'negative' damping effect.
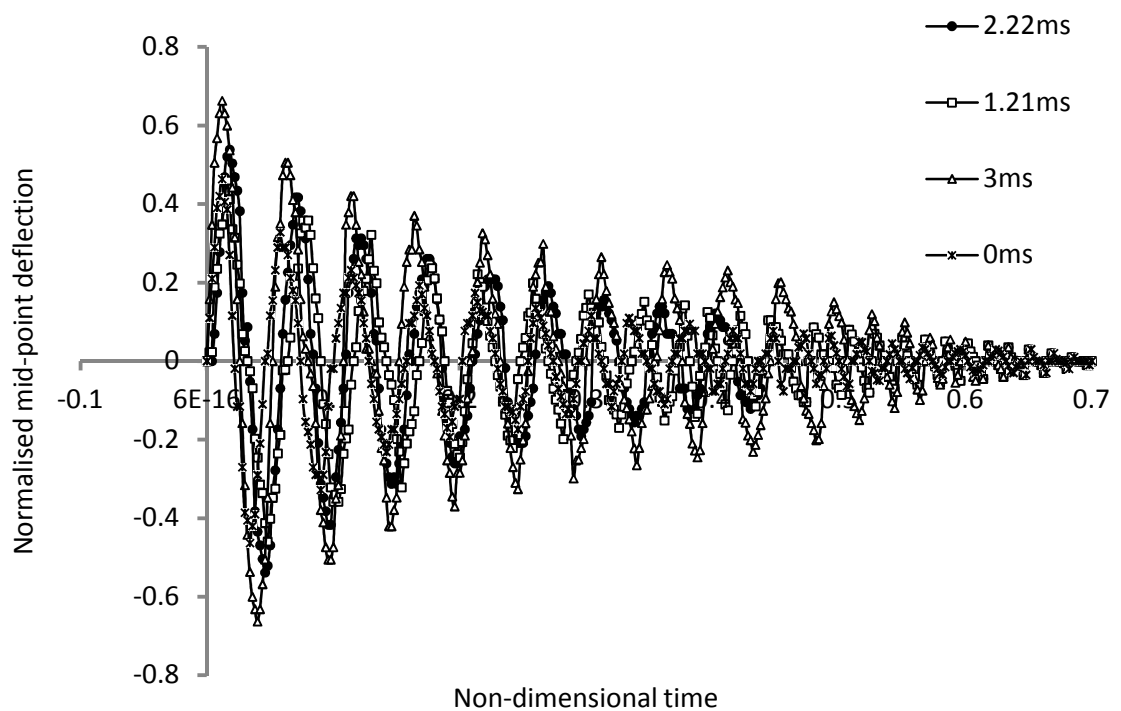
Figure 6.22: Transient response of pipe at mid-section at various speeds of the internal flow

In the previous chapter, the numerical simulations predicted the similar effect for the fixed-fixed boundary conditions as well as for other support conditions. Due to a very high internal damping due to friction, gravity and non-ideal support conditions, it was impossible to conduct a more detailed experimental investigation of the effects of the internal flow on the transient response of pipes transporting liquid, In particular, it was impossible to study higher harmonics of the transient response and the conditions corresponding to the initiation of pipe instability predicted analytically and via numerical modelling. This is something that was very difficult to predict at the earlier stage of the rig design. Nevertheless, it was demonstrated that even with a high positive damping the flow effects can be significant. In addition, the tendencies obtained from the experiments (the effect of 'negative' damping) fully agree with the previous analytical and numerical studies.

Further improvements and modifications of the test rig are required. This could involve redesign of supports and use of a more powerful pump to achieve higher flow speeds. Unfortunately, a comparison between experimental studies and analytical/numerical results was not conducted as the scale physical system had completely different properties to the idealised. However, this will be a subject of further work.

CHAPTER 7

SUMMARY AND CONCLUSION

The main objective of this project was to investigate effect of the flowing medium on the transient response of pipes conveying fluid or gas and subjected to impulse (impact-loading). To achieve this ambitious objective, analytical, numerical and experimental studies were conducted. This chapter presents a brief summary of the work conducted and the main results, and draws overall conclusions.

The selected topic is very important in many industrial and military applications such as offshore structures, oil and gas, power stations, petrochemical and defence industries where the critical pipe components transporting gas or liquid can be subjected to impact loading due to an accident, for example. On the other end of the structural length scale, in the last few years, micro-pipes carrying liquid or gas have been gaining popularity in various sensor technologies, which involve some dynamic measurements. Therefore, there is now a growing interest in studying the transient response of pipes with flowing media caused by dynamic loading.

However, the main motivation behind the current study was the recent release of AS 2885.1-2007, which includes a new section (5.8.3) on 'Pipeline with reduced cover or aboveground'. It makes it clear that pipelines may be installed aboveground. The reason for this revision was probably economical considerations because aboveground gas pipelines can offer significant benefits while posing relatively low risks. Some gas producers are interested in the application of aboveground gas lines so they can have this option available for production flowlines in remote areas. Hence, the issues surrounding safety and dynamic behaviour of aboveground high-pressure gas pipelines are very important, specifically for Australia.

A careful literature review was conducted, which indicated a significant amount of literature on the topic. The literature review presented in this thesis was limited to the issues that represent an interest for the current project. It was found that the previous studies mostly focused on vibration problems in pipes including the calculation of natural frequencies and vibration control. Despite the fact that the vibration and impact loading problems are closely related, it is surprising that not much research has been conducted on the dynamic response of pipes subjected to impulse loading, especially to understand how the internal flow changes the maximum deflections of the pipe.

110

Other gaps in the literature include a lack of analytical approaches and analytical solutions that can explicitly provide an estimate of the effect of the internal flow on the dynamic response of pipes and serve as a benchmark for numerical solutions. Driven mainly by the power chemical industries, the previous experimental studies mostly focused on vibration issues and vibration control of pipes conveying liquid; and not much work has been completed to investigate the response of pipe to impact (except the ballistic impact experiments on damage and perforation).

In Chapter 2, mathematical models describing a pipe conveying fluid were reviewed. It was found that the most popular models for long flexible pipes are based on Bernoulli-Euler beam theory. Many previous attempts to incorporate shear deformation using Timoshenko model or non-linear behaviour led to a significant complication of the governing equations, which make it virtually impossible to derive analytical solutions or validate numerical simulations. Therefore, the present work is based on the most simple yet reasonably accurate model utilising the classical beam theory.

In the third chapter, the governing equation for a long flexible pipe with flowing medium based on the classical Bernoulli-Euler beam theory was presented and analysed. After that, new scale transformations were conducted to demonstrate that only two parameters govern the transient dynamics of the pipe. This fact can be utilised to investigate various dynamic phenomena using reduced size or scaled physical models. Such scaled models would be adequate if the values of the governing parameters are kept the same for the scaled model and the reference system. Of course, the physical models have to meet all other conditions corresponding to the adopted assumptions in mathematical modelling. For example, the pipe has to be sufficiently long and flexible, and the loading should not significantly affect the internal flow characteristics.

Further, an original asymptotic approach was developed to investigate the transient response of pipes subjected to impulse loading. The approach is based on the standard perturbation technique widely applied elsewhere. The solution represents a recurrent system of equations, each term of which can be obtained by integration. The application of this approach was used to obtain the first-order correction to the classical solution for

the corresponding problem of both a cantilever beam and a simply supported pipe transporting gas or liquid. However, when higher order terms are required, the analytical procedure may become quite cumbersome and time-consuming.

In the fourth chapter, a central finite-difference scheme was developed for the fourth order governing equation and a validation study was completed. This demonstrated that the both approaches are free from errors and can be confidently applied to investigate the effect of parameters of the flowing medium on the transient response of pipes subjected to impulse loading.

A systematic study of these effects was conducted in Chapter 5. The suggested method of scaling of the governing equation proved very efficient, as there was significant controversy surrounding the effect of the flow speed on the dynamic behaviour of pipes. In some cases, it leads to negative damping, but in other cases, it leads to positive damping. With the introduced dimensionless parameters, which combine elastic, geometric properties of the pipe as well as properties of the internal flow, there was observed two tendencies. One of the non-dimensionless parameters increases damping properties of the system and the increase of its value leads to the faster dissipation of the energy supplied by the external loading (impact). The other non-dimensional parameter acts in an opposite way regardless of the boundary conditions and loading. An increase of its value reduces the damping properties of the system and can lead, eventually, to the initiation of dynamic instability.

The conditions of the initiation of dynamic instability were investigated using an analytical approach as well as the numerical central-difference approach. As stated in the literature review, the developed liberalised approaches are capable of determining the critical conditions for the initiation of dynamic instability. However, they are not capable of describing the dynamic behaviour near these conditions. As an example of the usefulness of the obtained results, a simple engineering criterion avoiding the dynamic instability of pipes conveying fluid or gas was suggested. The derived criterion of the initiation of instability can be considered a conservative estimate as the present mathematical model does not take into account other important factors, for example, friction or gravity, which can contribute significantly into the damping properties and

energy absorption mechanisms. The critical conditions derived in this chapter may also be useful in reducing potential damage by designing some measures from the pipe equipment working under high-pressure conditions.

In the sixth chapter, an experimental study was conducted to gain a further understanding of how the characteristics of the internal flow affect the transient response of circular pipes. The scope of the experimental study was limited to the case of a long flexible pipe with fixed-fixed support conditions. It was found the first resonant frequency of the pipe dominated in the dynamic response of the system. This is caused by the internal damping, which always exists in real systems. The resonant frequency of the pipe is almost unaffected by the flow speed, at least at the first few oscillations. From the comparison of the dynamic response of the pipe when all parameters were fixed and only fluid speed was varied, a significant influence of the parameters of the internal flow on the transient respond of the pipe was observed. It can be clearly seen that the increase of the flow speed leads to the increase of negative damping effect. As discussed in the literature review, the Coriolis force is responsible for the negative damping effect.

Due to very high internal damping due to friction, gravity and non-ideal support conditions, it was impossible to conduct a more detailed experimental investigation of the effects of the internal flow on the transient respond of pipes transporting liquid. In particular, it was impossible to study higher harmonics of the transient response and the conditions corresponding to the initiation of pipe instability predicted analytically and via numerical modelling. This is something that was very difficult to predict at the earlier stage of the rig design. Nevertheless, it was demonstrated that even with a high positive damping, the flow effects can be significant. In addition, the tendencies obtained from the experiments (the effect of negative damping) fully agree with the previous analytical and numerical studies summarised in the literature review. Further improvements and modifications of the test rig are required and specified in the conclusion section of Chapter 6. However, this will be a subject of further work.

Overall, the current work demonstrated the applicability of various approaches, analytical, numerical and experimental, to the investigation of extremely complex

phenomena. An excellent correlation between the analytical asymptotic approach and numerical approach was found. Unfortunately, a comparison between experimental studies and analytical/numerical results was not conducted as the scale physical system had completely different properties to the idealised. In particular, the test pipe had a very high internal damping, which was difficult to model analytically. Nevertheless, the result demonstrated a significant effect of the internal flow on the transient response of pipes.

A number of journal and conferences papers resulted from this work and were published in local and international journals and conference proceedings. One of the conference contributions won a prize for best student work at ACAM 7. This also represents one of main outcomes of the PhD project.

It is believed that the current theoretical and experimental work has made a notable contribution to the field of research. It has allowed a better understanding of the dynamic of pipes and the outcomes can be directly utilised to improve the safety of pipelines or develop more advanced procedures for analysis of the dynamic behaviour of pipes conveying gas or liquid. It is also believed that the current work can be further extended and new useful results can be obtained as a result of further in-depth study. The main area of the further research seems to be in the experimental field. Further improvements and modifications of the test rig are required. This could involve redesign of supports and use of a more powerful pump to achieve higher flow speeds and fully validate the theoretical models and solution presented in this thesis. However, full-scale experiments with high-pressure pipelines can be quite expensive and not feasible without an industry support.

APPENDICES

APPENDIX A

Mohammad, R., Kotousov, A., Codrington, J. and Blazewicz (2010)
Effect of flowing medium for a simply supported pipe subjected to impulse loading.
IN *6th Australasian Congress on Applied Mechanics, ACAM 6,*
12-15 December 2010, Perth, Australia.

APPENDIX B

APPENDIX C

fixed-free condition

```matlab
clear all; clc
clc
mm=20001;
nn=51;
%V=250;
L=10;
do=0.2;
di=0.19;
I=3.142/64*(do^4-di^4);
densp=7850;
densf=1000;
pvol=3.142/4*(do^2-di^2)*L;
fvol=3.142/4*(di^2)*L;
E=200e9;
force=5;
eta = 1.22807;
%alpha = 0;

%Mass of pipe and fluid
mp=pvol*densp;
mf=fvol*densf;
twt=mp+mf;

miu=twt/L;
gamma=2*sqrt(E*I*miu)*eta/L^2;
alpha=0; %gamma*L^2/sqrt(E*I*miu);
delx = 1/(nn-1);
delt = 0.00005;
%f(44,mm)=0;

lambp=densp/L;
lambf=densf/L;


eps=0.5
%eps=V*L*mf/L/sqrt(E*I*miu);
%eps=V*L*mf/sqrt(E*I*miu);
beta=0
%beta=V*L*sqrt(miu/E/I);

for n = 1:nn+1
    for m = 1:mm
        f(n,m) = 0;
    end
end
F = L^3*force/E/I;
f(ceil(nn/2),500)=F/delx/delt;

%eta = 1.22807;
```

134

```matlab
A = eye(nn+3);
A(1,3) = -1;
A(nn+2,nn) = 1;
A(nn+2,nn+1) = -2;
A(nn+3,nn-1) = -0.5;
A(nn+3,nn) = 1;
A(nn+3,nn+1) = 0;
A(nn+3,nn+2) = -1;
A(nn+3,nn+3) = 0.5;
for i = 3:1:nn+1;
        A(i,i-1) = -eps*delt/delx;
        A(i,i) = 2+alpha*delt;
        A(i,i+1) = eps*delt/delx;
end
Ainv = minv(A);

%Boundary and initial conditions
for n = 1:1:nn+3;
    W(n,1) = 0;
    W(n,2) = 0;
end

R(1:2,1)=0;
R(nn+2:nn+3,1)=0;
W(2,1) = 0;


for m = 2:1:mm;
      W(2,m) = 0;

      for n = 3:1:nn+1;
            R(n,1) = -2*(delt^2/delx^4)*(W(n+2,m)-
4*W(n+1,m)+6*W(n,m)...
                      -4*W(n-1,m)+W(n-2,m))+2*(2*W(n,m)-W(n,m-1))...
                      +eps*(delt/delx)*(W(n+1,m-1)-W(n-1,m-1))...
                      -2*beta*eps*(delt^2/delx^2)*(W(n+1,m)-2*W(n,m)...
                      +W(n-1,m))+alpha*delt*(W(n,m-1))+2*delt^2*f(n,m);
      end


Sol = transpose(Ainv*R);
        for n = 1:1:nn+3;
            W(n,m+1) = Sol(n);
        end

end

%CSVWRITE('Data-Eps_10-Beta_11',W)


%figure()
m=1:1:mm;
plot(m,W(nn+1,m)/F)
n=2:1:nn+1;
%plot(n,W(n,1000)/F)
hold on;
xlabel('m','Fontweight','Bold');
ylabel('w','Fontweight','Bold');
```

135

```matlab
title('Scaled deflection at n=10, Eps=0.35','Fontweight','Bold');

grid on;
hold on;

tip = max(W(nn+1,m))
mid = max(W(ceil(nn/2),m))
```

Fixed-fixed condition

```matlab
clear all; clc
clc
mm=20001;
nn=51;
%V=250;
L=10;
do=0.2;
di=0.19;
I=3.142/64*(do^4-di^4);
densp=7850;
densf=1000;
pvol=3.142/4*(do^2-di^2)*L;
fvol=3.142/4*(di^2)*L;
E=200e9;
force=5;

eta = 1.22807;
%alpha = 0;


%Mass of pipe and fluid
mp=pvol*densp;
mf=fvol*densf;
twt=mp+mf;

miu=twt/L;
gamma=2*sqrt(E*I*miu)*eta/L^2;
alpha=0; %gamma*L^2/sqrt(E*I*miu);
delx = 1/(nn-1);
delt = 0.00005;
%f(44,mm)=0;

lambp=densp/L;
lambf=densf/L;

eps=0.5
%eps=V*L*mf/L/sqrt(E*I*miu);
%eps=V*L*mf/sqrt(E*I*miu);
beta=30
%beta=V*L*sqrt(miu/E/I);

for n = 1:nn+1
    for m = 1:mm
        f(n,m) = 0;
```

136

```matlab
    end
end
F=L^3*force/E/I;
f(ceil(nn/2),500)=F/delx/delt;


A = eye(nn+1);
A(1,3) = -1;
A(nn+1,nn-1) = -1;



for i = 3:1:nn-1;
        A(i,i-1) = -eps*delt/delx;
        A(i,i) = 2+alpha*delt;
        A(i,i+1) = eps*delt/delx;

end
Ainv = minv(A);



for n = 1:1:nn+1;
    W(n,1) = 0;
    W(n,2) = 0;
end



R(1:2,1)=0;
R(nn:nn+1,1)=0;
W(2,1) = 0;
W(nn,1)= 0

for m = 2:1:mm;
      W(2,m) = 0;

      %for n = 3:1:40;
      for n = 3:1:nn-1;
            R(n,1) = -2*(delt^2/delx^4)*(W(n+2,m)-
4*W(n+1,m)+6*W(n,m)...
                        -4*W(n-1,m)+W(n-2,m))+2*(2*W(n,m)-W(n,m-1))...
                        +eps*(delt/delx)*(W(n+1,m-1)-W(n-1,m-1))...
                        -2*beta*eps*(delt^2/delx^2)*(W(n+1,m)-2*W(n,m)...
                        +W(n-1,m))+alpha*delt*(W(n,m-1))+2*delt^2*f(n,m);
      end


Sol = transpose(Ainv*R);
      %for n = 1:1:42;
      %    W(n,m+1) = Sol(n);
      %end

      for n = 1:1:nn+1;
            W(n,m+1) = Sol(n);
      end
end
```

137

```matlab
%figure()
m=1:1:mm;
plot(m,W(nn+1,m)/F)
n=2:1:nn+1;
%plot(n,W(n,1000)/F)
hold on;
xlabel('m','Fontweight','Bold');
ylabel('w','Fontweight','Bold');
title('Scaled deflection at n=10, Eps=0.35','Fontweight','Bold');

grid on;
hold on;


tip = max(W(nn+1,m))
mid = max(W(ceil(nn/2),m))
```

fixed ss condition

```matlab
clear all; clc
clc
mm=20001;
nn=51;
%V=250;
L=10;
do=0.2;
di=0.19;
I=3.142/64*(do^4-di^4);
densp=7850;
densf=1000;
pvol=3.142/4*(do^2-di^2)*L;
fvol=3.142/4*(di^2)*L;
E=200e9;
force=5;
eta = 1.22807;
%alpha = 0;


mp=pvol*densp;
mf=fvol*densf;
twt=mp+mf;

miu=twt/L;
gamma=2*sqrt(E*I*miu)*eta/L^2;
alpha=0; %gamma*L^2/sqrt(E*I*miu);
delx = 1/(nn-1);
delt = 0.00005;
%f(44,mm)=0;

lambp=densp/L;
lambf=densf/L;


eps=1.5
```

```matlab
%eps=V*L*mf/L/sqrt(E*I*miu);
%eps=V*L*mf/sqrt(E*I*miu);
beta=10
%beta=V*L*sqrt(miu/E/I);



%for n = 1:42
for n = 1:nn+1
    for m = 1:mm
        f(n,m) = 0;
    end
end
%f(20,500)=L^3*force/E/I;

F=L^3*force/E/I;
f(ceil(nn/2),500)=F/delx/delt;

%eta = 1.22807;
%A = eye(42);
A = eye(nn+1);
A(1,3) = -1;
%A(42,40)=1
A(nn+1,nn-1) = 1;

%for i = 3:1:40;
for i = 3:1:nn-1;
        A(i,i-1) = -eps*delt/delx;
        A(i,i) = 2+alpha*delt;
        A(i,i+1) = eps*delt/delx;
end
Ainv = minv(A);



%Boundary and initial conditions
%for n = 1:1:42;
for n = 1:1:nn+1;
    W(n,1) = 0;
    W(n,2) = 0;
end

R(1:2,1)=0;
%R(41:42,1)=0;
R(nn:nn+1,1)=0;
W(2,1) = 0;
%W(41,1) = 0
W(nn,1) = 0

for m = 2:1:mm;
    W(2,m) = 0;

    %for n = 3:1:40;
    for n = 3:1:nn-1;
        R(n,1) = -2*(delt^2/delx^4)*(W(n+2,m)-
4*W(n+1,m)+6*W(n,m)...
                -4*W(n-1,m)+W(n-2,m))+2*(2*W(n,m)-W(n,m-1))...
                +eps*(delt/delx)*(W(n+1,m-1)-W(n-1,m-1))...
                -2*beta*eps*(delt^2/delx^2)*(W(n+1,m)-2*W(n,m)...
                +W(n-1,m))+alpha*delt*(W(n,m-1))+2*delt^2*f(n,m);
```
139

```matlab
        end


Sol = transpose(Ainv*R);
        %for n = 1:1:42;
        for n = 1:1:nn+1;
            W(n,m+1) = Sol(n);
        end

end
```

ss ss condition

```matlab
clear all; clc
clc
mm=2000;
nn=51;
%V=250;
L=10;
do=0.2;
di=0.19;
I=3.142/64*(do^4-di^4);
densp=7850;
densf=1000;
pvol=3.142/4*(do^2-di^2)*L;
fvol=3.142/4*(di^2)*L;
E=200e9;
force=5;
eta = 1.22807;
%alpha = 0;

%Mass of pipe and fluid
mp=pvol*densp;
mf=fvol*densf;
twt=mp+mf;

miu=twt/L;
gamma=2*sqrt(E*I*miu)*eta/L^2;
alpha=0; %gamma*L^2/sqrt(E*I*miu);
delx = 1/(nn-1);
delt = 0.00005;
%f(44,mm)=0;

lambp=densp/L;
lambf=densf/L;


eps=0.5
%eps=V*L*mf/L/sqrt(E*I*miu);
%eps=V*L*mf/sqrt(E*I*miu);
beta=10
%beta=V*L*sqrt(miu/E/I);

for n = 1:nn+1
    for m = 1:mm
        f(n,m) = 0;
```

```matlab
        end
    end
F = L^3*force/E/I;
f(ceil(nn/2),500)=F/delx/delt;



%for n = 1:42
    %for m = 1:mm
        %f(n,m) = 0;
    %end
%end
%f(20,500)=L^3*force/E/I;

%eta = 1.22807;



%A = eye(42);
A = eye(nn+1);
A(1,3) = 1;
%A(42,40) = 1;
A(nn+1,nn-1) = 1;

%for i = 3:1:40;
for i = 3:1:nn-1;
        A(i,i-1) = -eps*delt/delx;
        A(i,i) = 2+alpha*delt;
        A(i,i+1) = eps*delt/delx;
end
Ainv = minv(A);



%Boundary and initial conditions
%for n = 1:1:42;
for n = 1:1:nn+1;
    W(n,1) = 0;
    W(n,2) = 0;
end

R(1:2,1)=0;
R(41:42,1)=0;
R(nn:nn+1,1)=0;
W(2,1) = 0;
W(nn,1)= 0
W(41,1)= 0

for m = 2:1:mm;
        W(2,m) = 0;

        %for n = 3:1:40;
        for n = 3:1:nn-1;
            R(n,1) = -2*(delt^2/delx^4)*(W(n+2,m)-
4*W(n+1,m)+6*W(n,m)...
                        -4*W(n-1,m)+W(n-2,m))+2*(2*W(n,m)-W(n,m-1))...
                        +eps*(delt/delx)*(W(n+1,m-1)-W(n-1,m-1))...
                        -2*beta*eps*(delt^2/delx^2)*(W(n+1,m)-2*W(n,m)...
                        +W(n-1,m))+alpha*delt*(W(n,m-1))+2*delt^2*f(n,m);
        end
```

141

```matlab
Sol = transpose(Ainv*R);
        %for n = 1:1:42;
        for n = 1:1:nn+1;
            W(n,m+1) = Sol(n);
        end

end


%figure()
m=1:1:mm;
plot(m,W(nn+1,m)/F)
n=2:1:nn+1;
%plot(n,W(n,1000)/F)
hold on;
xlabel('m','Fontweight','Bold');
ylabel('w','Fontweight','Bold');
title('Scaled deflection at n=10, Eps=0.35','Fontweight','Bold');

grid on;
hold on;

tip = max(W(nn+1,m))
mid = max(W(ceil(nn/2),m))
```

REFERENCES

[1]   Morgan B. The importance of realistic representation of design features in the risk assessment of high-pressure gas pipeline, 5th International Conference and Exhibition Pipeline Reliability, Houston, Texas; 1995, Sept.

[2]   Montiel H, Vilchez JA, Amaldos J, Casal J. Historical analysis of accidents in the transportation of natural gas. Journal of Hazardous Materials. 1996; 51:77–92.

[3]   Wang Z, Zhang Z, Zhao F. Stability analysis of viscoelastic curved pipes conveying fluid. Applied Mathematics and Mechanics. 2005; 6(26):807–813.

[4]   Sallstrom JH. Fluid-conveying damped Rayleigh-Timoshenko beams in transient transverse vibration studied by use of complex modal synthesis. Journal of Fluids Structures. 1993; 7:551–563.

[5]   Yigit F. Active control of flow-induced vibrations via feedback decoupling. Journal of Vibration Control. 2008; 14(4):591–608.

[6]   Fan CN, Chen WH. Vibration and stability of helical pipes conveying fluid. ASME. 1987; 402(109):402–410.

[7]   Ashley H, Haviland G. Bending vibration of a pipe line containing flowing fluid. ASME Journal of Applied Mechanics. 1950; 72:229–232.

[8]   Houser GW. Bending vibration of a pipe line containing flowing fluid. ASME Journal of Applied Mechanics. 1952; 74:206–208.

[9]   Diza M, Jain RK. Vibration analysis of pump discharge line. Journal of Hydraulic Division, ASCE 96. 1970; (HY11):2279–2296.

[10]   Chen SS, Rosenberg. Vibration and stability of tube exposed to pulsating parallel flow. ANS TRANS. 1970; 13:335–336.

[11]   Mulcahy TM, Wambsganss MW. Flow-induced vibration of nuclear reactor components. The Shock and Vibration Digest. 1976; 8(7):318–332.

[12]   Li T, DiMaggio OD. Vibration of a propellant line containing flowing fluid. AIAA Fifth Annual Structures and Material Conference, AIAA, No. CP-B: 194–199.

[13]   Brown S. Forensic engineering: reduction of risk and improving technology (for all things great and small). Engineering Failure Analysis. 2007; 14:1019–1037.

[14]   Sultan G, Hemp J. Modelling of the Coriolis mass flowmeter. Journal of Sound and Vibration. 1989; 132(3):473–489.

[15]   Feodos'ev VP. Vibrations and stability of a pipe when liquid flows through it. Inzhenernyi Sbornik. 1951; 10:169–170.

[16]   Housner GW. Bending vibrations of a pipe line containing flowing fluid. ASME Journal of Applied Mechanics. 1952; 19:205–208.

[17]   Paidoussis MP. 1992 Calvin rice lecture: Some curiosity-driven research in fluid structure interactions and its current applications. Journal of Pressure Vessel Technology. 1993; 115:2–14.

[18]   Foda MA, Abduljabbar Z. A dynamic green function formulation for the response of a beam structure to a moving mass. Journal of Sound and Vibration. 1998; 210(3):295–306.

[19]   Huang Y, Zeng G, Wei F. A new matrix method for solving vibration and stability of curved pipes conveying fluid. 2002; 251(2):215–225.

[20]   Niordson FI. Vibrations of a cylindrical tube containing flowing fluid. Kungliga Tekniska Hogskolans Handlingar (Stockholm); 1953. p. 73.

[21]   Semercigil SE, Turan OF, Lu S. Employing fluid flow in a cantilever pipe for vibration control. Journal of Sound and Vibration. 1997; 205(1):103–111.

[22]   Guran A, Plaut RH. Stability boundaries for fluid-conveying pipes with flexible support under axial load. Archive of Applied Mechanics. 1994; 64:417–422.

[23]   Kuiper GL, Metrikine AV. On stability of a clamped-pinned pipe conveying fluid. Heron. 2004; 49(3):211–232.

[24]   Paidoussis MP. Aspirating pipes do not flutter at infinitesimally small flow. Journal of Fluids and Structures. 1999; 13:419–425.

[25]   Huang CC. Vibrations of pipes containing flowing fluids according to Timoshenko theory. ASME J. Appl. Mech. 1974; 41(3):814–817.

[26]   Bratt JF. On lateral vibration of fluid conveying pipes. Proceedings of the ASME Energy-Sources Technology Conference, Petroleum Division Publication PD, New Orleans, LA. 1994; 63:1–4.

[27]   Stack CP, Garnett RB, Pawlas GE. Finite element for the vibration analysis of a fluid-conveying Timoshenko beam. Proceedings of the 34th AIAA/ASME Structures, Structural Dynamics and Materials Conference, La Jolla, CA. 1993; 4:2120–2129.

[28]   Lin YH, Tsai YK. Nonlinear vibrations of Timoshenko pipes conveying fluid. International of Journal Solids Structures. 1997; 34(23):2945–2956.

[29]   Chao Y, Menglin Y, Baoren L. Coupled vibration of piping system conveying unsteady flow. China Mech. Eng. 2008; 19(4):406–410.

[30]   Pramila A, Laukkanen J. Dynamics and stability of short fluid-conveying Timoshenko element pipes. Journal of Sound and Vibration. 1991; 144(3):421–425.

[31]   Tani J, Doki M. Effects of shearing loads and in-plane boundary conditions on the stability of thin tubes conveying fluid. ASME J. Appl. Mech. 1979; 46:779–783.

[32]   Paidoussis MP, Laithier BE. Dynamics of Timoshenko beams conveying fluid. J. Mech. Eng. Sciences. 1976; 18:210–220.

[33]   Paidoussis MP, Luu TP, Laithier BE. Dynamics of finite-length tubular beams conveying fluid. Journal of Sound Vibration. 1986; 106:311–331.

[34]   Maalawi KY, Ziada MA. On the static instability of flexible pipes conveying fluid. Journal of Fluids Structures. 2002; 16:685–690.

[35]   Semler C, Li GX, Paidoussis MP. The non-linear equations of motion of pipes conveying fluid. Journal of Sound and Vibration. 1994; 169(5):577–599.

[36]   Yoshizawa M, Ueno K, Hasegawa E, Tsujiioka Y. Lateral vibration of a cantilevered flexible pipe conveying fluid: a horizontal excitation at the upper end of the vertical pipe. Trans. Jpn. Soc. Mech. Eng. 1988; Ser C 54(497):100–107.

[37]   Miles WH, Pezeshki C, Elgar S. Bispectral analysis of a fluid elastic system: the cantilevered pipe. Journal of Fluids Structures. 1992; 6:633–640.

[38]   Ibrahim RA. Overview of mechanics of pipes conveying fluids—part I: fundamental studies. Journal of Pressure Vessel Technology. 2010; 132:034001–32.

[39]   Dzhupanov VA. Systematic review on the modes of a cantilevered pipe conveying fluid and lying on a multiparametric resisting medium. Journal of Theory. Appl. Mech. 1998; 28:34–53.

[40]   Paidoussis MP. Flow-induced vibrations in nuclear reactors and heat exchangers: practical experiences and state of knowledge. Practical experiences with flow-induced vibrations. Berlin: Springer; 1980. pp. 1–81.

[41]   Paidoussis MP. A review of flow-induced vibrations in reactors and reactor components. Nuclear Engineering Design. 1983; 74:31–60.

[42]   Paidoussis MP. Flow-induced instabilities of cylindrical structures. Applied Mechanic Revision. 1987; 40:163–175.

[43]   Paidoussis MP. The canonical problem of the fluid-conveying pipe and radiation of the knowledge gained to other dynamics problems across applied mechanics. Journal of Sound Vibration. 2008; 310:462–492.

[44]   Paidoussis MP, Li GX. Pipes conveying fluid: a model dynamical problem. Journal of Fluids Structures. 1993; 7:137–204.

[45]   Tijsseling AG. Fluid-structure interaction in liquid filled pipe systems: a review. Journal of Fluids Structures. 1996; 10:109–146.

[46]   Huang Y, Zhou S, Xu J, Qian Q, Li L. Advances and trends of nonlinear dynamics of pipes conveying fluid. Advanced Mechanical. 1998; 28(1):30–42.

[47]   Weaver D, Fitzpatrick J. A Review of cross-flow induced vibrations in heat exchanger tube arrays. Journal of Fluids Structures. 1988; 2:73–93.

[48]   Wiggert DC. Fluid transients in flexible piping systems. Proceedings of the Eighth International Association of Hydraulic Research IAHR Symposium on Hydraulic Machinery and Cavitation, Valencia, Spain. 1996; 58–67.

[49]   Wiggert DC, Tijsseling AS. Fluid transients and fluid-structure interaction in flexible liquid-filled piping. Applied Mechanic Revision. 2001; 54(5):455–481.

[50]   Xu J, Yang QB. Recent development on models and nonlinear dynamics of pipes conveying fluid. Advanced Mechanic. 2004; 34(2):1–13.

[51]   Chen SS. Flow-induced vibration of circular structures. Washington, DC: Hemisphere; 1987.

[52]   Paidoussis MP, Luu TP, Laithier BE. Dynamics of finite-length tubular beams conveying fluid. Journal of Sound and Vibration. 1986; 106(2):311–331.

[53]   Housner GW. Bending vibrations of a pipe when liquid flows through it. Journal of Applied Mechanics. 1952; 19:205–208.

[54]   Edelstein WS, Chen SS, Jendrzejczyk JA. A finite element computation of the flow-induced oscillations in a cantilevered tube. Journal of Sound and Vibration. 1986; 107(1):121–129.

[55]   Jendrzejczyk JA, Chen SS. Experiments on tubes conveying fluid. Thin-Walled Structures. 1985; 3:109–134.

[56]   Holmes PJ. Pipes supported at both ends cannot flutter. Trans ASME Journal Applied Mechanic. 1978; 45:619–622.

[57]   Singh K, Mallik AK. Wave propagation and vibration response of a periodically supported pipe conveying fluid. Journal of Sound and Vibration. 1977; 54(1):55–66.

[58]   Benjamin TB. Dynamics of a system of articulated pipes conveying fluid. I. Theory. Proceedings of the Royal Society (London). 1961; 261(A):457–486.

[59]   Paidoussis MP. Dynamics of tubular cantilevers conveying fluid. I. Mech. E. Journal of Mechanical Engineering Science. 1970; 12:85–103.

[60]   Paidoussis MP. Fluid–structure interactions: slender structures and axial flow. London: Academic Press; 1998.

[61]   Paidoussis MP. A note added to the discussion by Dupuis & Rousselet. Journal of Fluids and Structures. 1991; 5:600.

[62]   Benjamin TB. Dynamics of a system of articulated pipes conveying fluid. II. Experiments. Proceedings of the Royal Society (London). 1961; 261(A):487–499.

[63]   Gregory RW, Paidoussis MP. Unstable oscillation of tubular cantilevers conveying fluid. II. Experiments. Proceedings of the Royal Society (London). 1966; 293(A):528–542.

[64]   Paidoussis MP, Luu TP. Dynamics of a pipe aspirating fluid, such as might be used in ocean mining. ASME Journal of Energy Resources Technology. 1985; 107:250–255.

[65]   Langthjem M. Finite element analysis and optimization of a fluid-conveying pipe. Journal of Mechanics Based Design of Structures and Machines. 1995; 23(3):343–376.

[66]   Liang B, Tang JX. Analysis of dynamic characteristic and stability of pipe conveying fluid by finite element method. Acta Mech. Solida Sinica. 1993; 14(2):167–170.

[67]   Shizhong W, Yulan L, Wenhu H. Research on solid-liquid coupling dynamics of pipe conveying fluid. Applied Mathematics and Mechanics. 1998; 19(11):1065–1071.

[68]   Wang SZ, Yu SS, Zho Y. Solid-liquid coupling characteristics of fluid-conveying pipes. Journal Harbin Inst. Technology 2002; 34(2):241–244.

[69]   Cui HW, Tani J. Effect of boundary conditions on the stability of a cantilever pipe discharging and aspirating fluid. JSME Int. J. Ser. C: Dyn. Control, Robotics, Des. Manuf. 1996; 39:20–24.

[70]   Hongwu C, Junji T. Effect of boundary conditions on the stability of a cantilever pipe discharging and aspirating fluid. JSME Int. J., Series. 1996; 39(C):20–24.

146

[71]   Lee U, Oh H. The spectral element model for pipelines conveying internal steady flow. Eng. Structures. 2003; 25:1045–1055.

[72]   Lee U, Park J. Spectral element modeling and analysis of a pipeline conveying internal unsteady fluid. Journal of Fluids Structures. 2006; 22:273–292.

[73]   Stein RA, Tobriner WM. Vibrations of pipes containing flowing fluids. ASME Journal Applied Mechanic. 1970; 37(6):906–916.

[74]   Mizoguchi K, Komori S. Vibration and dynamic instability of a cylindrical shell conveying a compressible fluid. Bull. JSME. 1978; 21:628–636.

[75]   Wang X, Bloom F. Stability of concentric pipes conveying steady and pulsatile fluids. Journal of Fluids Structures. 1999; 13(4):443–460.

[76]   Lee SI, Chung J. New nonlinear modeling for vibration analysis of a straight pipe conveying fluid. Journal of Sound Vibration. 2002; 254(2):313–325.

[77]   Yang XD, Jin JD. Comparison of Galerkin method and complex mode method in natural frequency analysis of tube conveying fluid. Zhendong yu Chongji/Journal Vibration Shock. 2008; 27(3):80–86.

[78]   Maalawi KY, Ziada MA. On the static instability of flexible pipes conveying fluid. Journal of Fluids Structures. 2002; 16:685–690.

[79]   Ganesan R, Ramu SA. Vibration and stability of fluid conveying pipes with stochastic parameters. Struct. Eng. Mech. 1995; 3(4):313–324.

[80]   Lifshitz JM, Gov F, Gandelsman M. Instrumented low-velocity impact of CFRP beams. International Journal of Impact Engineering. 1995; 16(2):201–215.

[81]   Daniel CB. Denting of pressurised pipelines under localised radial loading. International Journal of Mechanical Sciences. 2004; 46:1783–1805.

[82]   Kumar DR, Vidivelli B. Acrylic rubber latex in ferrocement for strengthening reinforced concrete beams. American Journal of Engineering and Applied Sciences. 2010; 3(2):277–285.

[83]   Kotousov A, Mohammad R. Analytical modeling of the transient dynamics of pipe with flowing medium. J. of Physics: Conf. Series. 2009; 181:8.

[84]   Feodosiev VI. Advanced stress and stability analysis. Berlin: Springer-Verlag; 2005.

[85]   Païdoussis MP, Issid NT. Dynamic stability of pipes conveying fluid. Journal of Sound Vibration. 1974; 33:267–294.

[86]   Kreyszig E. Advanced engineering mathematics. Hoboken: John Wiley; 2006.

[87]   Barhen S. Analytic and numerical modeling of the transient dynamics of a microcantilever sensor. Phys. Letters. 2008; 372(A): 947–957.

[88]   Steidel R. An introduction to mechanical vibrations. John Wiley; 1989.

[89]   Jo Y-D, Ahn BJ. Analysis of hazard area associated with hydrogen gas transmission pipelines. Int. J. Hydrogen Energy. 2006; 31:2122–2130.

[90]   Shilling R, Lou YK. An experimental study on the dynamic response of a vertical cantilever pipe conveying fluid. Journal of Energy Resources Technology. 1980; 102:129–135.

[91]   Long RH Jr. Experimental and theoretical study of transverse vibration of a tube containing flowing fluid. ASME Journal of Applied Mechanics. 1955; 22:65–68.

[92]   Gregory RW, Paidoussis MP. Unstable oscillation of tubular cantilevers conveying fluids. I. Theory. Proceedings of the Royal Society (London). 1966b; 293(A):528–542.

[93]   Gregory RW, Paidoussis MP. Unstable oscillation of tubular cantilevers conveying fluid. II. Experiments. Proceedings of the Royal Society (London). 1966b; 293(A):528–542.

[94]   Kotousov AG. Method of integral inequalities to impact dynamics problems. Int. J. Eng. Science. 1999; 37:1737–1746.

[95]   Kotousov AG. A method for obtaining approximate solutions for highly dynamic problems. Int. J. Eng. Science. 2001; 39:477–489.

[96]   Toophanpour-Rami M, Hassan ER, Kelso RM, Denier JP. Preliminary Investigation of impulsively blocked pipe flow. 16th Australasian Fluid Mechanics Conference Crown Plaza, Gold Coast, Australia; 2007. pp. 1–4.

[97]   Smith CR, Seal CV, Praisner TJ, Sabatini DR. Hydrogen bubble visualisation in flow visualisation. In: Lim TT, Smits A, editors. Journal of Imperial College Press; 2000. pp. 27–42.

[98]   Vardi AE, Hwang KL. A characteristics model of transient friction in pipes. Journal of Hydraulic Research. 1992; 29(5):669–684.

[99]   Wang XJ, Lambert MF, Simpson AR. Detection and location of a partial blockage in a pipeline using damping of fluid transients. Journal of Water Resources and Planning Management. 2005; 131(3):244–492.

[100]   Wallis A. Axial-flow fans and ducts. Krieger Publishing Company; 1991.

[101]   Weinbaum S, Parker KH. The laminar decay of suddenly blocked channel and pipe flows. Journal of Fluid Mechanics. 1975; 69(4):729–752.